Y/NSP-252

National Security Program Office

Final Report

Ultrasonic Communication Project, Phase 1, FY 1999

H. D. Haynes
M. A. Akerman
Engineering Technology Division

V. M. Baylor
National Security Program Office

June 2000

June 2000 **Y/NSP-252**

Final Report

Ultrasonic Communication Project
Phase 1, FY 1999

H. D. Haynes
M. A. Akerman
Engineering Technology Division

V. M. Baylor
National Security Program Office

Prepared by
National Security Program Office
Oak Ridge Y-12 Plant
Oak Ridge, Tennessee 37831-8260
managed by
Lockheed Martin Energy Systems, Inc.
for the
U.S. Department of Energy
under contract DE-AC05-84OR21400

DISCLAIMER

Contents

Executive Summary

The primary objective of this Phase 1 project was to explore, demonstrate, and document methods for ultrasonic-based communication with an emphasis on the application of digital signal processing techniques. During the project, at the direction of the agency project monitor, particular attention was directed at sending and receiving typed messages and computer files ultrasonically through air and through pipes that would be commonly found in buildings.

Ultrasound communication hardware was initially developed by Oak Ridge National Laboratory in 1993 and was based on frequency modulation electronics. This hardware provided a means of transmitting audio information (e.g., voice and music) through the air as a continuous (analog) signal. During the Phase 1 project, efforts were focused on the development of methods for transmitting computer files using a technique called discrete frequency shifting (DFS). With DFS, individual alphanumeric characters are broken down into a sequence of bits, where each bit is used to generate a discrete ultrasonic frequency. Characters can then be transmitted one-bit-at-a-time and reconstructed by the receiver. This technique was put into practice through the development of LabVIEW™ virtual instruments (VIs). Together with specially designed electronics, these VIs provide a system for transmission and reception/reconstruction of typed messages and computer files.

In addition, signal-conditioning elements were identified, evaluated, and selected based on the required function. For example, several commercial integrated circuits were tested for converting the frequency of the received ultrasonic signal to a corresponding direct current voltage level. Two of these devices (a phase-locked loop and a frequency-to-voltage converter) were later incorporated into the final system hardware.

Considerable testing was performed to study how ultrasound is transmitted through pipes filled with air or water. These tests resulted in a number of reference charts that illustrate the absorption of ultrasound through different pipe materials, both with and without water, as a function of distance. These charts show that ultrasound is least attenuated by copper pipe and most attenuated by polyvinylchloride pipe. The major influence of water in the pipe appears to be as an additional damping mechanism (resulting in additional signal attenuation); however, dramatic improvements are observed in ultrasound signal strength if the transducers are directly coupled to the water, rather than simply attaching them to the outside of the pipe.

A major accomplishment of this project was the development and integration of hardware and software into a fully functional ultrasonic communication system for demonstration purposes. All aspects of this system are described in detail in this report, and recommendations for further improvements are given. This report also provides a discussion of major system considerations, including signal conditioning electronics, speed and distance of transmission, triggering and noise filtering, and error checking. This system is a major deliverable of this project and has been successfully demonstrated to the program monitor.

1. Background

1.1 Initial Developments (1993 Work)

In 1993, Oak Ridge National Laboratory (ORNL) developed methods and devices to allow people to communicate using inaudible (ultrasonic) sound pressure. Applications of this technique include

- communication through air when radio frequencies are monitored and communication must be secure and undetected;
- communication near explosive detonators where radio is forbidden; and
- communication within a building, ship, etc., by transmitting ultrasonic signals through existing structural components (e.g., beams and pipes).

A transmitter and receiver were developed (see Figure 1.1) for converting audio signals (including human voice) to ultrasonic signals, transmitting these ultrasonic signals, and reconverting the ultrasonic signals back to the audio range. The developed hardware was demonstrated on several occasions, most notably at the Special Technologies EXPO ’93 held in Oak Ridge, Tennessee, on May 3–6, 1993.

Through a careful selection of transmitter and receiver subcomponents, voice and music were transmitted over 100 ft in air using less than 1 mW of electrical power. System subcomponents include signal translation and detection circuits, efficient horn tweeters, specially designed parabolic dish collectors, and sensitive microphone elements. Analytical models predict that a useful range of 250 ft in still air could be achieved with less than 5-W input power. In addition it was demonstrated that a person outside a building could communicate with someone inside the building by transmitting ultrasonically through a glass window.

Follow-on work was suggested that would lead to the optimization of the technique to meet specific applications having unique requirements. These requirements could include

- extended distance (e.g., using higher power, larger collector dish, etc.);
- miniaturization of transmitter and receiver devices (e.g., for concealment in clothes, for integration in other equipment such as binoculars or rifles); and
- modification for use underwater and through structures (e.g., devices that strap on to piping or beams for communicating within a building).

It is expected that each new application could utilize transducers that are specially designed to unique size and performance specifications.

1.2 Patent 5,539,705

A patent was issued on July 23, 1996, for “Ultrasonic Speech Translator and Communication System.” The patent describes in detail the methods and devices that were developed for voice and music transmission through air via ultrasound and the potential for adapting these methods and devices for a variety of communications through solid materials. The reader is encouraged to review this patent if additional information is desired.

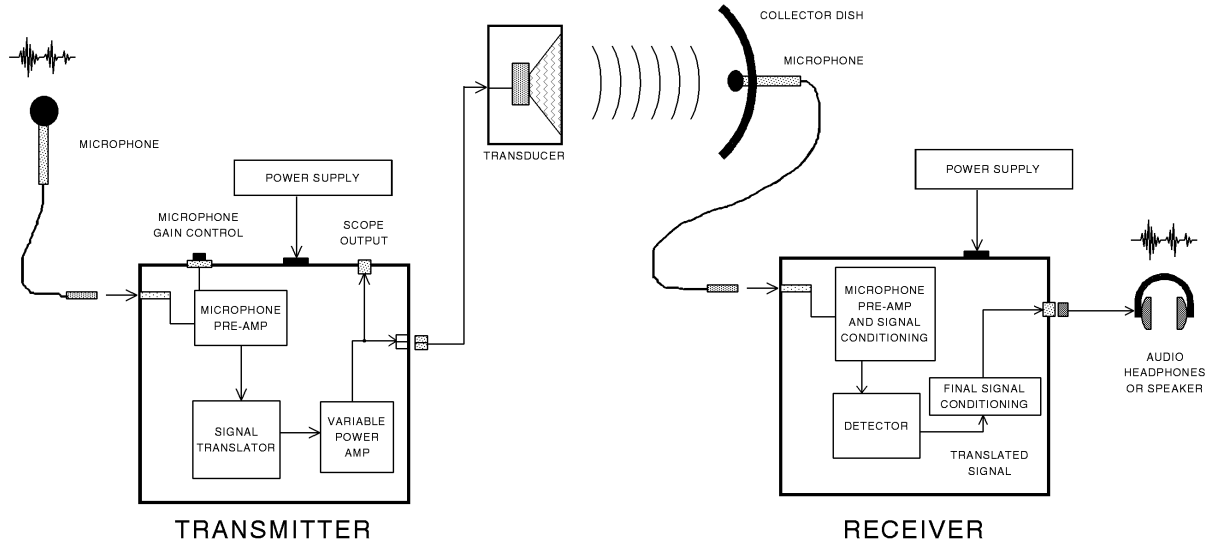

Figure 1.1 Illustration of initial development (1993) resulting in U.S. Patent 5,539,705.

2. Objectives of NN-20 Phase 1 Project

The primary objective of this project was to explore, demonstrate, and document methods for ultrasonic-based communication with an emphasis on the application of digital signal processing techniques. During the project, at the direction of the agency project monitor, particular attention was directed at sending and receiving ultrasonic data through pipes that would be commonly found in buildings. Efforts were also focused on development of a method for transmitting computer files ultrasonically. The project statement of work is reprinted here for reference purposes.

Task 1 Identify and evaluate new methods for ultrasonic communication. Determine the level of improvement that can be achieved from use of state-of-the-art electronics and digital signal processing (DSP) techniques. Comparisons between methods and circuits are to be based on their impact on signal-to-noise ratio, system efficiency, data conditioning, and other measurable characteristics of interest. Evaluations of DSP options will be enhanced through the utilization of virtual instrument (VI) techniques. Virtual instruments allow DSP algorithms to be evaluated and optimized, prior to their incorporation into application specific integrated circuits (ASICs) or other hardware.

Task 2 Perform tests to determine the envelope for ultrasound transmission through solids versus through air. While most of the physics of propagation is known, the emphasis here will be on the practical aspects of connections, efficient electronics, impedance matching, and the effect of damping mechanisms. Evaluate and/or develop transducers for efficiently transmitting and receiving ultrasound through various common hardware including water pipes, steel support beams, ductwork, etc.

Task 3 Identify and evaluate automatic low energy usage electronic control options that would permit ultrasonic communication systems to be used effectively under specified conditions.

Task 4 Develop at least one working demonstration of ultrasonic communication based on the findings of Tasks 1, 2, and 3. The DSP attributes of the demo will likely be handled by VIs developed during the project.

Task 5 Provide short quarterly progress reports. Prepare a final report and an executive summary that documents the major findings of this project, including recommendations for further work.

Deliverables Deliverables will include the quarterly reports, a final report, an executive summary, and at least one working demonstration that reflects an application chosen by the sponsor.

Reporting Informal reports will be provided periodically using means appropriate for the type and classification of the transmitted information.

Schedule The duration of this project is one year.

3. Evaluation of Communication Methods

3.1 Frequency Modulation

As previously discussed, initial developments of ultrasonic communication hardware by ORNL utilized frequency modulation (FM) circuitry. The FM method is attractive since FM signals are inherently more immune to extraneous noise than amplitude modulated (AM) signals. If FM signals are transmitted via a transducer having a relatively flat amplitude response to all transmitted frequencies, the resulting ultrasound will be inaudible; however, if the transducer does not transmit all frequencies with equal intensity, amplitude modulations will occur. These amplitude modulations can be heard, even though the frequencies being transmitted are above the normal hearing range.

Creating an FM signal involves a voltage-controlled oscillator (VCO). The VCO generates an output signal at a frequency that corresponds to the input voltage magnitude. For ultrasonic communication applications, the input voltage signal contains the information that is to be transmitted. The resulting FM signal is then fed to an ultrasonic transducer for conversion of the electrical signal to a FM pressure wave. The pressure wave is transmitted through the medium of interest, detected by another ultrasonic transducer, and converted back to an electrical signal. The electrical signal is then demodulated by an electronic circuit, which provides an output signal containing the transmitted information. Figure 3.1 is provided to illustrate these steps graphically.

Several integrated circuits (ICs) have been specifically designed to generate and demodulate FM signals. One IC that may be used as a VCO is the NE/SE566 Function Generator. The NE/SE566 is a highly linear VCO that provides buffered square wave and triangle wave outputs. In an ultrasonic communication system, the NE/SE566 can drive an ultrasonic transducer directly or can be used to trigger a higher-voltage transducer drive circuit.

One commonly used IC for demodulating FM signals is the phase-locked loop (PLL). A PLL contains a built-in VCO for generating a reference signal and a phase comparator, which essentially compares the frequencies of the input signal and the reference signal and generates an error voltage proportional to the frequency difference between the two signals. The error voltage is then used internally to adjust the VCO until the VCO and input signal frequencies are equal. At this point the PLL has locked onto the signal. A low-pass loop filter is normally used to smooth the pulsating error voltage into a dc error signal and, consequently, limits the speed with which the PLL can track changes in the input frequency. The error signal magnitude thus reflects the frequency of the input signal. The PLL can continuously follow the frequency of an FM signal and provide a voltage output that corresponds to the frequency, thus providing a method for reproducing the original input signal.

Another IC for demodulating FM signals is the voltage-to-frequency converter (VFC), which normally functions as a frequency-to-voltage converter as well. After alternating current (ac) coupling a transistor-transistor logic (TTL) version of the FM signal (as required by the VFC), the VFC detects the falling edges of the input signal as it crosses zero and outputs a direct current (dc) voltage proportional to the frequency of the zero crossings.

Both PLL and VFC methods can track the frequency of an input signal that varies in frequency. Frequency variations can be continuous (analog) or discrete (digital). Since the primary objective of the Phase 1 Ultrasonic Communication Project was to evaluate DSP techniques, considerable effort was therefore directed towards evaluation and demonstration of methods where digital information could be sent via ultrasound. The following discussion summarizes that effort.

3.2 Discrete Frequency Shifting

Ultrasound communication hardware, developed in 1993 by ORNL, transmitted audio information (e.g., voice and music) as a continuous (analog) signal. By converting analog information to digital, dynamic range (signal-to-noise ratio) can often be improved. During this Phase 1 project, efforts were focused on the development of methods for transmitting computer files using a technique called discrete frequency shifting (DFS). With DFS, individual alphanumeric characters are broken down into a sequence of bits, where each bit is used to generate a discrete ultrasonic frequency. Characters are then transmitted one-bit-at-a-time, and reconstructed by the receiver. LabVIEW™ virtual instruments (VIs) have been developed and used thus far in conjunction with specially designed electronics for transmission and reception/reconstruction of typed messages and computer files.

As an example, Figure 3.2 illustrates a simple typed message (“This is a test.”) that has been converted to a series of integer levels. In the top plot, two discrete levels are used, requiring a sequence of eight bits to represent a single character whose ASCII equivalent can range from 0 to 255. The bottom plot shows the data compression that occurs when the number of levels is increased from 2 to 16. When 16 levels are used, only 2 bits are required to construct a character. Thus, to transmit the message (“This is a test.”) containing 15 characters (including the period), 120 bits of information are required when using 2-bit levels. The number of required bits drops to 30 when 16-bit levels are used. Table 3.1 shows the two-number codes for the first 128 ASCII characters. For example, the word (“This”) is constructed by the following number sequence: 5,4,6,8,6,9,7,3. Each bit is transmitted ultrasonically by converting each bit level to a unique frequency at the transmitter location and converting the frequency back to the bit level at the receiver location (Figure 3.3).

Several electronic circuit designs have been evaluated in conjunction with these VIs in an effort to obtain maximum transmission speed without sacrificing transmission accuracy and reliability. These efforts focused on evaluation of ICs used to convert frequency to voltage. Initial baseline tests were carried out using the LM565 PLL. This PLL was an integral part of the 1993 ultrasonic communication system and thus provided a good place to start on this project. Of initial concern was the speed at which the PLL could track a moving step change in input frequency. A more modern PLL, the CD74HCT4046AE (hereafter called the 4046), was tested for tracking speed in a similar manner. As shown in Figure 3.4, the 4046-based circuit was clearly faster than the LM565 in tracking a frequency shift from 28 to 30 kHz. In addition to the 4046, a frequency-to-voltage converter IC (VFC320) was also evaluated and shown to provide comparable response to the 4046. Both the 4046 and the VFC320 were selected for incorporation into the demonstration system hardware.

3.3 Response to Phase Distortion Effects

Ultrasonic signals can follow many different paths from the transmitter to the receiver. Although the majority of the signal may follow a direct route, reflections can also occur, resulting in multipath interference that introduces amplitude and phase distortion at the receiver location. Since the PLL circuitry is sensitive to phase as well as frequency of the ultrasound signal, changes in phase produce variations in the final demodulated signal that can produce errors in the ultrasound transmission. This effect is illustrated by Figures 3.5a, 3.5b, and 3.5c, which show the PLL output signal distortion that occurs when the ultrasonic signal path from transmitter to receiver is altered. In contrast to the PLL output signal distortion, the output from the frequency-to-voltage (F-to-V) circuit remains relatively unaffected by phase effects since it responds directly to frequency, not phase. The stable output signal of the F-to-V circuit makes it suitable for ultrasonic communication through solids as well as through air.

3.4 Other Methods

Another promising method that has yet to be fully explored is ultrasonic communication using a fixed frequency but with varying phase. A voltage-to-phase converter circuit would be used at the transmitter and a phase detector circuit would be used at the receiver. Circuit designs have been identified but have not yet been explored due to project budget considerations. Other methods can be explored that would identify and exploit the unique frequency “windows” where phase distortion is minimal. Many methods for noise reduction are also worth evaluating.

Table 3.1 First 128 ASCII characters, their decimal equivalent, and their two-number sequence for use in a 16-bit level code.

Dec	Char	1st no.	2nd no.	Dec	Char	1st no.	2nd no.	Dec	Char	1st no.	2nd no.
--	-----			44	,	2	12	89	Y	5	9
0	NUL	0	0	45	-	2	13	90	Z	5	10
1	SOH	0	1	46	.	2	14	91	[	5	11
2	STX	0	2	47	/	2	15	92	\	5	12
3	ETX	0	3	48	0	3	0	93	]	5	13
4	EOT	0	4	49	1	3	1	94	^	5	14
5	ENQ	0	5	50	2	3	2	95	_	5	15
6	ACK	0	6	51	3	3	3	96	‘	6	0
7	BEL	0	7	52	4	3	4	97	a	6	1
8	BS	0	8	53	5	3	5	98	b	6	2
9	TAB	0	9	54	6	3	6	99	c	6	3
10	LF	0	10	55	7	3	7	100	d	6	4
11	VT	0	11	56	8	3	8	101	e	6	5
12	FF	0	12	57	9	3	9	102	f	6	6
13	CR	0	13	58	:	3	10	103	g	6	7
14	SO	0	14	59	;	3	11	104	h	6	8
15	SI	0	15	60	<	3	12	105	i	6	9
16	DLE	1	0	61	=	3	13	106	j	6	10
17	DC1	1	1	62	>	3	14	107	k	6	11
18	DC2	1	2	63	?	3	15	108	l	6	12
19	DC3	1	3	64	@	4	0	109	m	6	13
20	DC4	1	4	65	A	4	1	110	n	6	14
21	NAK	1	5	66	B	4	2	111	o	6	15
22	SYN	1	6	67	C	4	3	112	p	7	0
23	ETB	1	7	68	D	4	4	113	q	7	1
24	CAN	1	8	69	E	4	5	114	r	7	2
25	EM	1	9	70	F	4	6	115	s	7	3
26	SUB	1	10	71	G	4	7	116	t	7	4
27	ESC	1	11	72	H	4	8	117	u	7	5
28	FS	1	12	73	I	4	9	118	v	7	6
29	GS	1	13	74	J	4	10	119	w	7	7
30	RS	1	14	75	K	4	11	120	x	7	8
31	US	1	15	76	L	4	12	121	y	7	9
32		2	0	77	M	4	13	122	z	7	10
33	!	2	1	78	N	4	14	123	{	7	11
34	"	2	2	79	O	4	15	124	|	7	12
35	#	2	3	80	P	5	0	125	}	7	13
36	$	2	4	81	Q	5	1	126	~	7	14
37	%	2	5	82	R	5	2	127	DEL	7	15
38	&	2	6	83	S	5	3				
39	’	2	7	84	T	5	4				
40	(	2	8	85	U	5	5				
41	)	2	9	86	V	5	6				
42	*	2	10	87	W	5	7				
43	+	2	11	88	X	5	8				

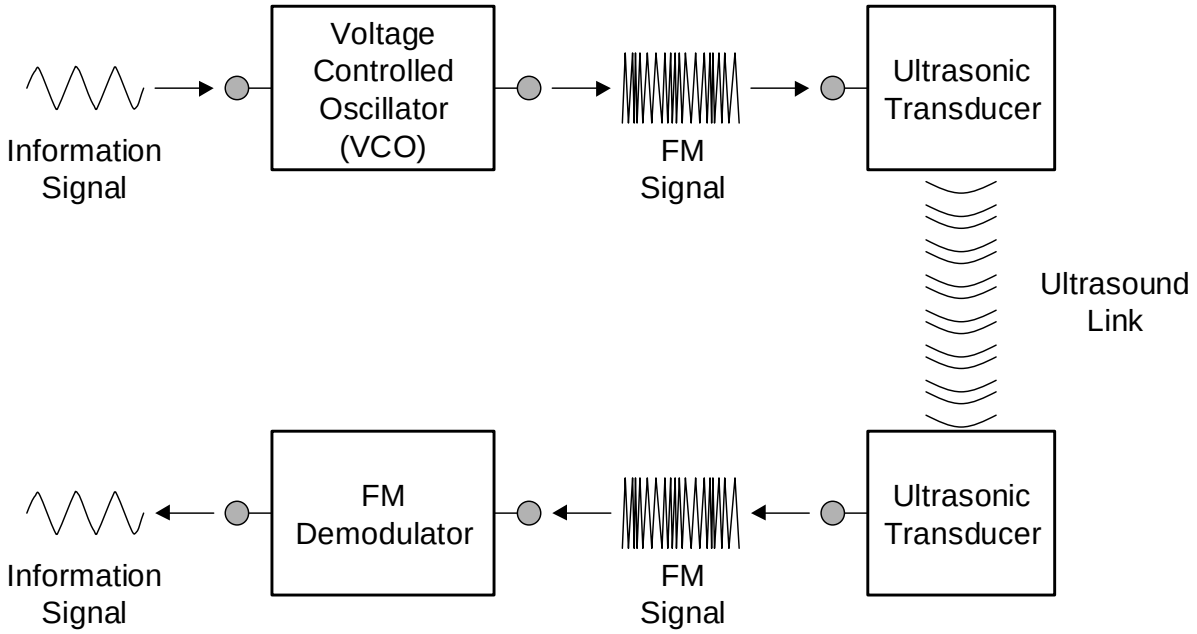

Figure 3.1 Graphical representation of a FM-based ultrasonic communication system.

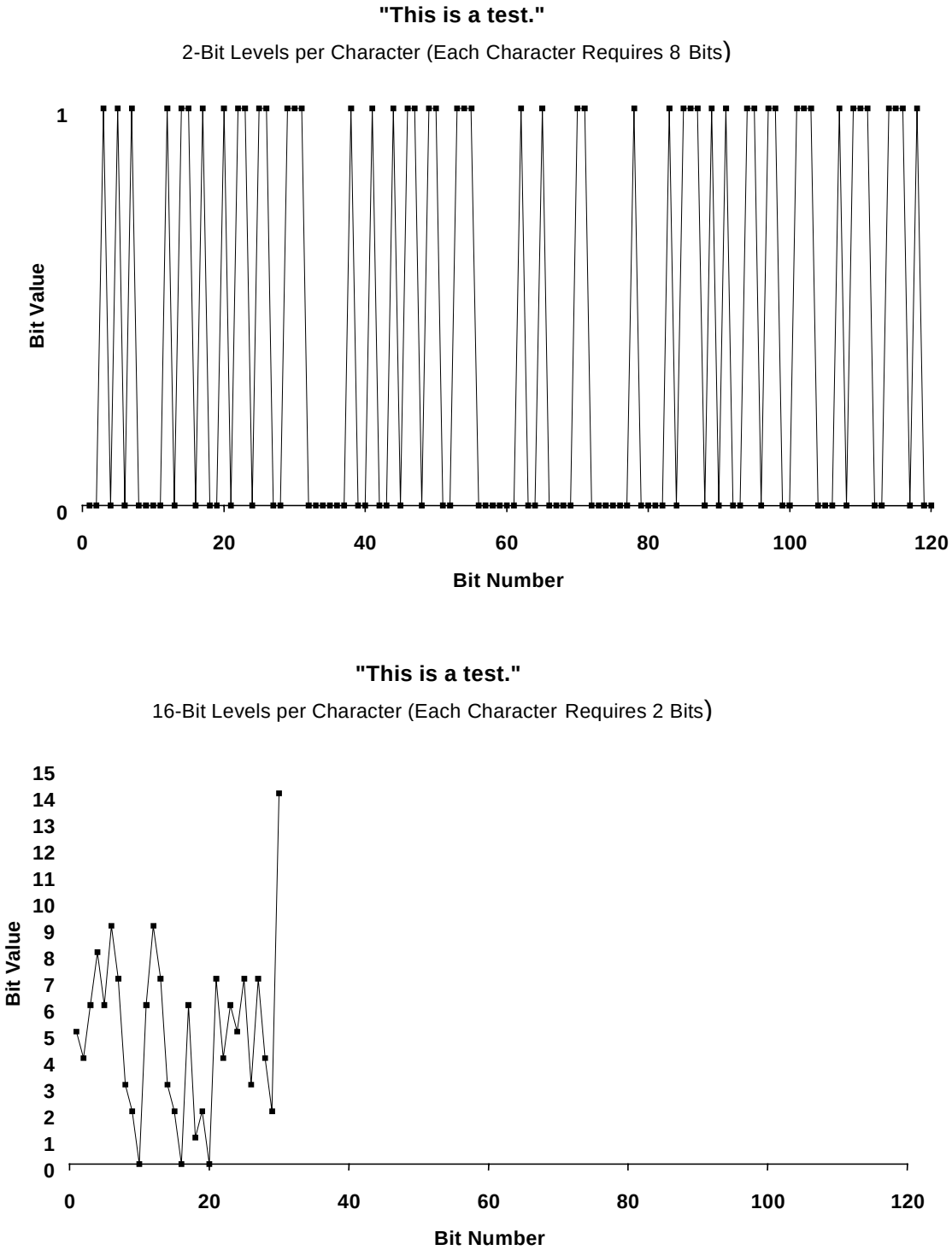

Figure 3.2 The message ("This is a test.") represented by two digital sequences: (top) 2-bit levels per ASCII character and (bottom) 16-bit levels per ASCII character. For application to ultrasonic communication, each bit level generates a discrete frequency.

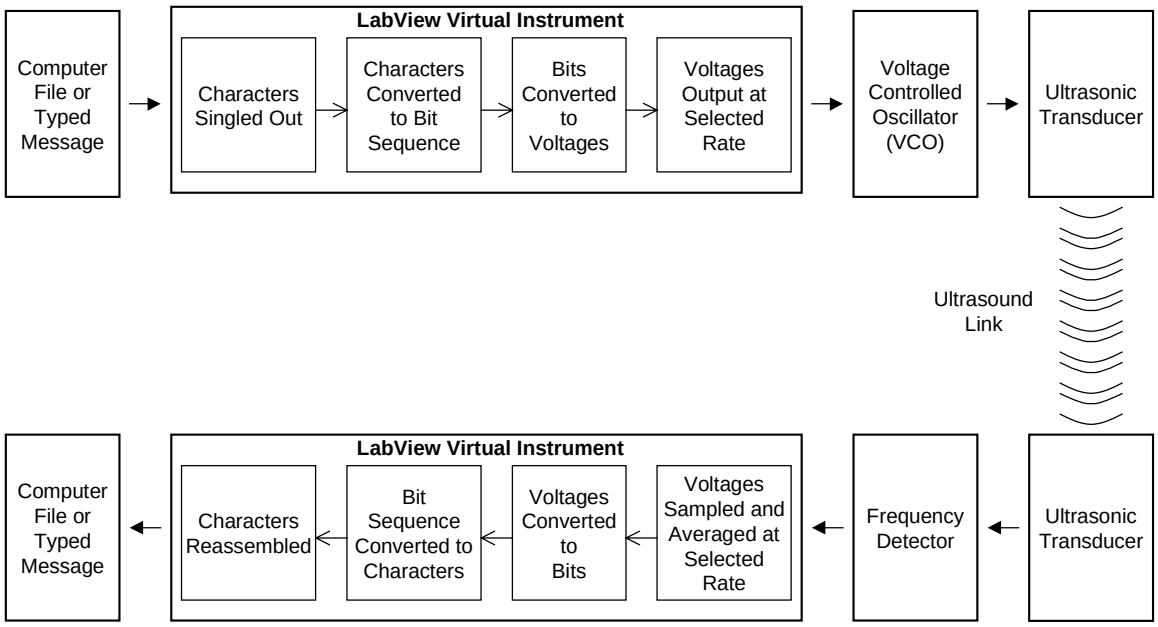

Figure 3.3 Block diagram illustrating how a computer file or typed message can be transmitted ultrasonically using DFS and LabVIEW™ VIs.

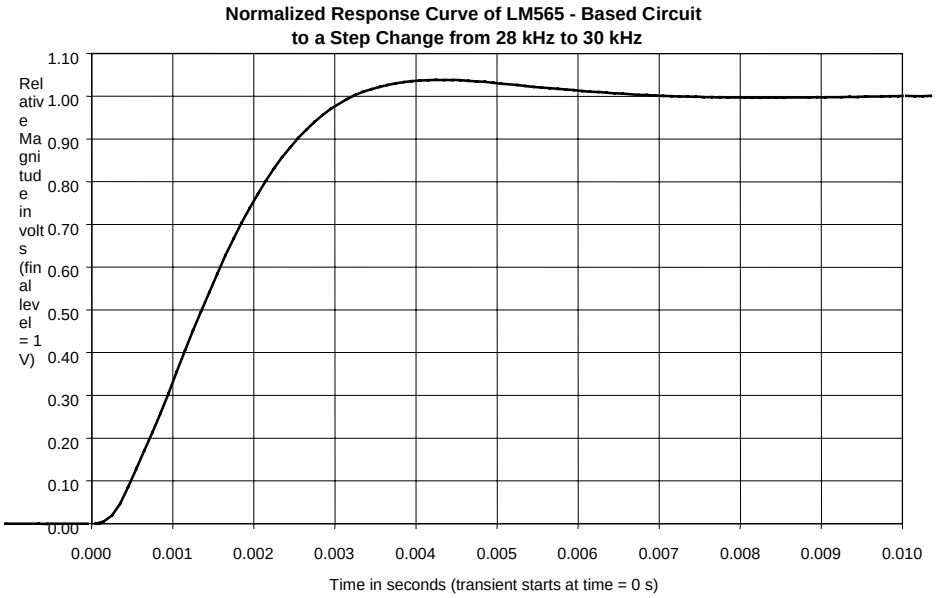

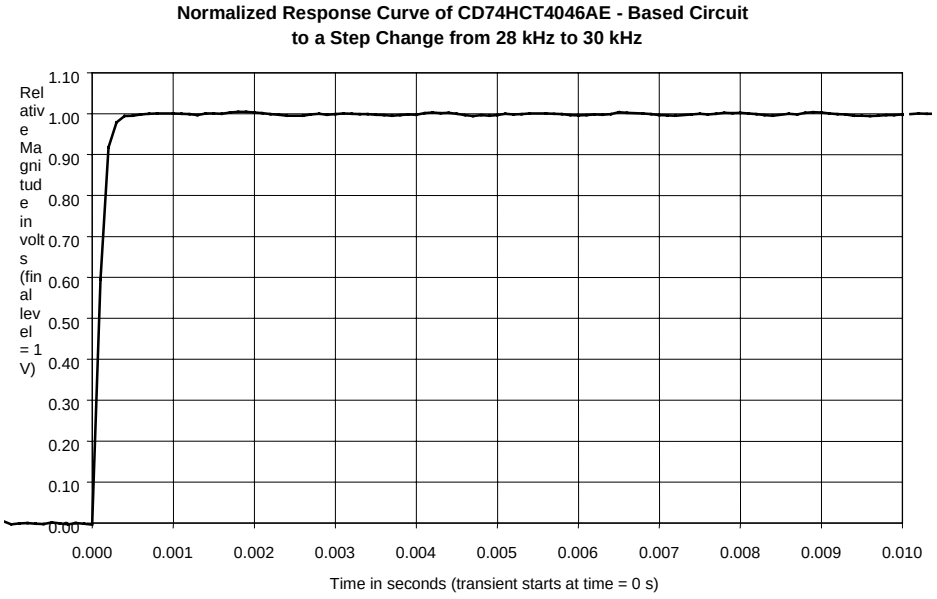

Figure 3.4 Comparison between two PLL circuits to a step change in input frequency from 28 to 30 kHz. The 4046-based circuit is observed to have a much faster response time.

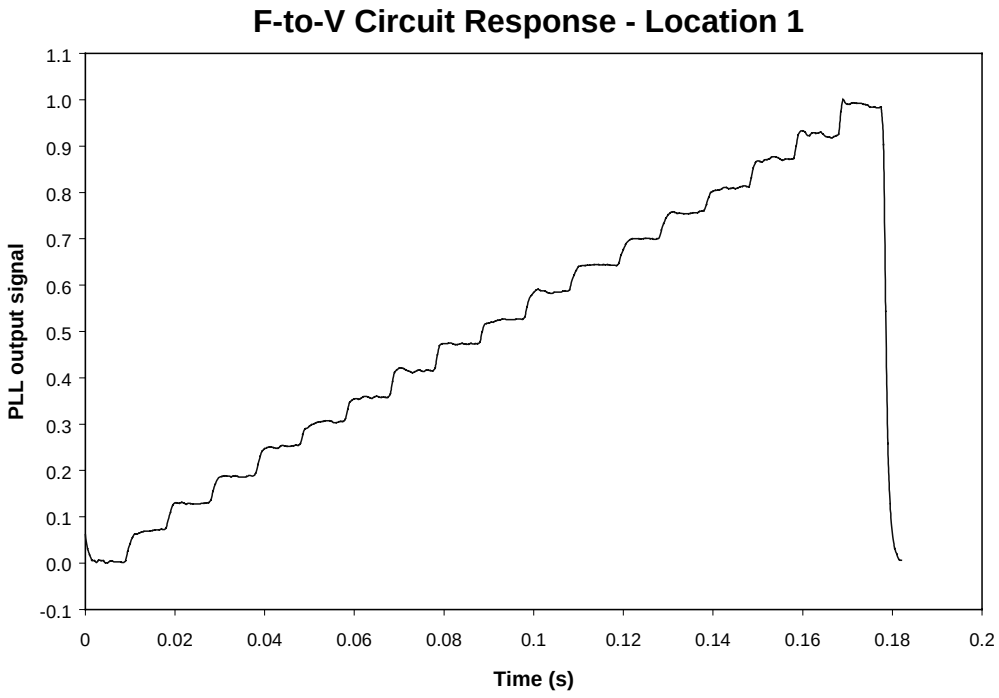

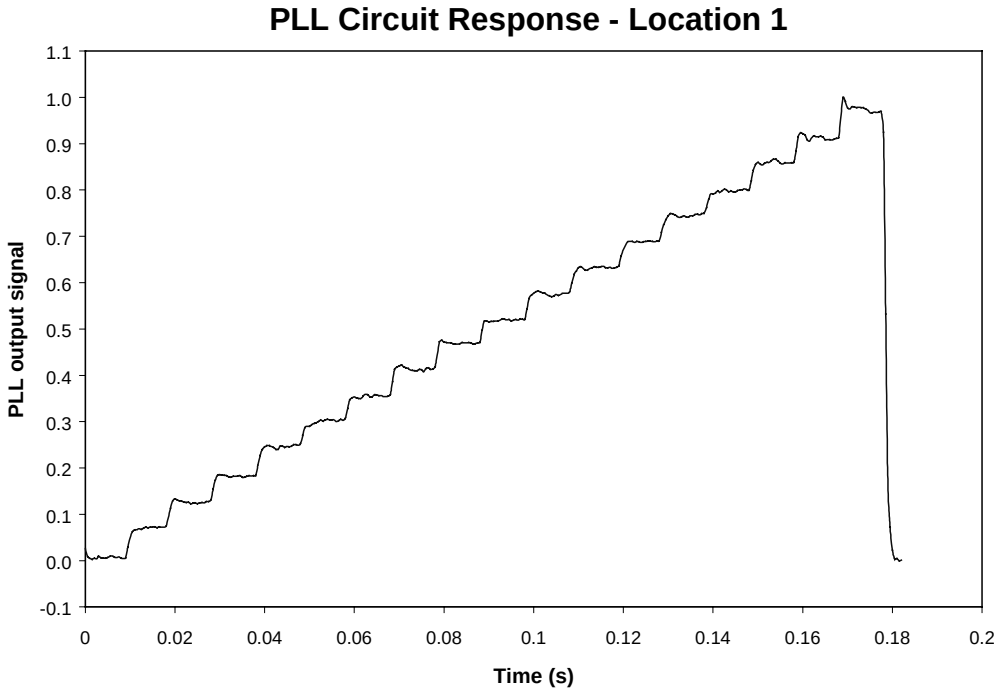

Figure 3.5a Comparison between the F-to-V circuit (top) and the PLL circuit (bottom) to a "staircase" of eighteen discrete and evenly spaced frequencies. Signals were transmitted through air using commercially available ultrasound transducers at a distance of approximately 6 ft. Both circuits provide outputs that vary in magnitude linearly with the frequency of the transmitted ultrasonic signal.

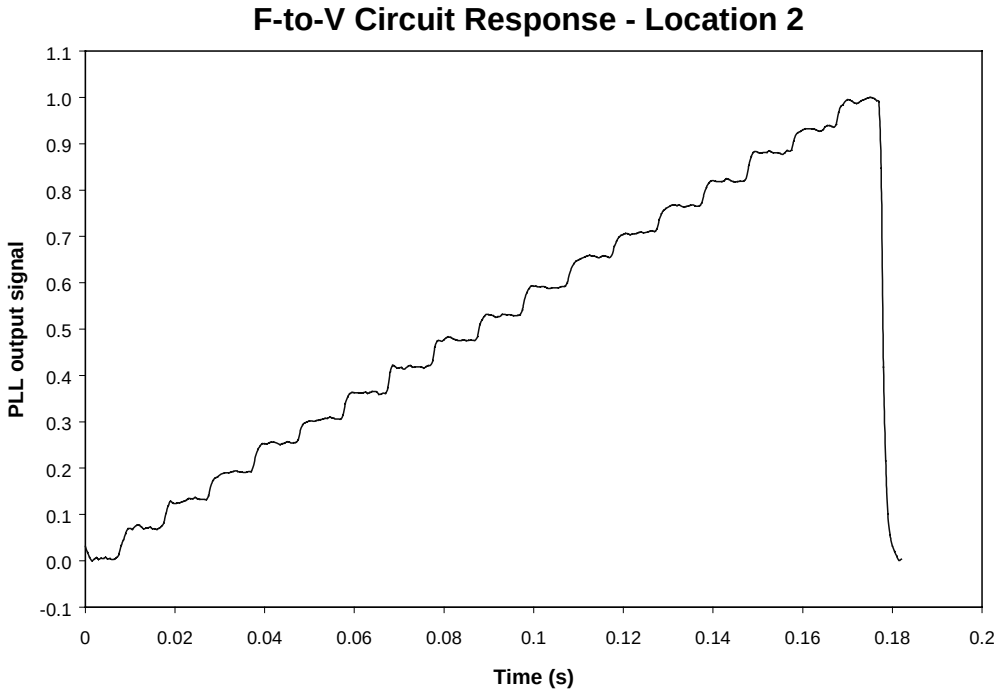

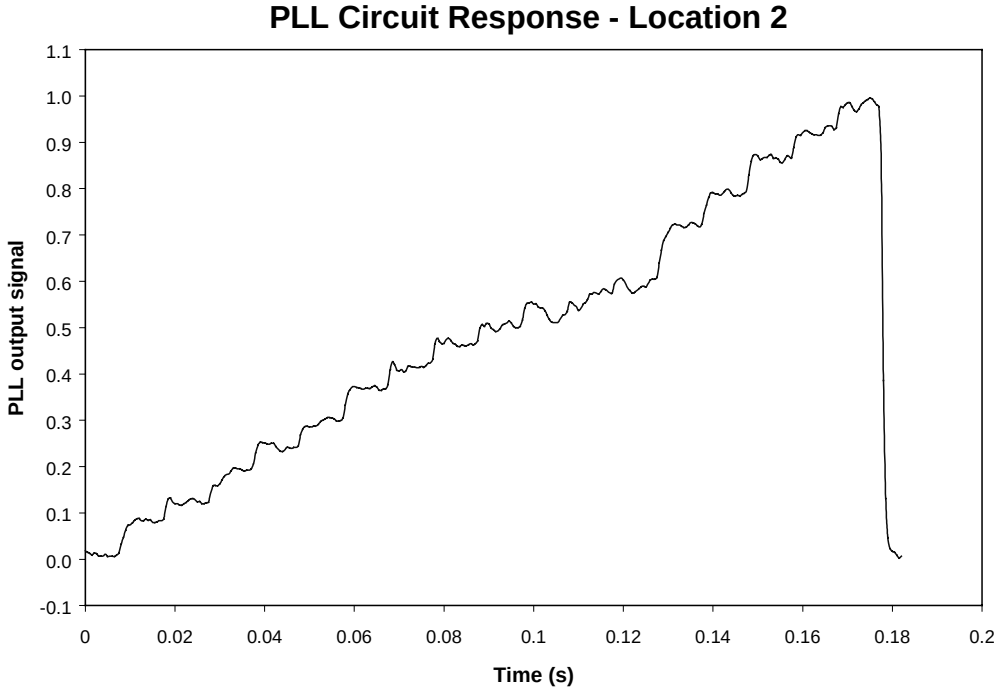

Figure 3.5b Similar comparison plots to Figure 3.5a after moving the receiver transducer slightly to introduce mild phase distortion that shows up as a nonlinear response in the PLL circuit output. The F-to-V circuit is relatively unaffected by this phase distortion.

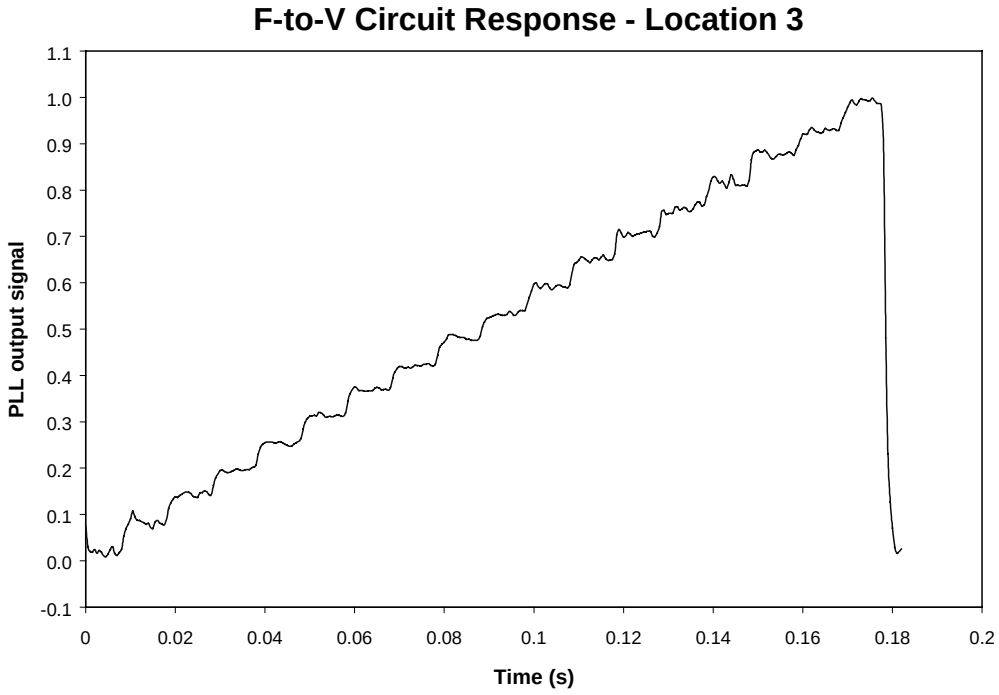

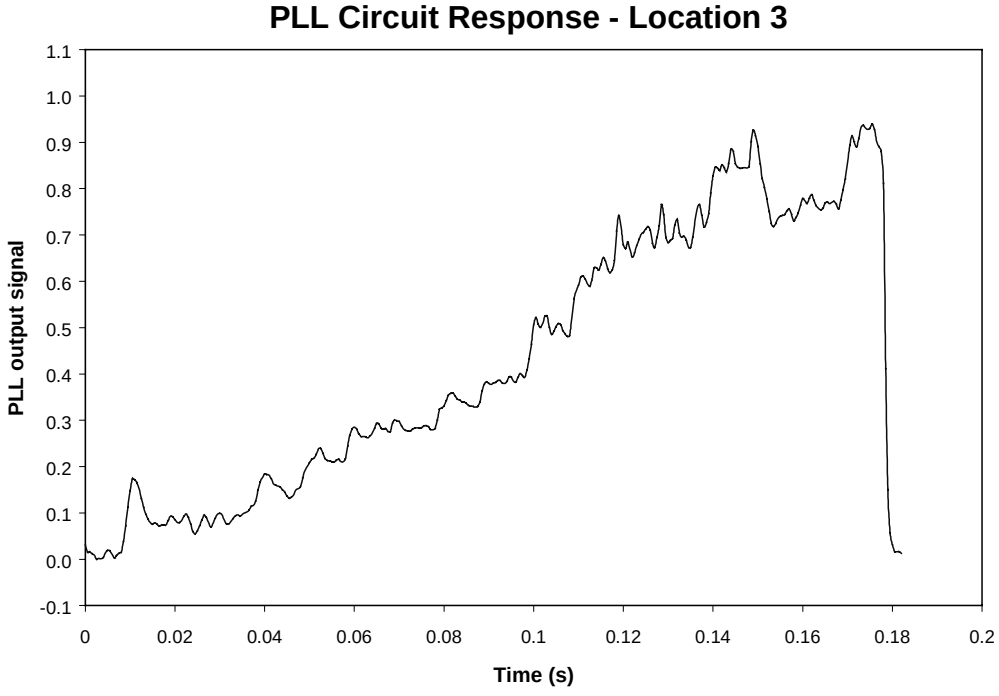

Figure 3.5c Similar comparison plots to Figures 3.5a and 3.5b after moving the receiver transducer again to introduce more severe phase distortion. The PLL output signal is greatly affected by this distortion whereas the F-to-V circuit is only slightly affected.

4. Ultrasound Transmission Through Water Pipes

A major goal of this project was to investigate ultrasound transmission through media other than air. Discussions with the program monitor prompted a focused effort to study ultrasound transmission through water pipes. The following two sections describe the significant findings from that work.

4.1 Transducers Connected to Outside of Pipe

Measurement of the rate at which signals attenuate in different pipes used in ordinary construction can help in estimating the distances over which information may be practically conveyed ultrasonically. Additional useful information would include the speed at which signals move and the changes in the attenuation and speed with and without water in the pipes.

Figure 4.1 illustrates the method used to accomplish these measurements. A transmitter transducer was placed near the end of a pipe and connected to a signal generator. The transducer and pipe were surrounded by 2 in. of closed cell foam to minimize the transmission of sound through the air. The receiver transducer was mounted on the pipe in a manner allowing it to be moved along the pipe without disturbing the pipe. The signal detected by the receiver transducer was amplified using a low-noise preamplifier, further conditioned by a narrow-band filter and viewed by an oscilloscope and a spectrum analyzer. In all cases, measurements were made at 40 kHz, and the band pass was set between 38 and 42 kHz. The receiver and transmitter were electrically isolated from one another in all cases as an additional precaution to guarantee that the measured signal was indeed from ultrasound in the pipe.

Since ultrasound waves are moving away from the transmitter in a coherent way, their phase may be observed easily using an interferometer set up using standard laboratory equipment. The transmitter signal is taken directly from the signal generator to channel 1 of an oscilloscope. The receiver signal after amplification and band pass is fed into channel 2. By using the x-y function of the oscilloscope, one may easily see regularly changing Lisajous patterns as the receiver is moved along the pipe. By taking measurements at complete wavelength intervals the complex system of maxima and minima that exists may be unfolded to the degree necessary to observe absorption along the pipe.

In the arrangement described here, the pipe is excited at 40 kHz at one end and thus becomes a vibrating rod with waves moving away from the transducer along the pipe at the speed of sound in the pipe. At the ends of the pipe, the waves reflect and move back toward the origin. The amount of end effect would depend on the amount of absorption along the pipe and in each case was judged to be small.

The pipes were excited primarily perpendicular to their length, thus mainly generating transverse waves, whose primary oscillation is perpendicular to the pipe. Some portion of this energy is spontaneously converted into other forms (e.g., longitudinal waves). This effect also occurs at interface points such as a tee joining two long sections of pipe. Theoretically, the speed of sound in a solid medium is equal to the square root of the modulus divided by the density. Since the transverse and longitudinal moduli are different, one expects the speed of sound to be different. For instance, the transverse speed will be smaller than the longitudinal speed by an amount equal to Poisson's ratio. For ultrasound transmission in pipes, several effects should be present that are not generally mentioned in textbook values of speed of sound in materials. One effect is that, in finite media, the speed of sound can be lower than the speed

of sound in a so-called infinite medium. In addition, it is theoretically possible for a pipe to effectively "confine" a wave, resulting in little or no transmission when the wavelength of the transmitted ultrasound is equal to the dimension of the pipe, even though transmission will occur readily above and below this point. A third effect is that water in the pipe increases the weight of the pipe and changes the way the waves propagate. This effect can be significant in relatively lightweight polyvinylchloride (PVC) pipes.

For the pipe absorption measurements, the receiver transducer is attached in such a way that it sees mainly transverse excitations, just as the transmitter transducer primarily generates transverse excitations. Longitudinal excitations are still observed because any pipe movement is translated to the detector, albeit with a lower efficiency. The result is that transverse waves are emphasized in the figures that follow.

4.1.1 ½-in. Galvanized Pipe Absorption Measurements

Two 10-ft sections of standard galvanized plumbing pipe were joined with a tee in the middle and brass ball valves at each end. The joints were sealed using Teflon tape. An ultrasonic transmitter was placed at one end just inboard of the ball valve, and, with the receiver transducer at the 1-m mark, a signal generator was adjusted to produce the strongest signal (near 40.5 kHz) that occurs at the resonant operating point of the transducers.

Two types of measurements were made in this configuration. First, data points were taken every centimeter from 1 to 1.8 m. This allows an overview of the peaks and valleys expected as the signal is transmitted down the tube. Second, data points were taken in clumps near the expected maximum points along the entire 20-ft length of the pipe, using the interferometer (phase relationship) approach to identify maxima. For instance, up to 10 measurements 1 cm apart may be made to be sure the maximum point is recorded. These measurements were accomplished first with water in the pipe and then with no water in the pipe.

Additionally, the transmitter was encased with 2-in. semirigid foam on each side, clamped together. With this arrangement, the background signals detected by the receiver transducer were always less than 3% of the total measured signal from the pipe. In addition, the receiver signals were amplified, filtered, and recorded from the digital readout provided by a spectrum analyzer.

When water was added, the pipe was situated on four foam-padded supports with the center slightly higher than the two ends. Water was poured into the open top of the tee until the pipe was full, and then the ball valves at each end were cracked several times, adding water to the tee as air and water escaped making more room. When the pipe was judged to be full, a plastic threaded cap was screwed into the tee making the assembly water and air tight.

Figure 4.2 demonstrates the first type of measurement and shows prominent cycles repeating every 24 cm, approximately double the expected wavelength of 12.5 cm. A second pattern is superimposed that repeats every 4.2 cm. A third observation is that the signal actually appears to increase over the 80-cm measurement distance. This is partly due to the interaction of the two cyclic effects, resulting in situations where the actual peak of the long cycle is unavailable and partly due to the measurements being taken every centimeter, leaving the possibility that the actual maximum points may be between measurements. Overall, the lack of a clear downward trend is an indication of a very low absorption across this distance and at this frequency.

Another possible explanation for the oscillations shown in Figure 4.2 is that the ultrasonic energy is being transmitted in different modes and that the energy is moving between these modes as it is being transmitted down the pipe. The nature of the test results points to the need to explore further the different transmission modes that can occur in simple and complex pipe systems.

Figure 4.3 demonstrates the second type of measurement, over the length of the pipe. The trend is smoother since only the maximum values are plotted at the distance where they occur. After one measurement sequence down the pipe, the points were plotted, and then additional points were taken where there was the appearance of a gap or the possibility that a maximum was missed. The additional data points acquired in this way have been added to Figure 4.2. As shown in Figure 4.3, the additional points from 100 cm to 180 cm do indeed produce a downward slope.

Subsequent to the measurements above, the water was drained from the pipe. The frequency was readjusted for maximum signal strength at 100 cm, and the following measurements were made at a slightly lower frequency, 40.3 kHz.

Figure 4.4 shows the minimum/maximum patterns over an 80-cm distance. Large-scale maxima again appear at approximately 24-cm intervals, and small-scale maxima appear every 2.1 cm. Figure 4.5 shows the position of the large-scale maxima, again based on multiple measurements near each expected maximum. The overall slope is less than the earlier measurement with water in the pipe.

Some variations are inevitable in experimental measurements. Other variations provide information that must be considered when developing an effective system. The most striking effect may be the 2.1-cm spikes that appear both with and without water coupled with the 22-cm, large-scale wavelength. It is expected that these two wavelengths are the result of two waves propagating more or less independently, one propagating at 840 m/s and the other at 8,800 m/s. This is to be compared with the expected velocities of 5000 m/s longitudinal, 3097 m/s transverse for steel, and 1440 m/s for water, 340 m/s for air. The sound pressure is halved every 2.6 m along this pipe.

4.1.2 ½-in. Copper Pipe Absorption Measurements

These measurements were accomplished with the identical experimental arrangement described above; however, the interferometer approach was used to identify maxima for the whole-pipe measurement series instead of taking multiple data points near a maxima.

Figure 4.6 displays an 80-cm segment of copper pipe from 1 to 1.8 m with water in it. An overall wavelength of 10 cm is apparent, indicating a sound velocity of 4000 m/s. Smaller wavelengths are present as well, repeating every 2.5 cm, with a smaller amplitude indicating a lower-intensity wave with a velocity of 1000 m/s. Figure 4.7 shows the measurements made over the 20-ft length of pipe, including the tee at the middle (used to insert the water). From this chart, one may derive an absorption coefficient of 0.00069/cm before the tee and 0.00043/cm after the tee, both based on a base 10 exponential model. The tee itself results in a loss of 6 dBV. Overall, the pipe absorption with water is slightly higher than without it.

Figure 4.8 displays test results from an 80-cm segment of copper pipe from 1 m to 1.8 m with no water in it. The overall features are similar to those of the water-filled copper pipe. Just as with water, there are weaker wavelengths displayed every 2.5 cm as well as the stronger

maxima at 9- to 10-cm separation. The main effect of water appears to be a slight change in the absorption. Using Figure 4.8 as a guide, measurements were made over the entire pipe selecting maximum points based on the Lisajous patterns. Results are shown in Figure 4.9, which is used to estimate an absorption coefficient of 0.00059/cm before the pipe tee and 0.00026/cm after the tee. The tee results in a loss of 4 dBV.

4.1.3 ½-in. PVC Pipe Absorption Measurements

Measurements were made on PVC pipe duplicating those described above. The interferometer approach was used to find maxima for the longer distances. Figure 4.10 shows a 30-cm segment with water in the pipe. The absorption coefficient is estimated to be 0.012/cm and the velocity of sound is 400 m/s.

Figure 4.11 shows an 80-cm segment without water in the pipe. The absorption coefficient is 0.0076/cm, not quite half the absorption of the water-filled PVC pipe. In addition, there appears to be a conversion from 1600-m/s waves to 400-m/s waves over the 80-cm distance.

The PVC pipe measurements with water were drastically different than those without water, and overall, PVC is not as good a transmission medium as the metal pipes at 40 kHz (or at other frequencies). In general, the velocity of sound in PVC is lower than for metal pipes, and a 1600-m/s wave appearing in dry PVC is damped in the water-filled pipe.

Using the same experimental method described for the metal pipes above, the amplification was increased significantly in order to make the measurements, and the “noise floor” was reached at a distance of only 1 m from the transmitter transducer. Of course, longer distances are possible; however, they would require increased transmission power, better coupling to the pipe, and/or electronics having lower noise. The absorption measurements will be useful in determining just what those modifications would need to be.

An alternative strategy would be to inject longitudinal waves from the beginning since the expectation is that these propagate at a higher velocity and with lower absorption. The test arrangement used for the measurements in this section utilized a simple transverse coupling that could be applied anywhere with ease.

4.1.4 Summary of Velocities and Absorption Coefficients

Table 4.1 summarizes the velocities and absorption coefficients measured, and Figure 4.12 displays the same information graphically:

Table 4.1 Summary of sound velocities and absorption coefficients for three pipes, both dry and with water.

Pipe	Velocities observed (m/s)	Absorption coefficient before the pipe tee (/cm)	Absorption coefficient after the pipe tee (/cm)
Galvanized	8000	0.0003 dry 0.0013 water	0.0018 dry 0.004 water
Copper	4000	0.00059 dry 0.00069 water	0.00026 dry 0.00043 water
PVC	400	0.0076 dry 0.012 water	Noise Noise

4.1.5 Air Absorption Measurements

Using the same type of transducers, the absorption of ultrasound in air was measured. Textbook values of 1440 m/s were observed for the sound velocity in air. Figure 4.13 shows the decrease in signal with distance.

At close range, the direct signals between transducers were 90 times greater in air than through copper at the same distance with the same power delivered to the transducer (approximately 0.1 W). Due to the much greater absorption in air, the signal is already weaker in air at 3 m than when transmitted through copper pipe. There are at least two conclusions that may be drawn from this observation. First, nearly 100 times more signal could be injected into a pipe with a suitable arrangement that matches the impedance of an efficient transducer with the impedance of the pipe. Some of the options for achieving this are discussed in other sections of this report. Second, there are clearly situations in which greater distance may be achieved using ordinary piping than might otherwise be achieved using signals in air.

4.2 Transducers Directly Coupled With Water

The previous section describes the transmission of ultrasound through a water pipe using resonant transducers attached to and moved along the outside of the pipe, with and without water in the pipe. In response to an interest by the program monitor, additional tests were performed in order to determine how effectively ultrasound can be directly coupled to the water in a pipe, how well it propagates, and what the absorption of the ultrasound is as a function of distance. These issues were investigated using the experimental arrangement shown in Figure 4.14. As illustrated in this figure, measurements were made using different lengths of galvanized pipe in order to determine the absorption of ultrasound with distance.

When in contact with the water, a major shift in the transducer resonance was observed. The same 40-kHz transducer, designed for use in air, operated with a new, broader resonance of approximately 28 kHz when in direct contact with water. In addition, the direct coupling with the water dramatically improved the efficiency of the transmission. For the same electrical signal at the transmitter transducer, direct water coupling led to an increase in the receiver signal of a factor of 1,000 over that observed when the transducers were coupled to the outside of the pipe.

Tests showed that the absorption coefficients measured with the water-coupled transducers were almost identical to the previously measured coefficients for galvanized pipe with water in it. When the water was removed and the transducers were reconnected as shown in Figure 4.14, the absorption coefficients were determined to be intermediate between the previous measurements for “open” air (no pipe) and the previous measurements for air-filled galvanized pipe (when the transducers were connected to the outside of the pipe). One could easily draw the conclusion that the efficiency of the transducers is improved by water coupling or that the coupling of the transducers to the pipe/water system is improved. It appears that the actual mode of transmission had not changed, other than the likelihood of launching longitudinal waves directly down the pipe rather than launching transverse waves that are continually changing to longitudinal waves during propagation. Additional tests were then performed to improve our understanding of this experiment.

Holding the pipe securely with one hand while transmitting ultrasonically down the length of pipe resulted in an approximate 50% reduction in the signal strength provided at the receiver. Foam pieces were then placed down the water-filled pipe (Figure 4.14) in such a way as to block the ultrasonic transmission path through the water. The signal strength did not decrease at the detector; rather, the signal strength increased slightly. The same thickness of foam was then cut in a circular shape with a circular hole in the middle the size of the pipe opening. This foam washer was placed between the receiver transducer and the ball valve. This de-coupling of the transducer from the pipe wall resulted in a signal approximately 50 times weaker than without the washer, even though the water path to the transducer had not changed. The receiver transducer was once again removed and a second foam piece was inserted in such a way as to fill the center hole in the first foam piece. This further reduced the received signal by a factor of 2. It is noted that the foam washer and plug were both approximately 0.25 cm thick, much smaller than a wavelength of sound in any of the materials used.

A significant conclusion that one may draw from the discussion above is that signals should be measurable above noise over a distance of greater than 63 m (200 ft). In fact, computer files were transferred using the demonstration equipment over a distance of 8 m (24 ft) through a water-filled galvanized pipe using transducers directly coupled with the water. This distance was limited only by the major diagonal length available in the laboratory. It is likely that computer files could be transferred at much greater distances through water pipes using this technique.

Also illustrated in Figure 4.14 is a variable-length pipe configuration that was constructed to allow the length of the pipe to be continuously adjusted up to 37 cm. With this arrangement, the pipe length and thus the distance between the ultrasonic transducers could be adjusted in small increments so that absorption measurements could be made with water-coupled transducers at integral wavelengths of the transmitted ultrasound.

Using this adjustable pipe, it was immediately apparent that the strength of the received signal had dropped several orders of magnitude from the previous measurements without the adjustable PVC, thus requiring signal amplification to make measurements with this pipe configuration. This is further evidence that the signal is being carried by the pipe/water system, and not by the water alone, since the overall distance to the transmitter had not significantly changed.

The wavelength measured in the variable length pipe was 6.2 cm, and the absorption coefficient derived from the absorption measurements was 0.014/cm, a little greater than previously measured for PVC pipe with water in it. The wavelength of 6.2 cm, coupled with the frequency of 28.5 kHz, yields a sound velocity of 1770 m/s, not significantly higher than previously measured in PVC pipe over short distances.

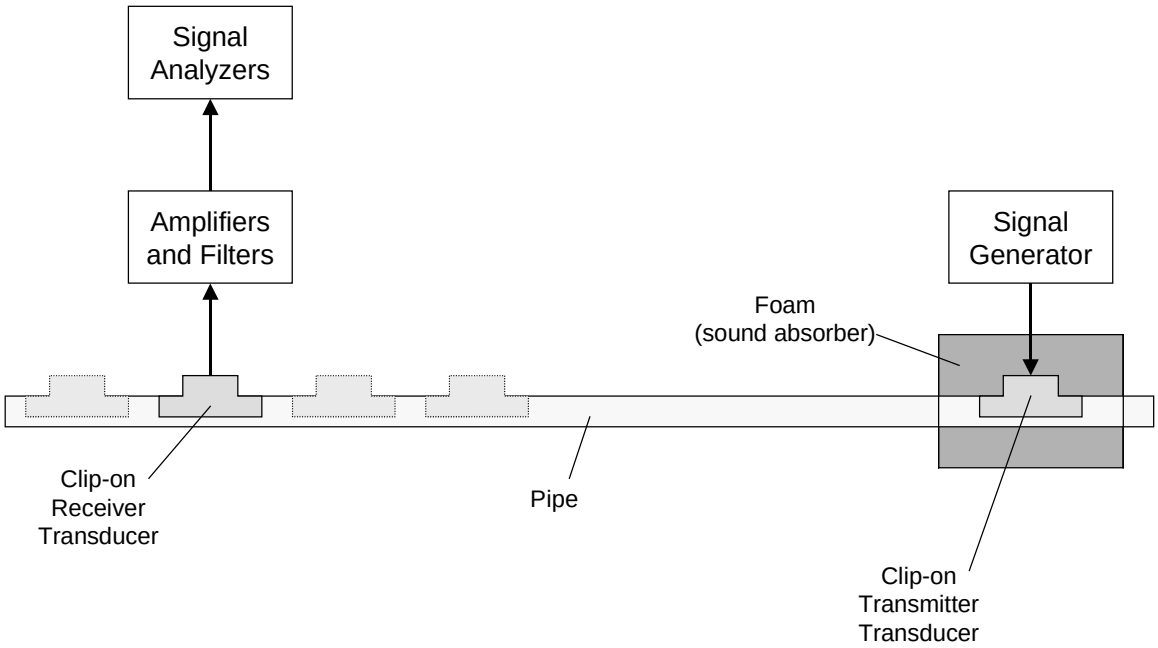

Figure 4.1 Experimental arrangement for pipe absorption measurements.

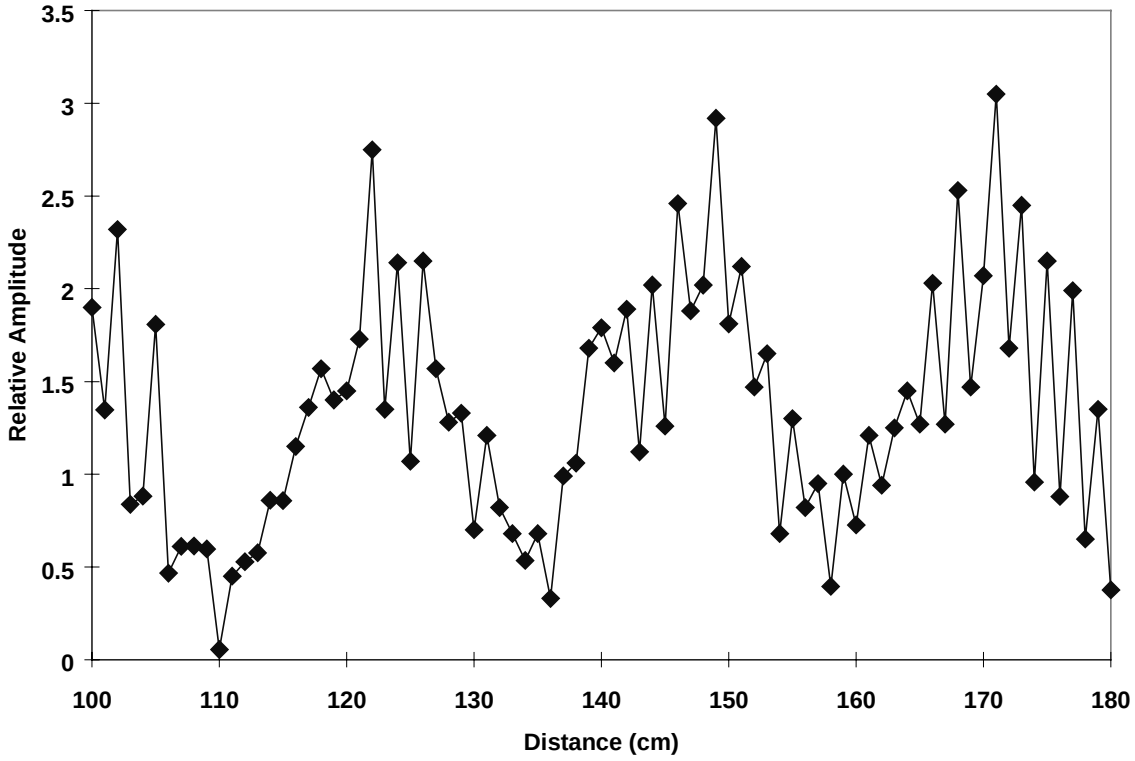

Figure 4.2 Absorption measurements (every centimeter) over an 80-cm distance for a galvanized pipe filled with water.

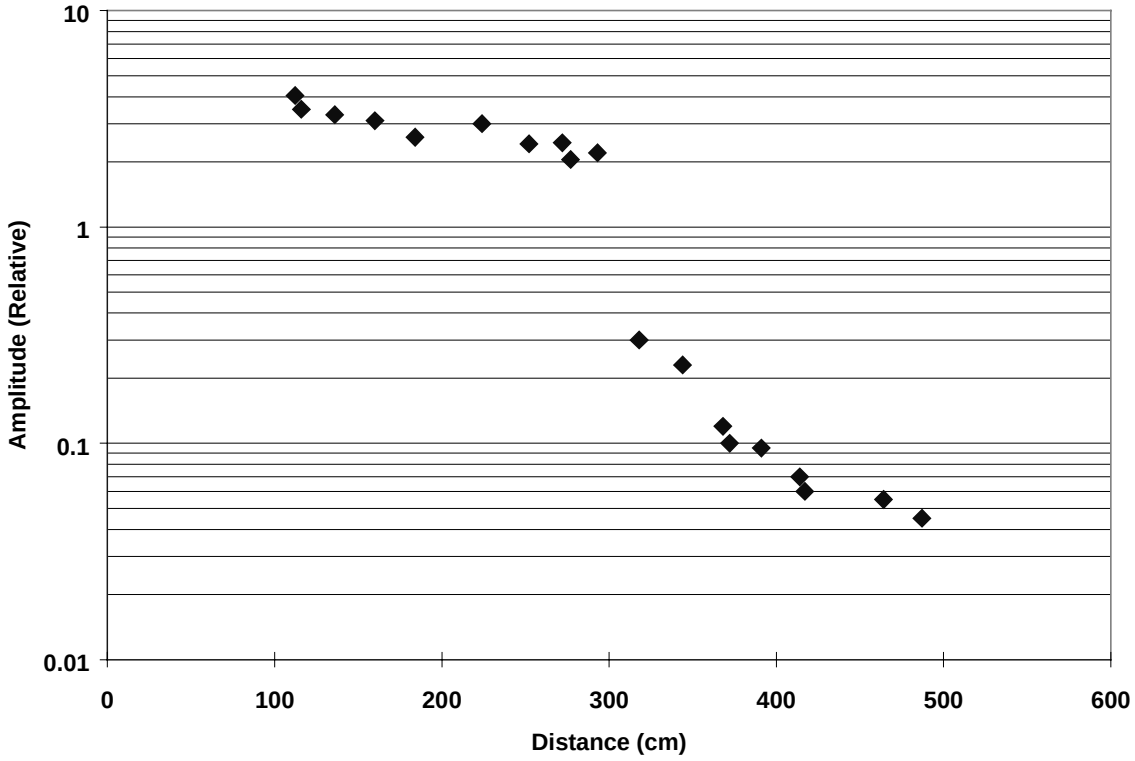

Figure 4.3 Absorption measurements (maxima only) over a 400-cm distance for a galvanized pipe filled with water.

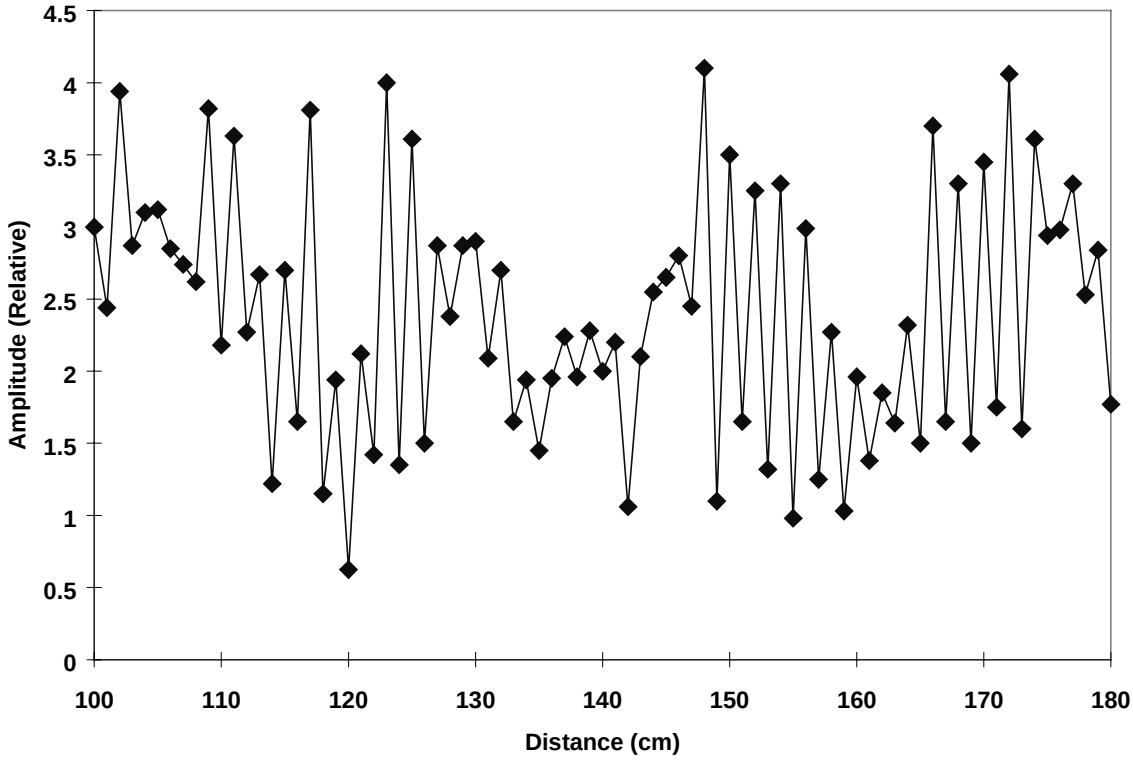

Figure 4.4 Absorption measurements (every centimeter) over an 80-cm distance for a dry galvanized pipe.

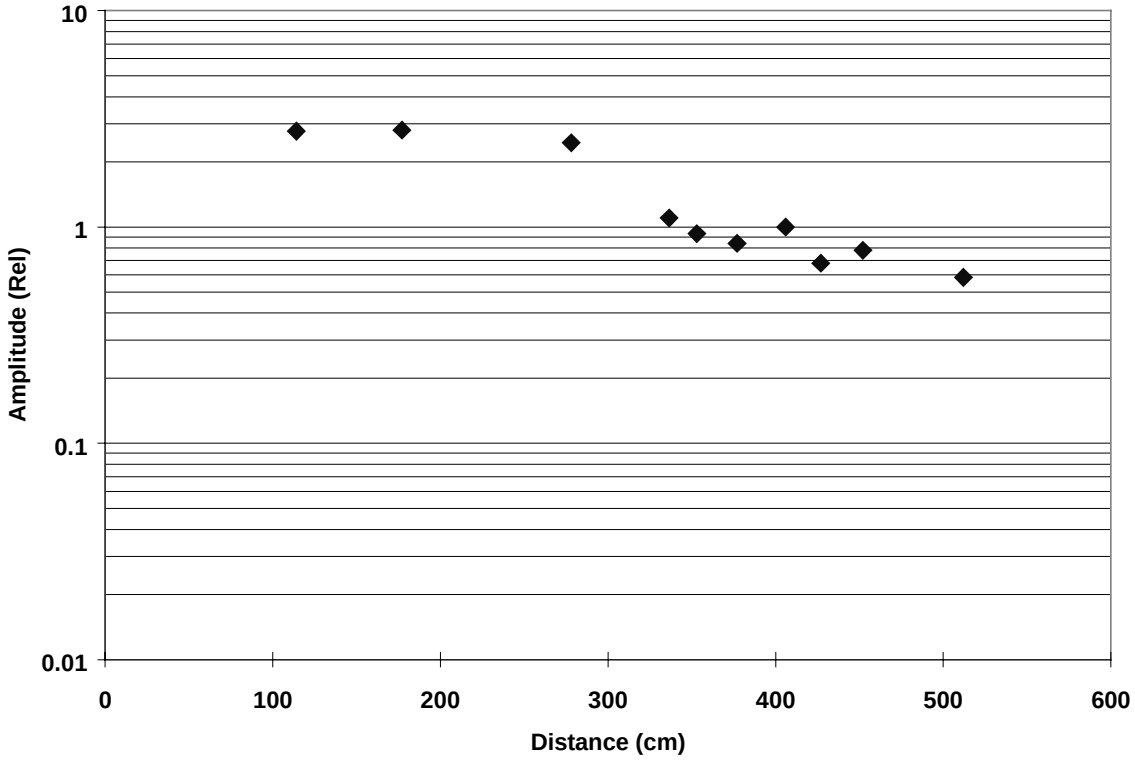

Figure 4.5 Absorption measurements (maxima only) over a 400-cm distance for a dry galvanized pipe.

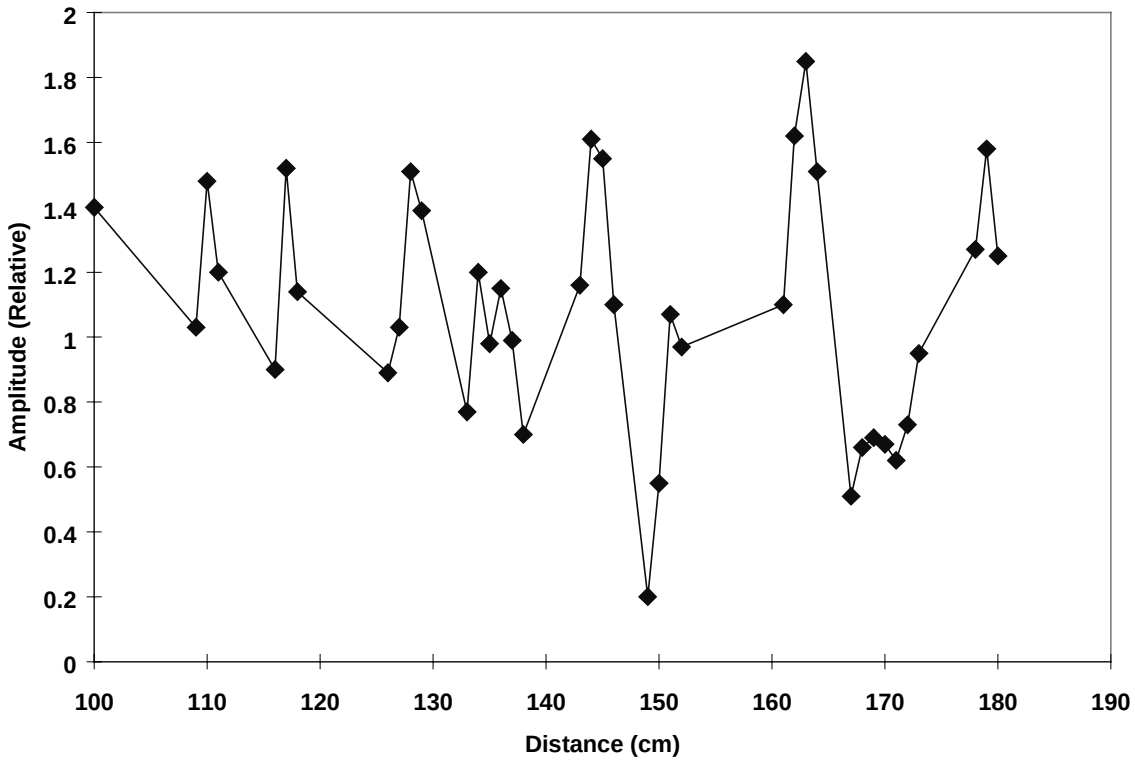

Figure 4.6 Absorption measurements (every centimeter) over an 80-cm distance for a copper pipe filled with water.

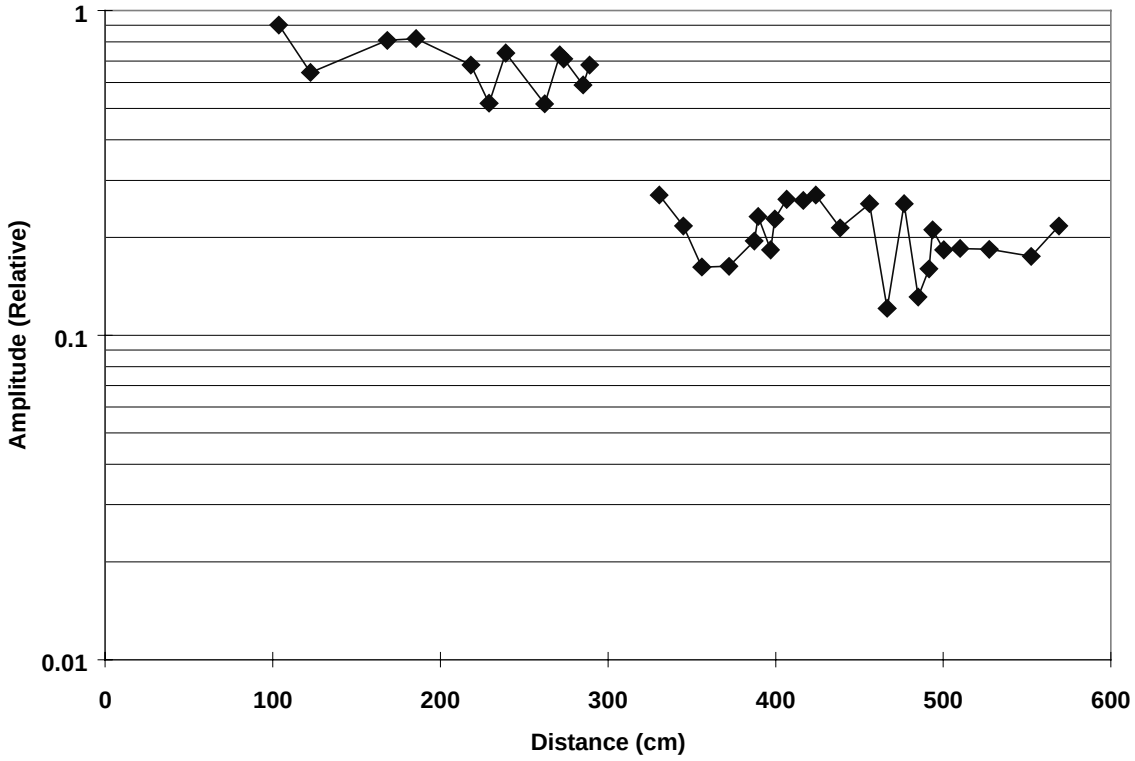

Figure 4.7 Absorption measurements (maxima only) over a 480-cm distance for a copper pipe filled with water.

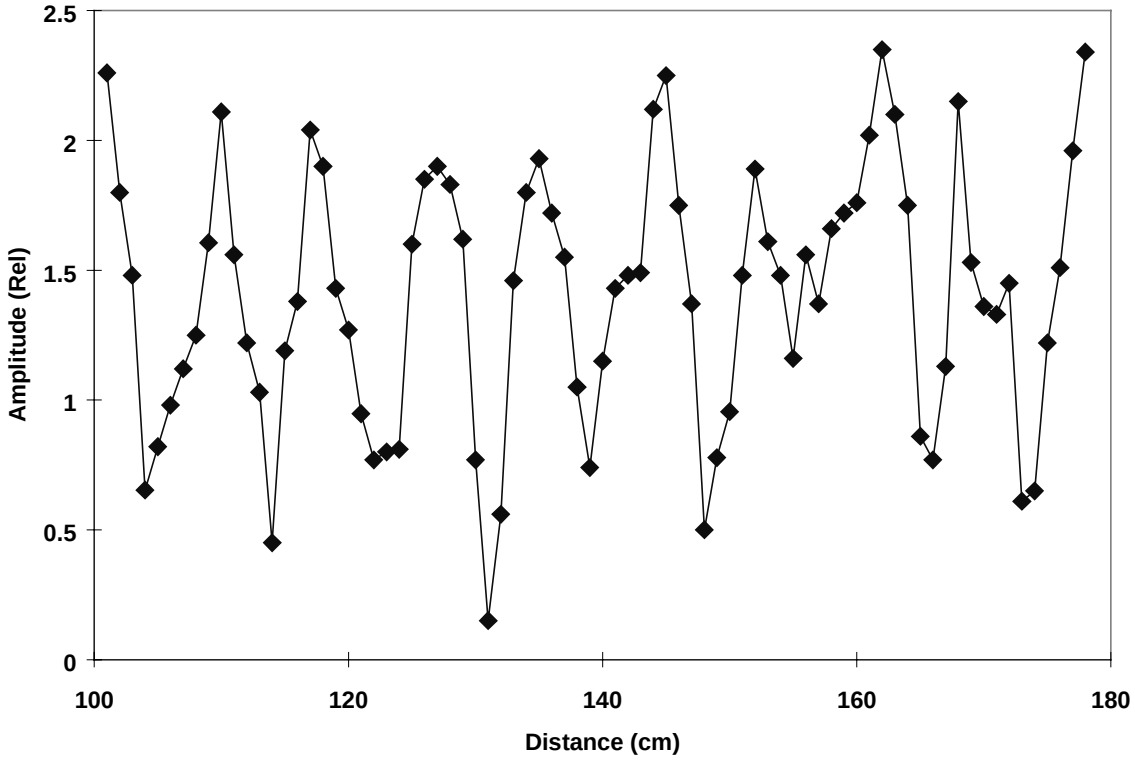

Figure 4.8 Absorption measurements (every centimeter) over an 80-cm distance for a dry copper pipe.

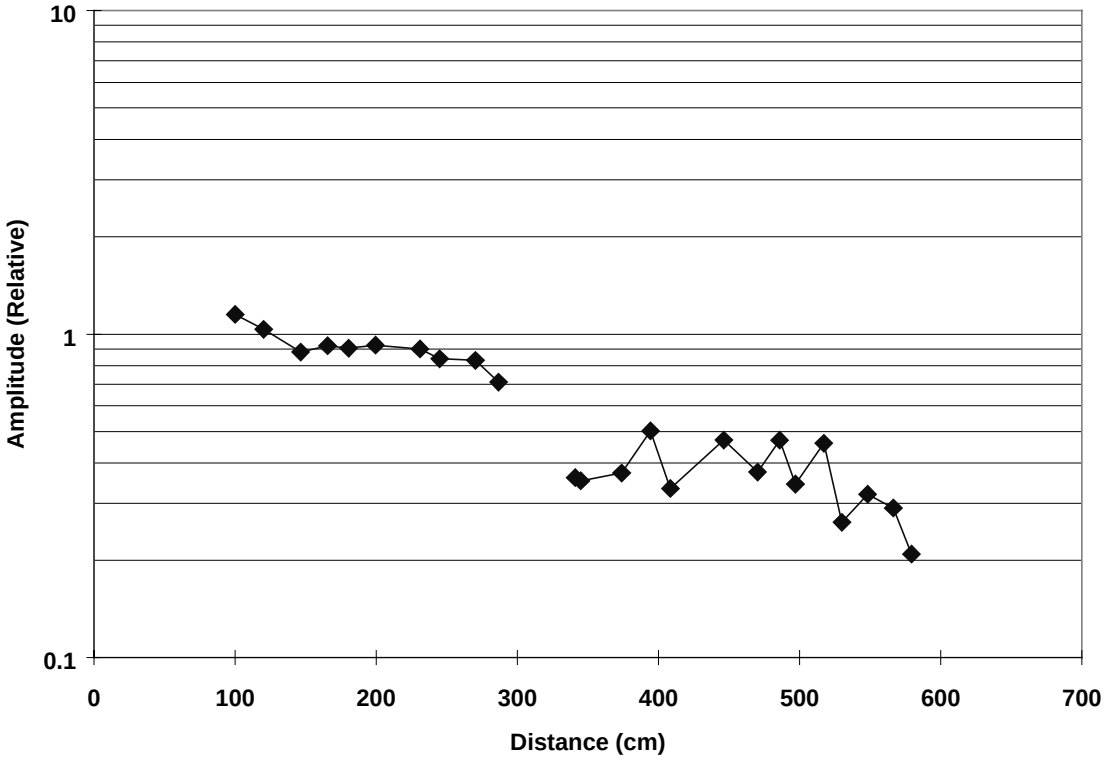

Figure 4.9 Absorption measurements (maxima only) over a 480-cm distance for a dry copper pipe.

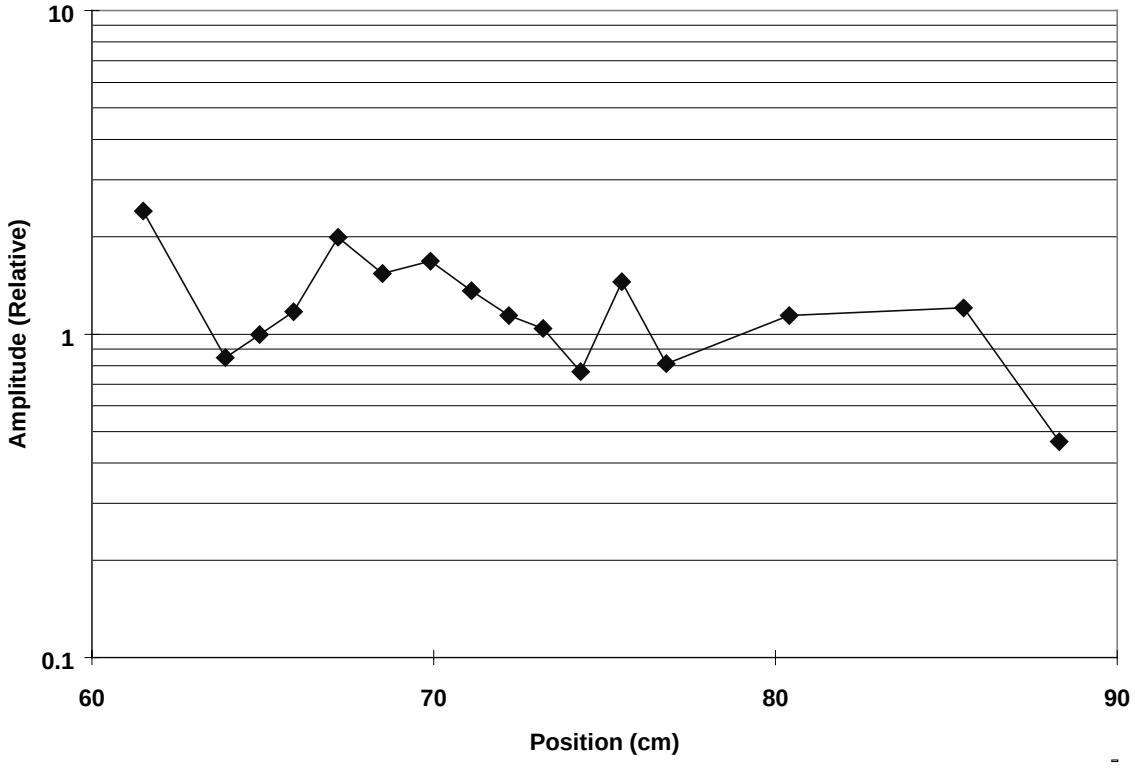

Figure 4.10 Absorption measurements over a 30-cm distance for a PVC pipe filled with water.

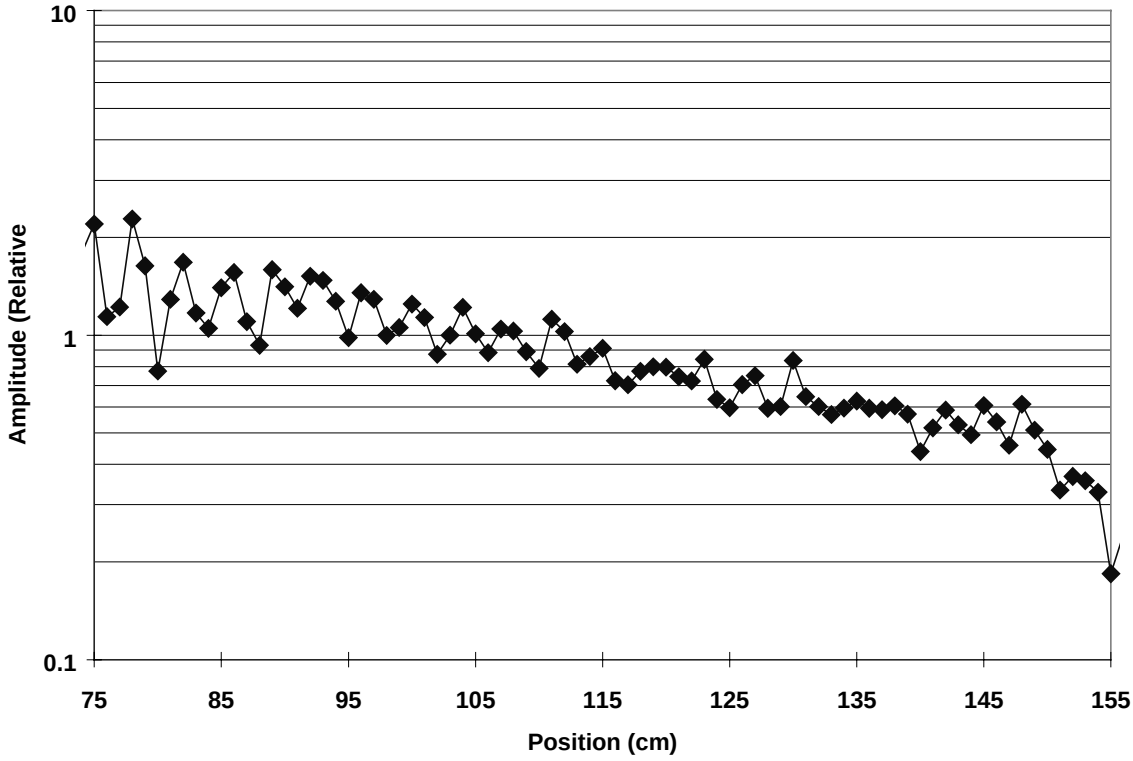

Figure 4.11 Absorption measurements (every centimeter) over an 80-cm distance for a dry PVC pipe.

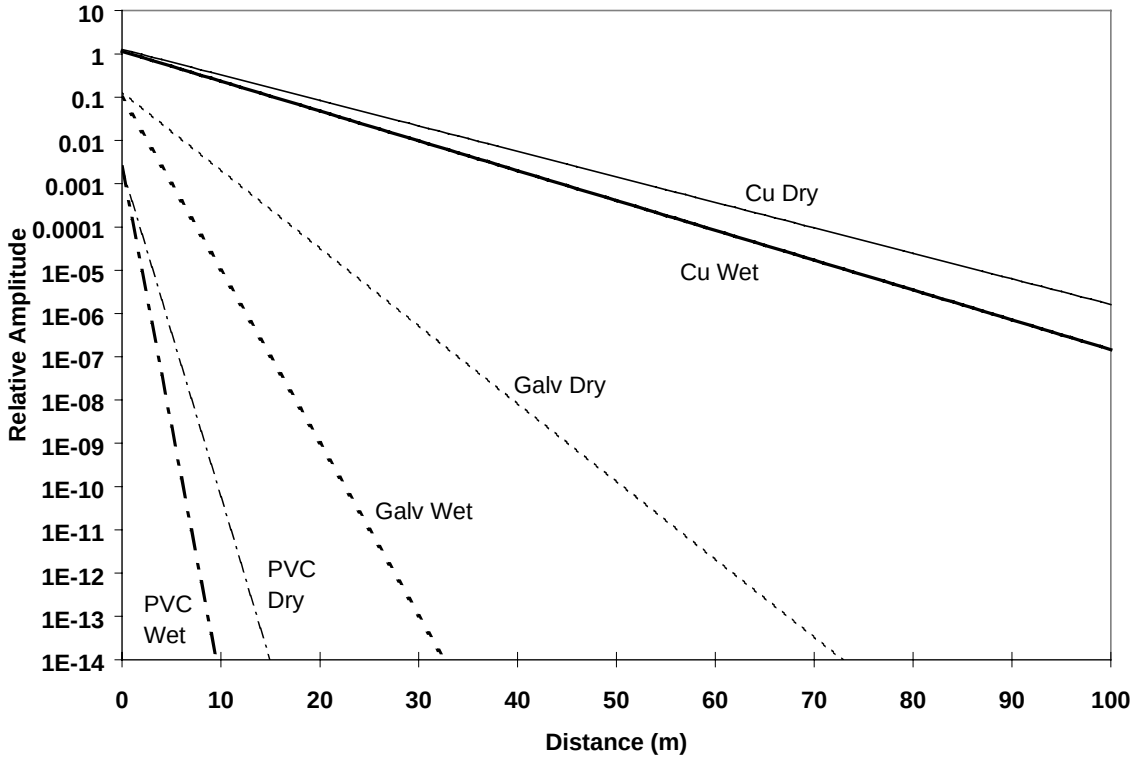

Figure 4.12 Summary of absorption for all pipes measured. In all cases, absorption with water was greater than absorption in a dry pipe.

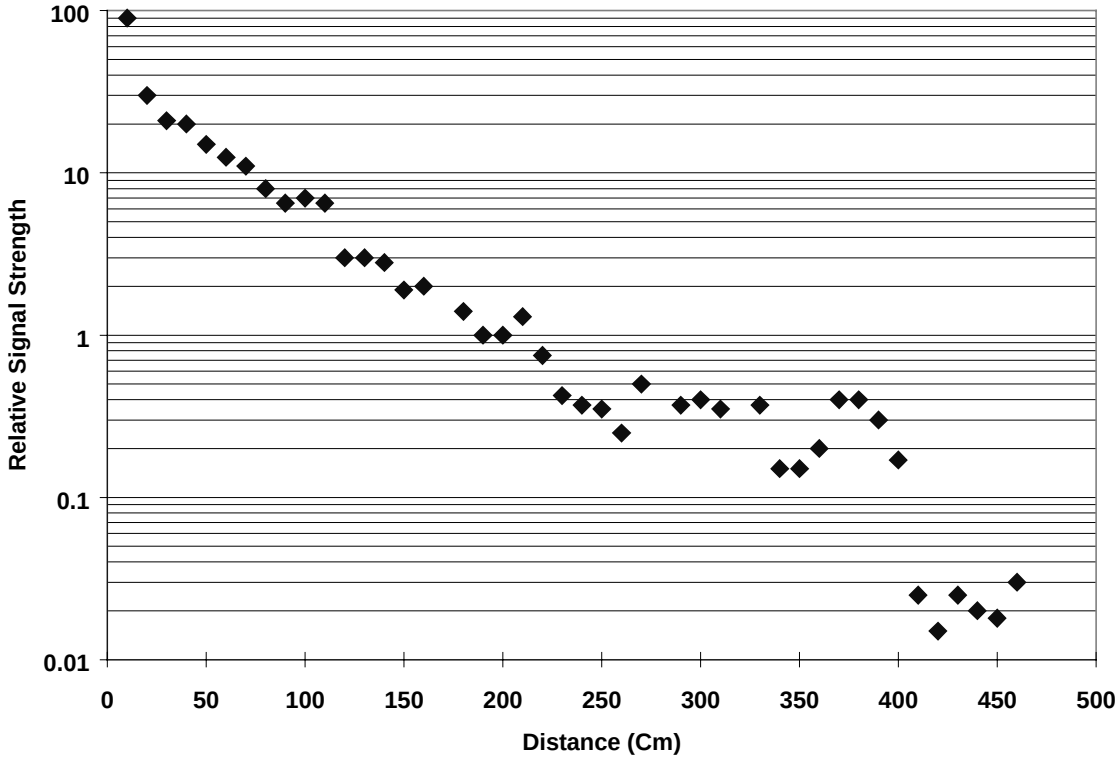

Figure 4.13 Absorption measurements over a 450-cm distance through air.

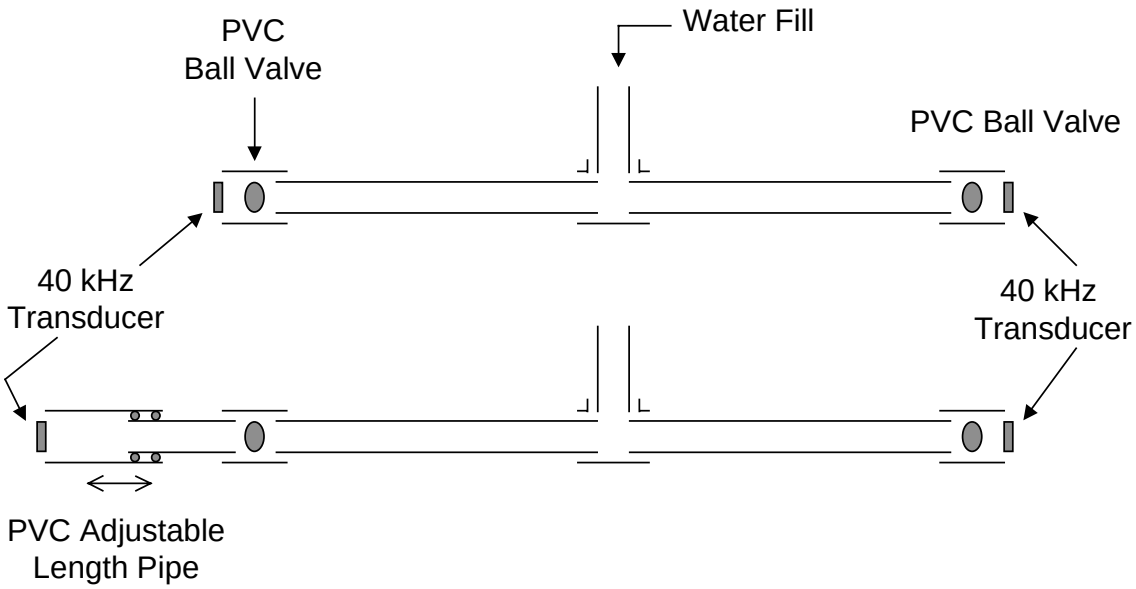

Figure 4.14 Methods used to investigate the transmission of ultrasound through a water-filled pipe. In both the fixed-length pipe (top configuration) and the adjustable-length pipe (bottom configuration), the ultrasound transducers are directly coupled with the water.

5. Methods of Generating Ultrasound

5.1 Piezoelectric Transducers

Throughout this project, commercially available piezoelectric transducers were utilized in systems that were developed to demonstrate ultrasonic communication methods. This section of the report is intended to provide background information about those transducers and other methods that could be used to generate and detect ultrasound.

Ultrasonic transducers are often fabricated from piezoelectric materials because of the capabilities of these materials for converting mechanical motion into an electrical signal and vice versa. This conversion occurs because mechanical motion induces stress in the material that is then converted by the material into an electrical signal. The reverse is equally true—an electrical signal imposed across a piezoelectric material results in an induced strain and motion. The motion is usually small, but, if applied repetitively, the motion is sufficient to produce periodic sound pressure in the audible or ultrasonic ranges. This effect is commonly used to produce and detect ultrasound, and many piezoelectric ultrasonic transducers are commercially available. Ultrasonic transducers are often designed to emphasize a particular characteristic, such as efficiency or bandwidth. Unfortunately, transducers having high efficiency are usually designed to operate at a resonant condition and are therefore limited to a small frequency range. Conversely, transducers designed for wide bandwidth response are usually much less sensitive than resonant transducers.

Several materials exhibit piezoelectric characteristics. Some of these materials are identified in Table 5.1 along with their calculated electrical-to-mechanical conversion efficiency.

Table 5.1 Piezoelectric materials and conversion efficiencies.[1]

Material	Conversion efficiency (%)
Quartz	0.01
ADP	0.7
BaTiO3	4.0
PZT#5 (Lead Zirconate-Lead Titanate Mixture)	20.0

For comparison, the efficiencies of converting electrical energy to ultrasound for three commercially available piezoelectric transducers were estimated to be 0.8%, 0.11%, and 0.2%, with the later employed in an ultrasonic communication system that was developed for demonstration purposes. A transducer designed to move air for cooling was also studied. The power equivalent of the moving air was divided by the electrical power applied to the unit, and an efficiency of 6% was derived.

[1] Data from the American Institute of Physics Handbook, Kingsport Press, 1972.

These examples show that piezoelectric transducers leave room for potential improvements in performance. Conversion efficiencies for piezoelectric crystals have been reported to be as high as 60%; [2, 3] however, these efficiencies are not observed in the final commercial products.

One application investigated during this project was the transmission of ultrasound through small diameter (<3-in.) pipe. To achieve maximum efficiency of transmission, it was desired to utilize a transducer that generated and "launched" ultrasound in the proper direction, that is, "longitudinally" down the pipe. Since a transducer for this purpose was not commercially available, one was constructed. The transducer utilized a commercially available piezoelectric ceramic element that resonates at 220 kHz. The resonator was extracted from its commercial packaging and remounted as shown in Figure 5.1. The resulting transducer was able to generate ultrasound in the frequencies of interest (20 to 80 kHz); however, the efficiency of this transducer was very low (due to operating off-resonance), which limited its ultrasound output.

5.2 Impedance Matching

An important element of ultrasound generation is impedance matching at two key locations: the interface between the electronic circuit and the transducer and the interface between the transducer and the transmission medium. Improvements in these areas can significantly impact the efficiency and thus the performance of an ultrasonic communication system..

For electronic impedance matching, consider an electrical transmission line with insignificant resistance and distributed elements of inductance and capacitance:

$$Z = \sqrt{\frac{L}{C}}$$

where Z = impedance, L = inductance, and C = capacitance.

Three conditions can result at the end of the transmission line. A short results in a wave of equal and opposite polarity at the short. An impedance equal to that of the transmission line absorbs a wave completely with no transmission or reflection. An open circuit results in the voltage being double at the end and the current zero. Each of these conditions has an analogous effect in sound.

In understanding sound equivalents, it is useful to make use of analogies with electrical terms:

Electrical Term	Sound Term
Voltage	Pressure
Current	Particle Speed
Inductance/unit length	Density
Capacitance/unit length	Inverse bulk modulus of elasticity

If a sound wave is generated in one medium and then comes in contact with a material differing in density and sound speed, then the wave will be partially reflected at the border.

---

[2] Prof. Michael Goldfarb, Vanderbilt University for Intelligent Mechatronics. Personal conversation (1999).

[3] Kornbluh, R., et al., "Electrostrictive Polymer Artificial Muscle Actuators," Proceedings of the 1998 IEEE International Conference on Robotics and Automation, Belgium (1998).

For ultrasound impedance matching,

$$Z = (\rho)(c)$$

where Z = impedance, ρ = density, and c = the velocity of sound, all in the medium the wave is traveling through. Another useful expression is

$$c = \sqrt{\frac{E}{\rho}}$$

where E is the bulk elastic modulus of the medium, or in the case of a solid, E is the modulus of elasticity. As shown in Table 5.2, the values for c, E, and ρ will be greatly different for typical media of interest in this project—air, water, and iron.

Table 5.2 Density, speed of sound, and impedance values for different media of interest.

Medium	ρ **(**$\frac{kg}{m^3}$**)**	**c (**$\frac{m}{s}$**)**	**Impedance (**$\frac{kg}{(m^2)(s)}$**)**
Air	1.29	331	427
Water	1000	1450	1450000
Iron	7600	5130	39000000
PZT Transducer	7500	3120	24000000

From the table, one can see that using the same transducer for each of these media would result in large losses for two out of the three, assuming that at least one was impedance-matched.

Another useful characteristic of a sound wave is its wavelength:

$$\lambda = \frac{c}{\nu}$$

where λ = wavelength, c = speed of sound, and ν = the frequency of the sound. These values are different for different media, as illustrated by Table 5.3.

Table 5.3 Wavelength of 25-kHz ultrasound in different media.

Material	c ($\frac{m}{s}$)	Wavelength (mm)
Air	331	13
Water	1450	58
Iron	5130	205
PZT Transducer	3120	125

Often the thickness of an impedance-matching material may be determined in terms of wavelengths of the sound to be transmitted or reflected. More specifically, an impedance matching interface layer may be fashioned from a material that is 1/4 wavelength thick and having an impedance of $\sqrt{(Z_1)(Z_2)}$, where Z_1 and Z_2 are the impedances of the two materials to be coupled by the impedance-matching material.

Based on Table 5.2, if one were transferring ultrasound from air to water, one would fashion an impedance-matching layer from a material having an impedance of

$$\sqrt{(427)(1450000)} = 24900 \frac{kg}{(m^2)(s)}$$

and 1/4 wavelength thick for the interface material. This could be achieved by finding the ideal interface material or, better yet, by fashioning a suitable material by altering the density of an otherwise acceptable choice and by keeping voids small compared to the wavelength of sound in the material. To continue the example, if tallow is used as the impedance-matching material, the following values can be used:

$$\text{Density} = 0.9 \frac{g}{cm^3}$$

$$\text{Velocity of sound} = 390 \frac{m}{s}$$

$$\text{Impedance} = 35000 \frac{kg}{(m^2)(s)}$$

The impedance of tallow can be seen to be close to the ideal impedance of $24900 \frac{kg}{(m^2)(s)}$. A thickness of 1/4 wavelength would then be

$$(0.25) \frac{390 \, m/s}{25000 Hz} = 3.9 \; mm$$

An impedance-matching interface designed in this manner can also provide beneficial filtering by rejecting frequencies outside the band of interest.

5.3 Alternative Transducers

Alternative methods were identified that might provide means of creating or detecting ultrasound efficiently within the frequencies of interest.

For ultrasound coupling to pipes,

- use a surface acoustic wave generator mounting (a means of making the equivalent of a multi-beam antenna in radio),
- lock a longitudinal bar transducer to the pipe (or use a cylindrical longitudinal transducer), or
- place a water-matched transducer directly in contact with the water at the faucet.

For ultrasound coupling in air, use compressed air with electrical actuation and or modulation:

- Variants include a whistle or other vortex shedding orifice.
- Other variations include Hartmann generator, jet-edge generator, siren generator, and a resonant capacitor with one surface moveable.

For ultrasonic coupling through water, use a water pump with electrical actuation and/or modulation, similar to air above.

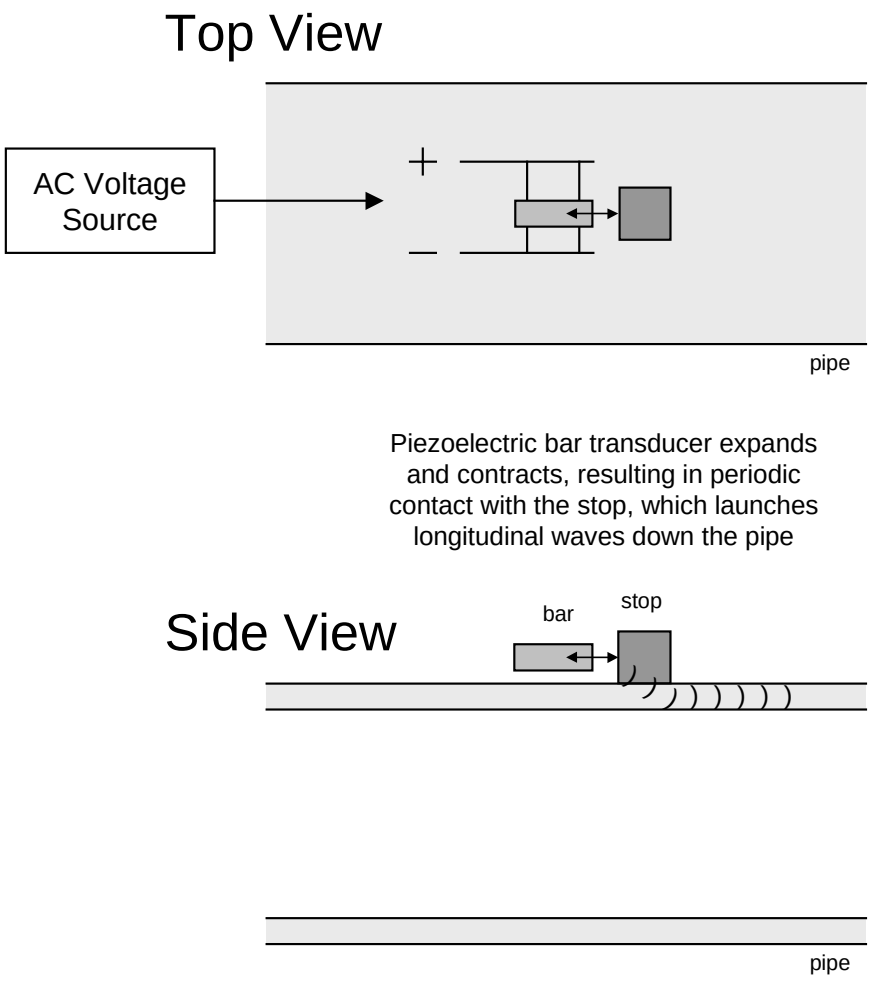

Figure 5.1 Method of generating ultrasonic longitudinal waves in a pipe.

6. Ultrasonic Communication System Considerations

6.1 Amplifier Considerations

Noise generated in a cable located between an ultrasonic transducer and the first signal amplifier may be minimized by placing a preamplifier close to the detector. Second, the preamplifier should be a low-noise amplifier with noise levels less than the noise expected in the signal. Third, attention should be paid to the impedance of the detector, and, while exact matching is not required, a low-impedance amplifier should not be used with a high-impedance detector.

Most, if not all, piezoelectric based detectors are high impedance. A further consideration is the signal-to-noise ratio, since for a particular detector/transducer there will be a baseline noise that no preamplifier will improve on. For the MASSA 89 series ultrasonic transducer used in most experiments, this noise floor is specified at $17nV/\sqrt{Hz}$. At a minimum, one should use amplifiers with input noise voltage at or below this value, with the understanding that the transducer itself sets the lower limit.

While operational amplifiers in general are considered high-impedance components, a number of them are not only high impedance, but also low noise, while providing more than adequate response in the ultrasound range. The BIFET, JFET, or MOSFET front end of modern operational amplifiers (op amps) guarantees high impedance—10^{12} Ω for instance, far higher than the typical 1,000–10,000 Ω impedance of an ultrasound transducer.

Three op amps were evaluated for their low-noise characteristics: the RCA CA3140E, the Texas Instruments TL071, and the Analog Devices AD795. Rather than redevelop the mechanism by which such a noise floor is measured, it was decided to do a simple comparison of these amplifiers with the same ultrasonic transducer, the same electrical hook-up, the same load resistance, the same gain, etc., but only vary the front-end op amp. Since the transducer is an electrical component, essentially a capacitor, one would expect a baseline noise floor at a given frequency below which no improvement in amplifier or hook-up will allow improvement.

Using the arrangement shown in Figure 6.1 and with no signal applied to the ultrasonic transducer other than room ambient noise, the noise associated with each of the three op amps was measured over a 100-kHz band (Figure 6.2). Each of the op amps was seen to possess low-noise characteristics; however, it can be seen that there is a noticeable advantage in baseline noise associated with matching components in a practical test.

The CA3140E is a good low-noise choice based on the discussion above. The TL071 provides a lower noise floor and is in the price range of the CA3140E. The AD795 is 10 times more expensive than the others, but also yields the lowest noise floor of the three op amps tested.

Figure 6.3 shows a back-to-back comparison between the best operational amplifier from the previous figure (AD795) and a high-quality, commercially acquired, laboratory-grade amplifier. In the frequency range of interest to this project, the ORNL-built, AD795-based amplifier is the clear winner by 12 dB, allowing a signal 15 times smaller to be observed at the low signal limit.

Although this work was performed to enhance the ability to make absorption measurements on pipes with low signal and low noise, the implication is that use of the lowest noise amplifier can permit longer distance ultrasonic communication in a practical system.

6.2 Voltage-Controlled Oscillator Considerations

Most ultrasound transducers are based on the piezoelectric effect and are high-impedance, low-current devices. This should be taken into consideration when designing transmitter drivers as well as receiver preamplifiers. As part of this project, several transmitter driver circuits were designed, built, and evaluated. These circuits were used for ultrasonic absorption measurements and as part of the demonstration communication system.

An initial transmitter was constructed using the NE/SE566, a commercially available VCO. The NE/SE566 provides both square and triangle waveform outputs. To interface the NE/SE566 VCO to the computer VI, a differential amplifier is used to convert the 0- to 10-V, dc control voltage from the computer into a smaller voltage range required to establish the correct NE/SE566 output frequency. The output of the NE/SE566 is then fed to a CD4093 Quad two-input NAND Schmitt trigger. Although the CD4093 contains four complete and independent Schmitt Triggers, the circuits described in this report never use more than two.

With the two inputs of the CD4093 connected (jumpered), the CD4093 acts as an inverter with a high-impedance output at the full power supply voltage (in this case 12 V dc). Another interesting feature of the CD4093 is that it could be used with suitable input logic to allow rapid shifting of the phase by 180 degrees, which could be useful in a binary digital signal transmission arrangement.

The linearity of the NE/SE566-based transmitter circuit (shown in block diagram format in Figure 6.4) was tested by connecting the transmitter output to an ultrasonic transducer and then monitoring the output frequency with a spectrum analyzer as the voltage was varied over the control range. The ultrasonic transducer used was a MASSA Model TR-89/B series, type 31 ultrasound transducer that was resonant at 31 kHz. Figure 6.5 shows that the NE/SE566 provides very good short-term linearity over a relatively wide frequency range (in this case from 26 to 40 kHz). Figure 6.6 shows the NE/SE566 output frequency as a function of control voltage over a smaller range, again with the ultrasonic transducer attached. There is a slight deviation from linearity as the output frequency passes through the transducer's resonance.

In addition to linearity, frequency stability was tested. For the frequency range of interest, it was discovered there can be considerable drifting in the output frequency (up to 100 Hz in 1 h) that is apparently due to temperature variations in the NE/SE566. This undesirable drifting led to the evaluation of other transmitter circuits that are described below.

A Schmitt trigger can also function as a VCO if wired as shown in Figure 6.7. The Schmitt trigger is accompanied with a resistor/capacitor network causing it to oscillate when an input control voltage is applied. The voltage supplied from the differential amplifier controls the frequency within a range set by the resistor/capacitor network. Another function of the resistor/capacitor network is to set the duty cycle of the output waveform. A second Schmitt trigger is then used to shape the output pulses from the first and to ensure that the full supply voltage is utilized to drive the ultrasonic transducer, regardless of frequency.

Figure 6.8 shows the linearity of the Schmitt trigger-based VCO without the ultrasonic transducer attached. It can be seen that the linearity is poor over a large frequency range. Figure 6.9 shows, however, that linearity over a small range can be good. Figure 6.10 shows that after attaching the ultrasonic transducer there is a significant deviation from linearity as the

frequency passes through the transducer resonance. Since a linear frequency response was desired, this transmitter design was not pursued.

One of the most common and least-expensive ICs on the market is the LM555 timer. A LM555CN (8-pin, dual inline package) version was evaluated as a potential VCO for ultrasonic communication. The LM555CN was integrated with the differential amplifier (computer interface), Schmitt trigger (pulse shaping), and ultrasonic transducer (Figure 6.11). The LM555CN-based transmitter was seen to exhibit superior frequency drift characteristics (only 10-Hz drift over 12 h) compared to the NE/SE566 (100-Hz drift over 1 h). Figure 6.12 illustrates that the LM555CN is also highly linear as a VCO. As shown in Figure 6.12, the LM555CN output frequency decreases with an increase in voltage, which is an opposite relationship from that provided by the other VCO circuits that were tested.

Figures 6.13 through 6.16 provide VCO frequency drift information by presenting the results of several “peak-hold” spectral acquisitions. The peak-hold process retains the peak amplitude of all frequencies during the time the data are being acquired. For comparison, Figures 6.13 and 6.14 show the small (about 4-Hz) frequency drift of the LM555CN-based VCO and the considerably larger (about 150-Hz) frequency drift of the NE/SE566-based VCO over a 5-min time span. Another interesting difference between the two VCO types is that the LM555CN is considerably less noisy (about 20 dBV less) than the NE/SE566. The frequency stability of the LM555CN is further characterized by Figures 6.15 and 6.16, which show the relatively insignificant frequency drift that occurs over a 5-s and 5-min time spans, respectively, after the LM555CN circuit had warmed up for 1 h. The frequency drift and noise characteristics of the NE/SE566 were examined on a second circuit that exhibited nearly identical characteristics to the first NE/SE566 circuit.

Finally, initial investigations were performed using the LM555CN as a means of controlling the pulse width or phase of an ultrasonic signal via a control voltage. Further study of variable-frequency shifting techniques for communication revealed that these frequency shifts resulted in shifts in waveform phase, as well as shifts in the position of nulls and peaks at the receiver site. One way to use this knowledge to advantage is to use a direct frequency sensitive detection (F-to-V converter) rather than a method that is overly sensitive to phase PLL. Possible alternative transmitting methods include: pulse width modulation (PWM), pulse position modulation (PPM), and phase modulation (PM). These promising methods have been initially investigated, and their development is highly recommended as part of a proposed follow-on project.

6.3 Speed Considerations

There are practical limitations as to how fast messages and computer files can be sent with the ultrasonic methods described in this report. The speed that information can be transmitted is influenced by many factors, including

- ultrasound carrier frequency,
- transducer characteristics (response time, “ringing,” etc.),
- electronic circuit characteristics (e.g., response characteristics of amplifiers, filters, F-to-V converters, etc.),

- VI settings (bit transfer rate; time duration of trigger signal, “wait” states, and calibration sequence; data averaging parameters), and

- computer characteristics (processor speed, RAM level, etc.).

Several of these factors (e.g., signal filtering, computer bit transfer rate, and data averaging parameters) are typically adjusted to compensate for transducer response deficiencies and weak or noisy signals.

Figure 6.17 illustrates one of these factors—transducer response time. As shown in the figure, a step change in magnitude of an electrical signal produces a delayed “ramp” response when converted to ultrasound and then back to an electrical signal. Since an ultrasonic transducer is an electromechanical device, this response characteristic is expected and understood.

Figures 6.18, 6.19, and 6.20 illustrate a “staircase” waveform that results from changing the frequency of the transmitted ultrasonic signal in steps. Figure 6.18 shows what happens if the speed of transmission is too high. The steps are smeared and otherwise distorted, making their interpretation difficult. The bottom few steps are further contaminated by transducer ringing. Figure 6.19 shows the beneficial effects of lowering the transmission speed. The steps are now much easier to see, thus improving the clarity of the transmitted information. Significant transducer ringing is still evident in the bottom few steps. Figure 6.20 demonstrates that by decreasing the transmission speed further and utilizing a low-pass filter the staircase waveform has been “cleaned up” significantly. Information, including computer files, may now be reliably transmitted using these speed and filter settings.

6.4 Distance Considerations

This project has focused on the identification and development of methods for ultrasonic communication that utilize digital signal processing and that are capable of being used in multiple media (including air, liquids, and solids). Particular attention has been directed at transmission of typed messages and computer files through air and water pipes. These methods can be used for relatively short-range communication (e.g., less than 100 ft) and for extended distances as well. The distance over which ultrasound can be transmitted is influenced by many factors, including

- power level of transmitting system,

- efficiency of transmitter and receiver transducers,

- efficiency of coupling between the transducers and the media (impedance matching),

- amplification (gain) and noise rejection characteristics of electronics and receiver data acquisition system, and

- media ambient noise level.

This report has described several of these factors (transducer efficiency, impedance matching, and amplifier noise characteristics). Transmitter power level and media ambient noise level have not been extensively addressed during this Phase 1 project but would be determined based on the specific application (scenario) where ultrasonic communication is to be employed.

6.5 Triggering and Handshaking Considerations

The final system developed for demonstration purposes utilizes an ultrasonic triggering technique to initiate the information transfer and to coordinate the transfer of data blocks in a sequential manner so that large computer files can be transmitted. As long as more than one data block is to be sent from the transmitter station to the receiver station, some form of "handshaking" is required. This is accomplished in the final demonstration system by momentarily utilizing the receiver station as a transmitter and the transmitter station as a receiver. A separate pair of ultrasonic transducers is used to transmit and receive the trigger signal. The trigger signal transducers operate at a resonant frequency that is outside of the resonant response range of the communication signal transducers. The coordination of the transmit and receive modes of each station is controlled by computer VIs.

6.6 Noise Filtering and Error Checking Considerations

In the final demonstration system, extraneous noise is filtered via both analog and digital means. Analog filtering is accomplished by high-pass filtering of the raw received signal (to filter acoustic noise sensed by the transducer) and by low-pass filtering of the signal after the analog F-to-V conversion. The signal is then acquired (over-sampled) by the computer and averaged by a "smart" scheme that breaks down the acquired signal into individual steps, and ignores data that may be contaminated by transducer "ringing." The averaged data are then converted back into the bits and characters that constitute the transmitted message or computer file.

The development of error checking methods, while clearly beyond the scope of this Phase 1 project, would be required for absolute 100% accuracy of transmission, especially in relatively noisy environments as are likely to be encountered under many scenarios. One scheme for accomplishing this would be to develop a system with a receiver station that was capable of resending the received data block back to the transmitting station for full confirmation. The data block would be sent and resent until it was confirmed to have been sent with 100% accuracy. All remaining data blocks would then be transmitted in the same manner.

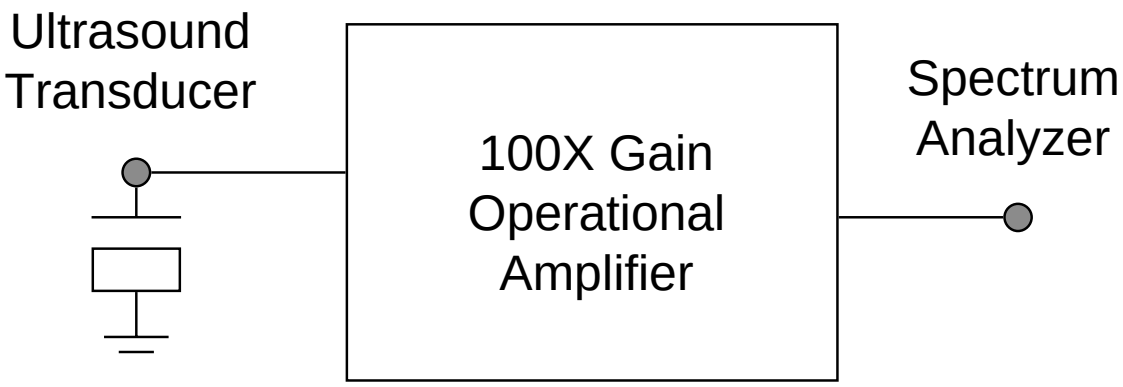

Figure 6.1 General test setup used to evaluate the noise floor of different amplifiers used for ultrasound communication purposes.

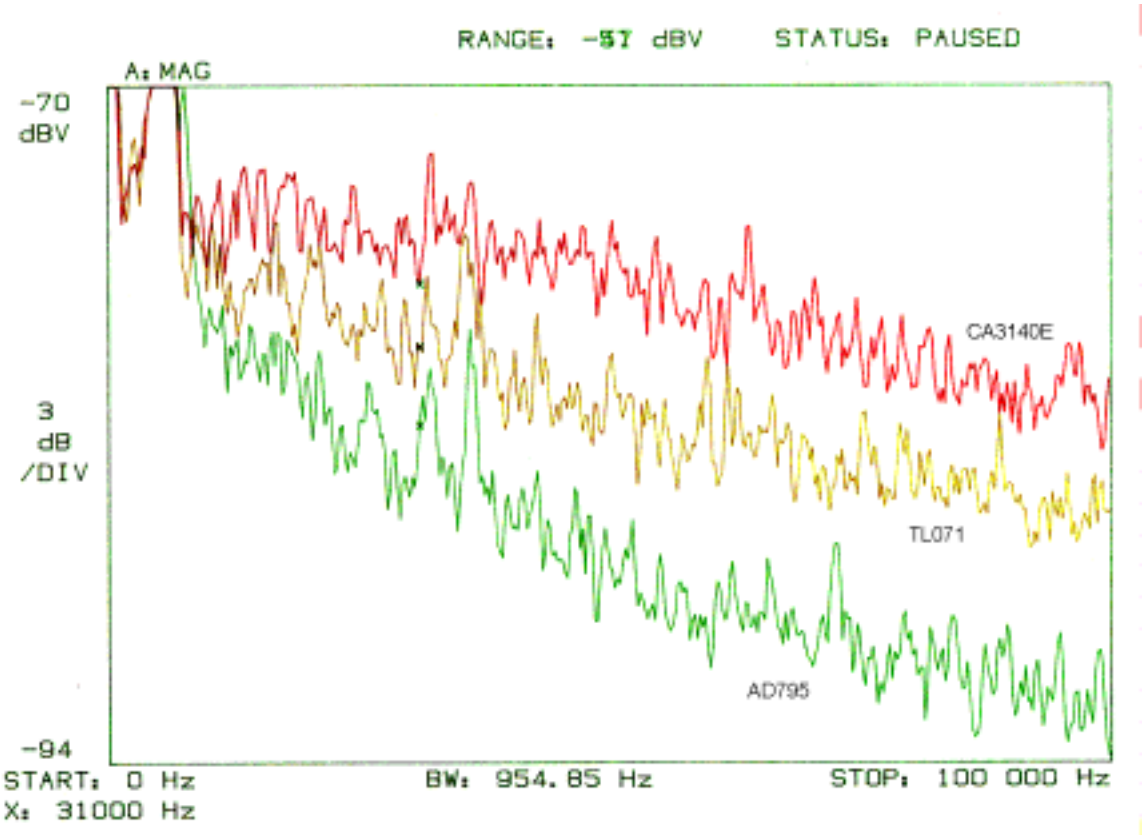

Figure 6.2 Noise floor measurements for three low-noise amplifiers.

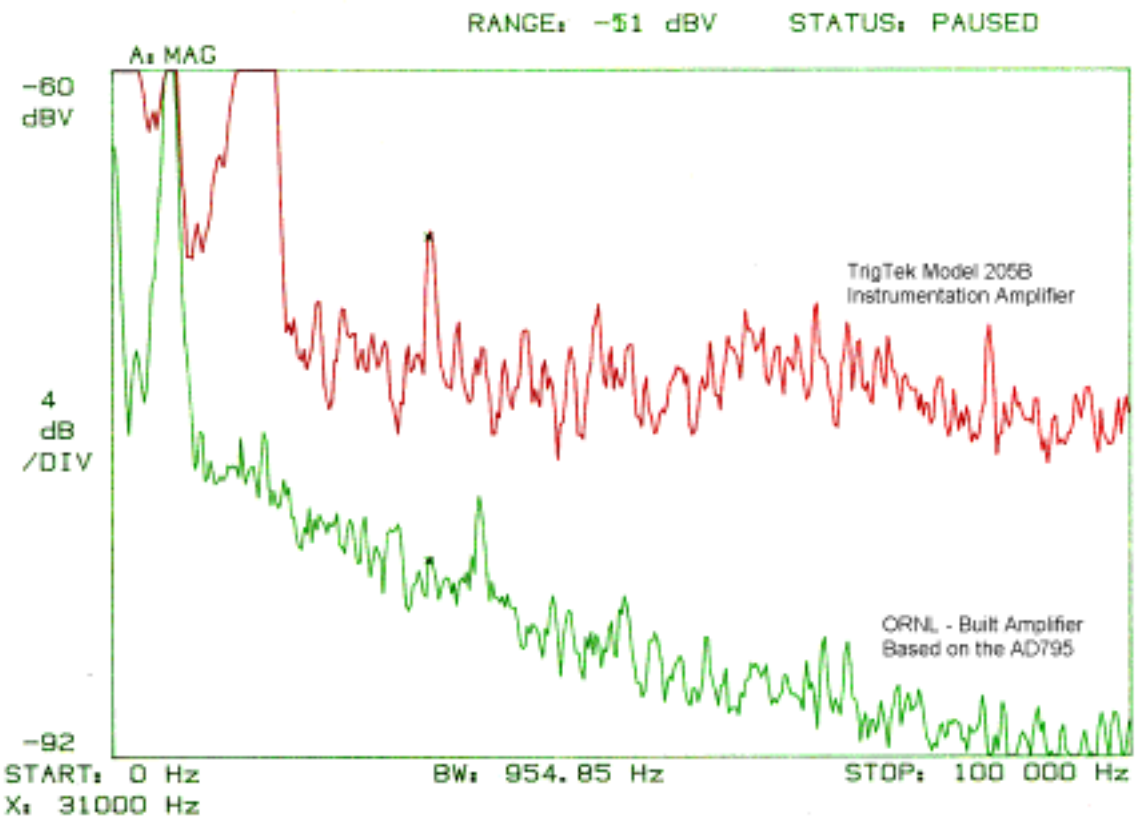

Figure 6.3 Noise floor comparison between a commercially acquired amplifier and the ORNL-built amplifier used for ultrasound absorption measurements.

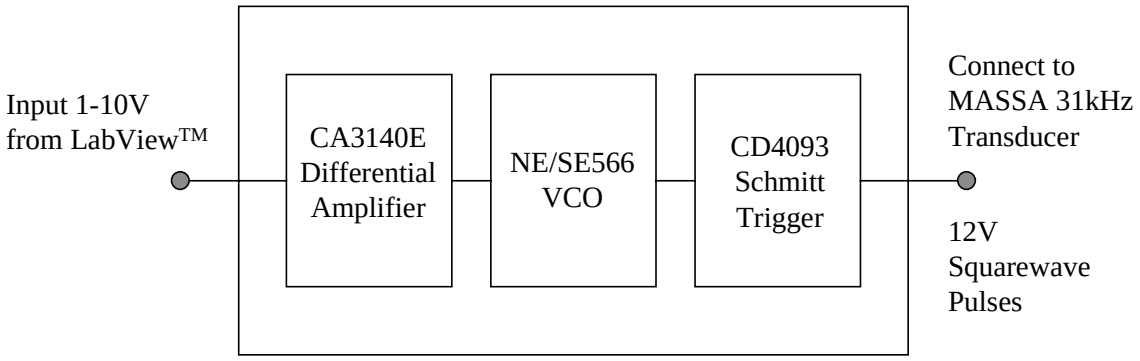

Figure 6.4 Block diagram of an ultrasonic transmitter circuit using a NE/SE566 as a VCO.

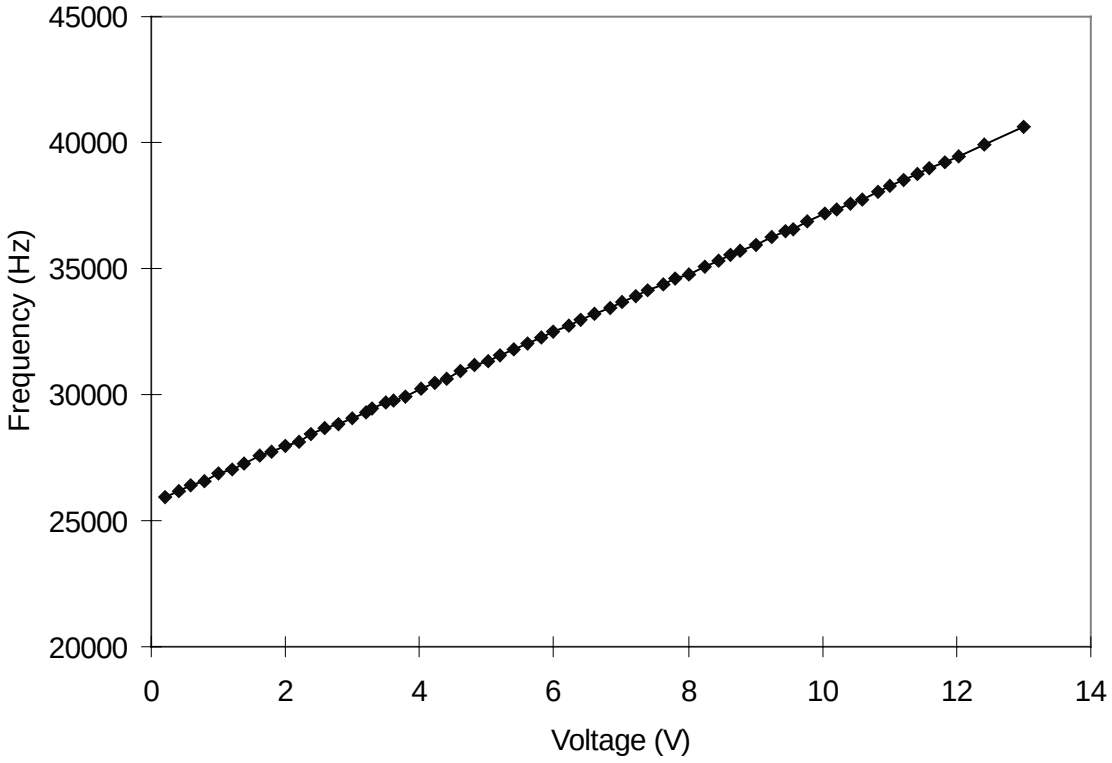

Figure 6.5 NE/SE566 short-term linearity over a 14-kHz band.

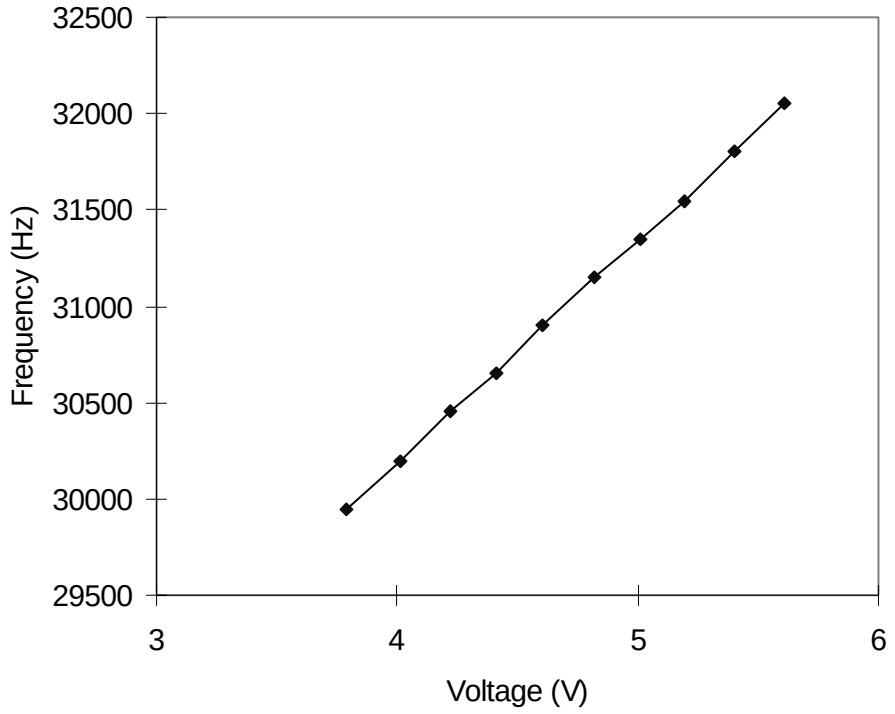

Figure 6.6 NE/SE566 short-term linearity over a 2-kHz band.

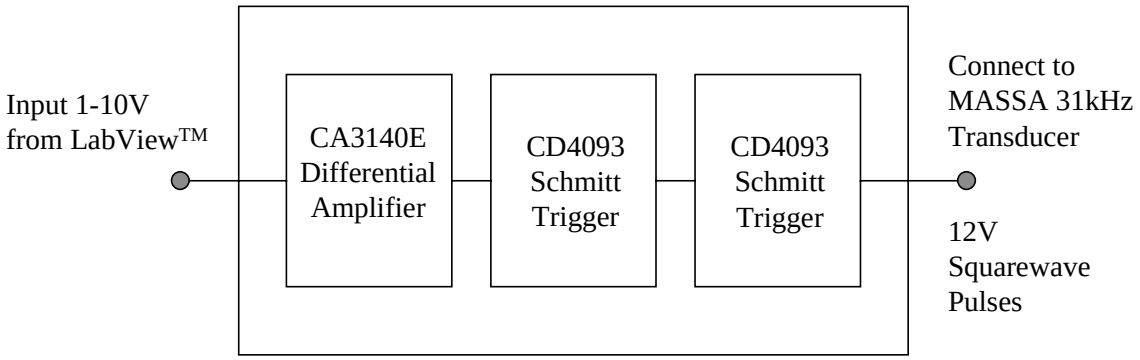

Figure 6.7 Block diagram of an ultrasonic transmitter circuit using a CD4093 as a VCO.

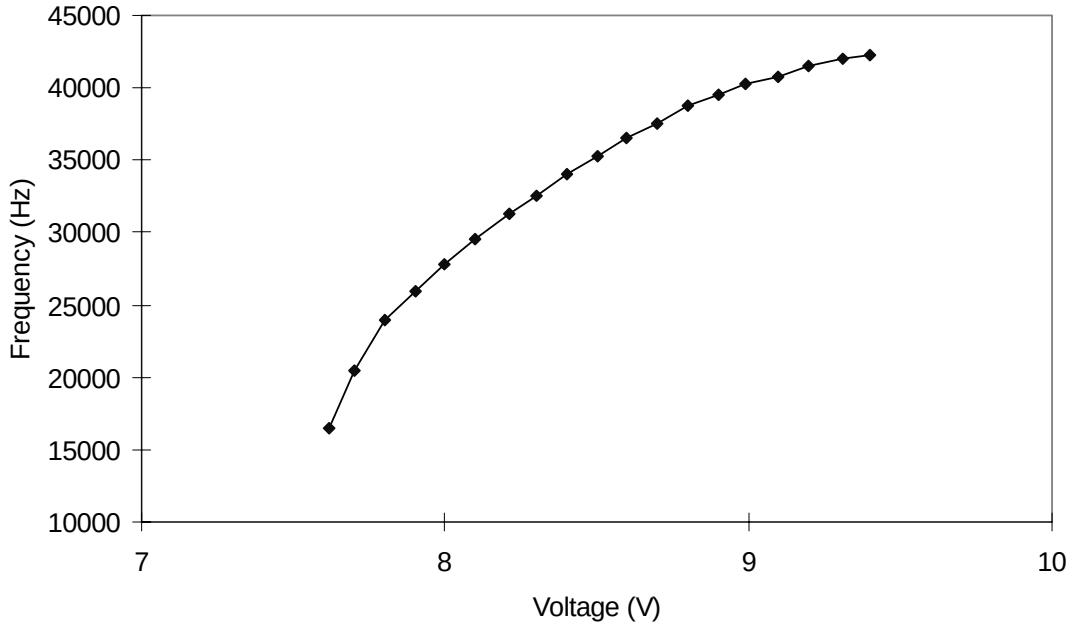

Figure 6.8 Schmitt trigger short-term linearity over a 25-kHz band without an ultrasonic transducer.

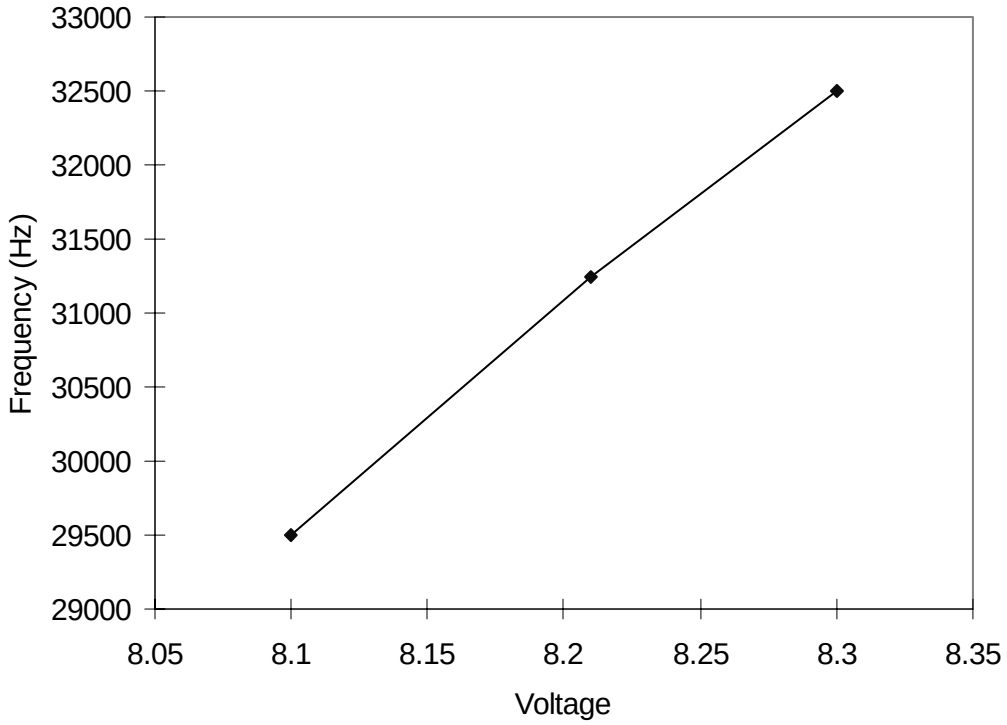

Figure 6.9 Schmitt trigger short-term linearity over a 3-kHz band without an ultrasonic transducer.

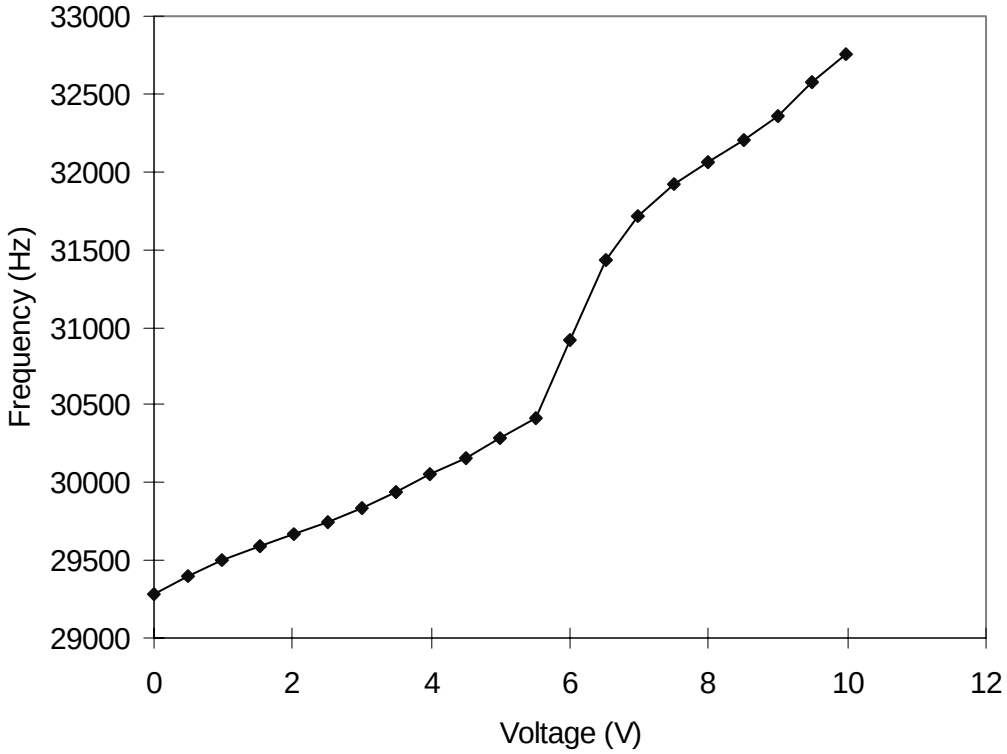

Figure 6.10 Schmitt trigger short-term linearity over a 3.5-kHz band after attaching an ultrasonic transducer.

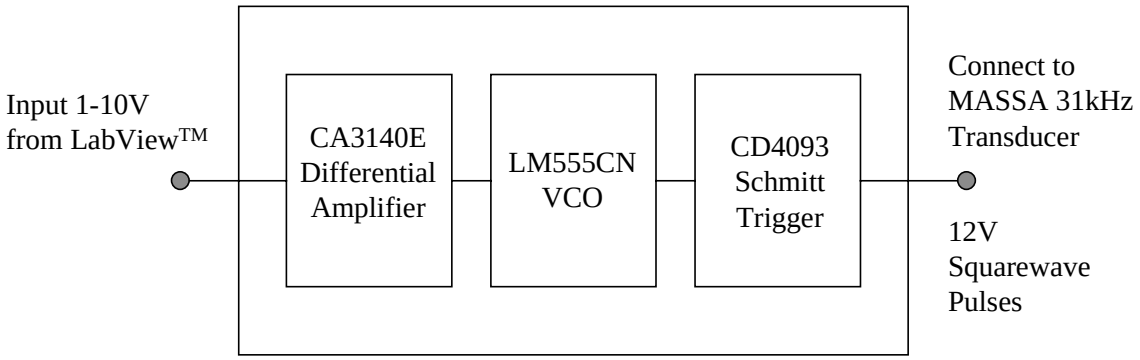

Figure 6.11 Block diagram of an ultrasonic transmitter circuit using a LM555CN as a VCO.

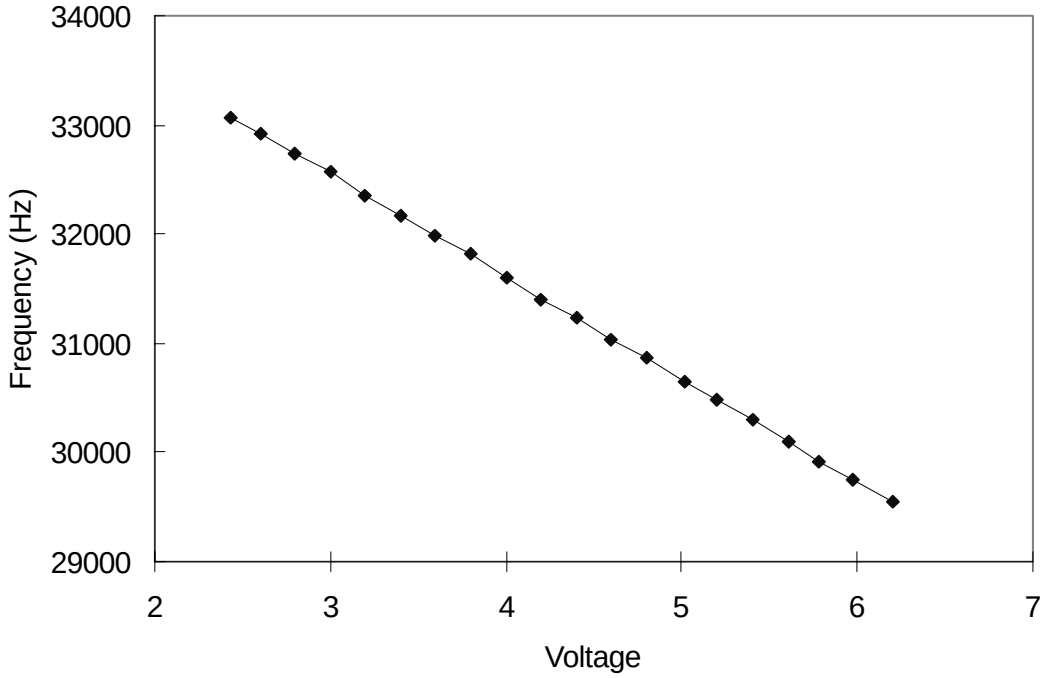

Figure 6.12 LM555CN short-term linearity over a 3.5-kHz band.

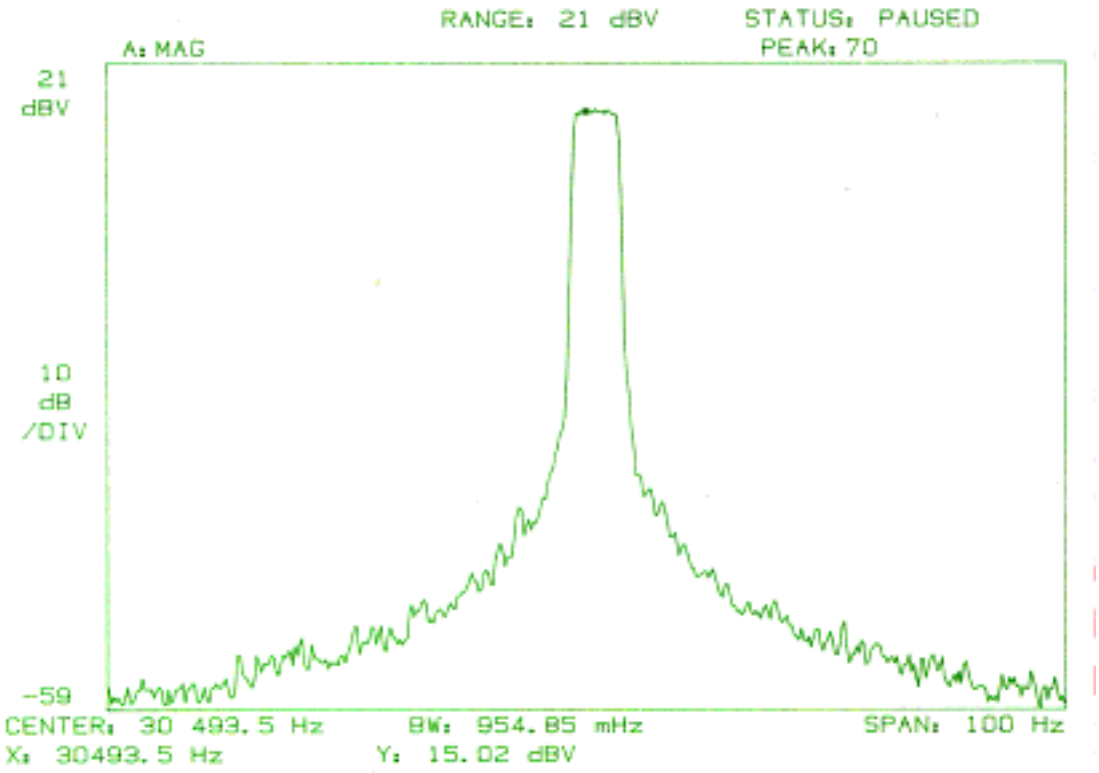

Figure 6.13 Frequency drift in LM555CN transmitter observed over a 5-min period during warm-up. (Note: data plotted over a 100-Hz span.)

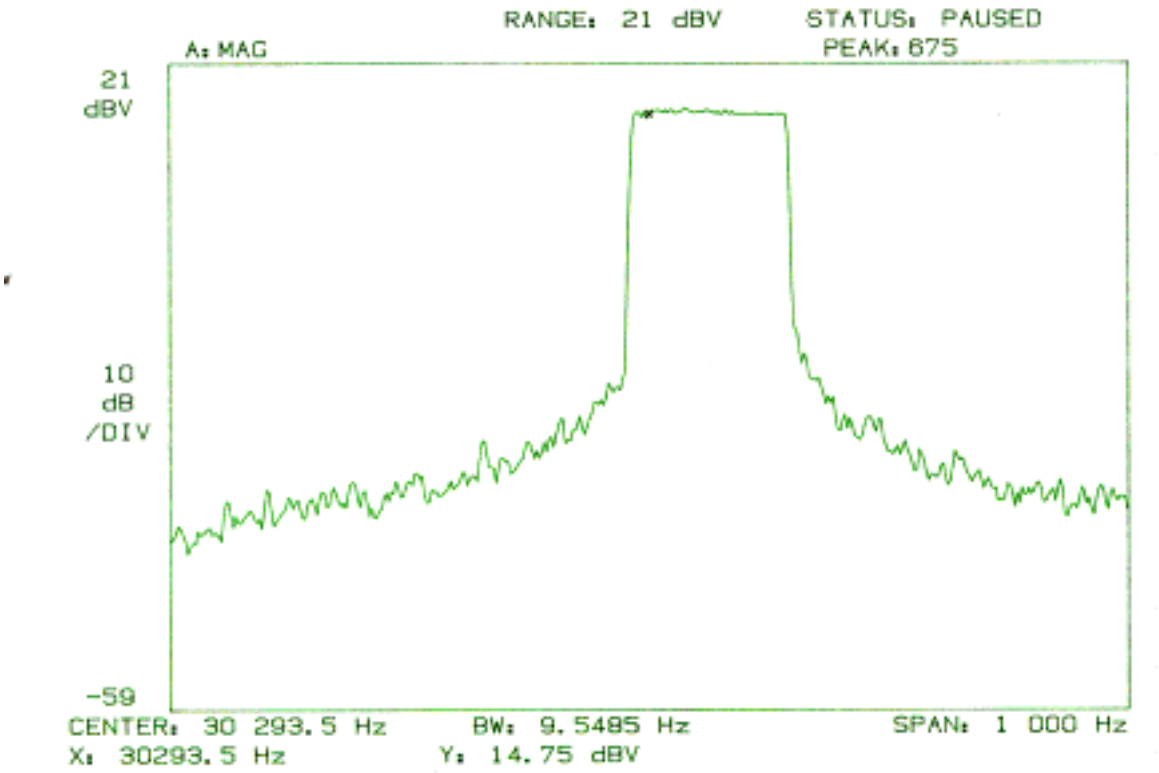

Figure 6.14 Frequency drift in NE/SE566 transmitter observed over a 5-min period during warm-up. (Note: data plotted over a 1000-Hz span.)

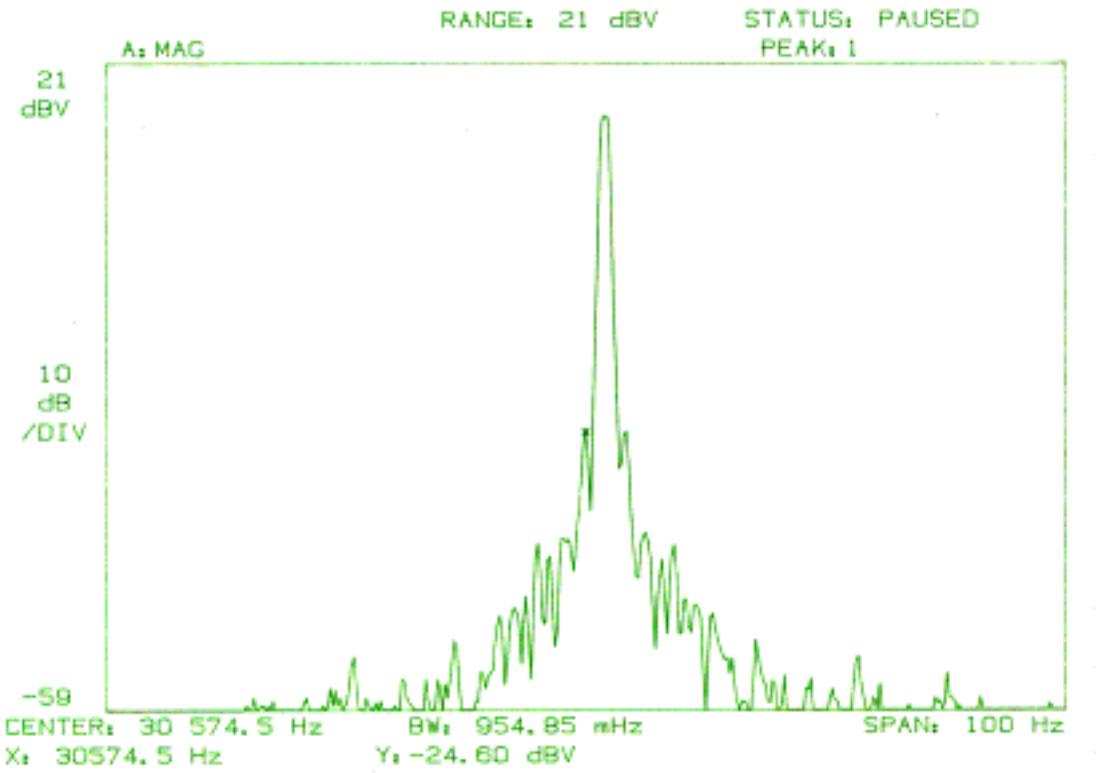

Figure 6.15 Frequency drift in LM555CN transmitter observed over a 5-s period after warm-up. (Note: data plotted over a 100-Hz span.)

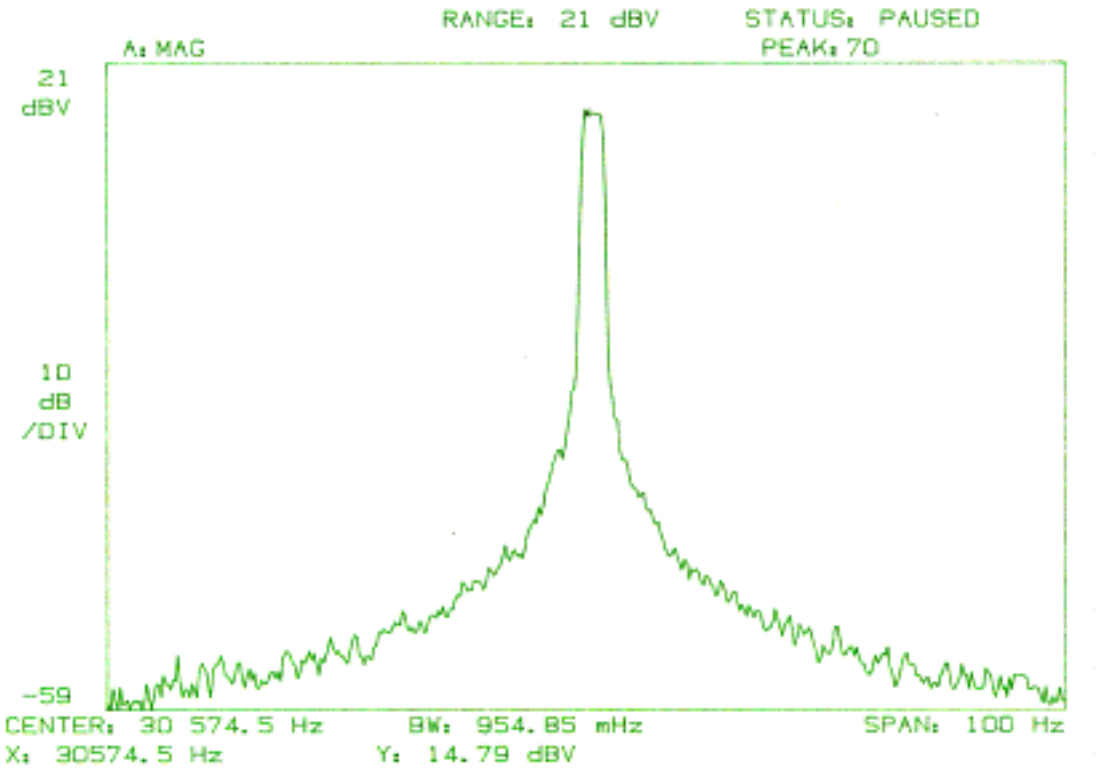

Figure 6.16 Frequency drift in LM555CN transmitter observed over a 5-min period after warm-up. (Note: data plotted over a 100-Hz span.)

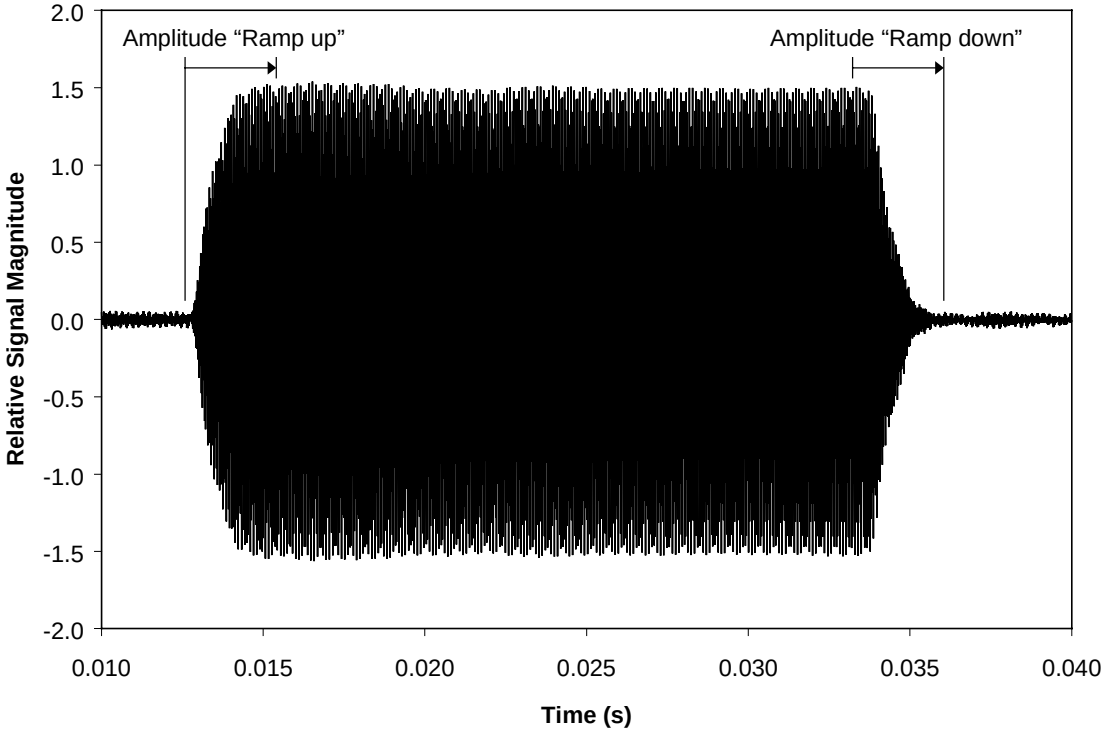

Figure 6.17 Receiver transducer output signal of a 30-ms ultrasonic burst that was transmitted approximately 12 ft through air. The “ramp up” and “ramp down” reflects the combined noninstantaneous response times of the transducers.

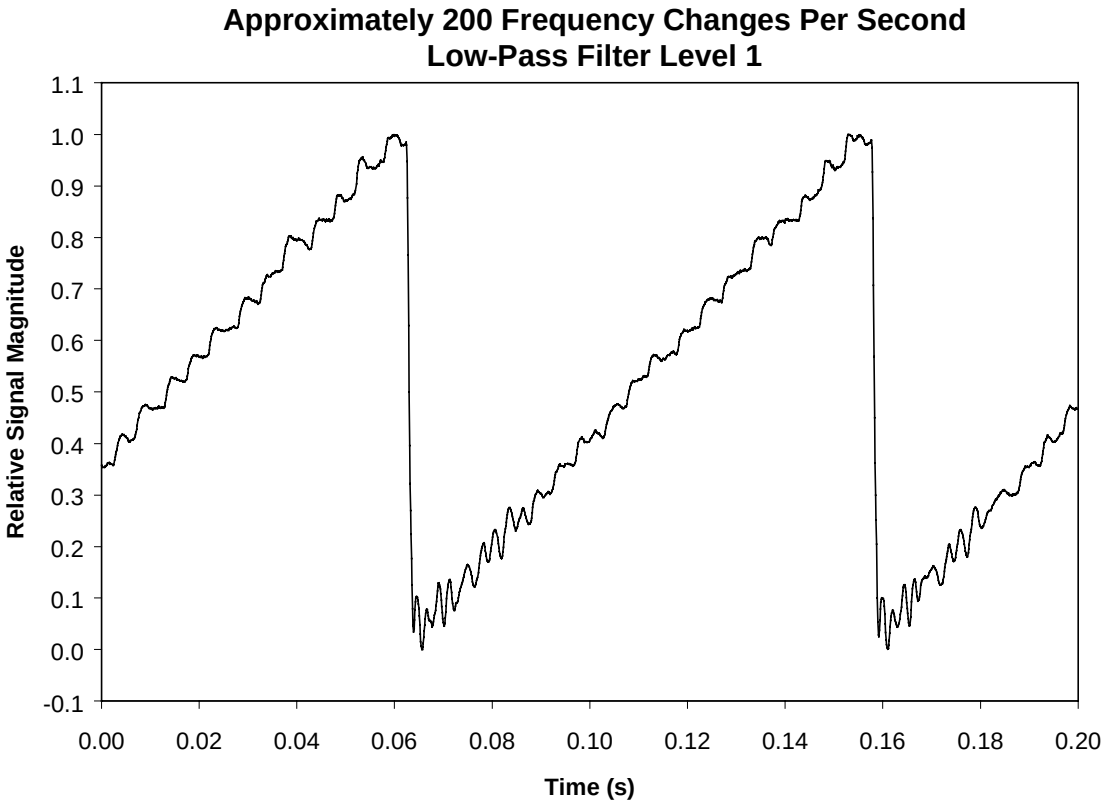

Figure 6.18 Received "staircase" waveform obtained by transmitting a repeated series of equally spaced ultrasonic frequencies through air over a distance of approximately 12 ft. The ragged response, especially near the bottom of the staircase, results from the speed of transmission being too high.

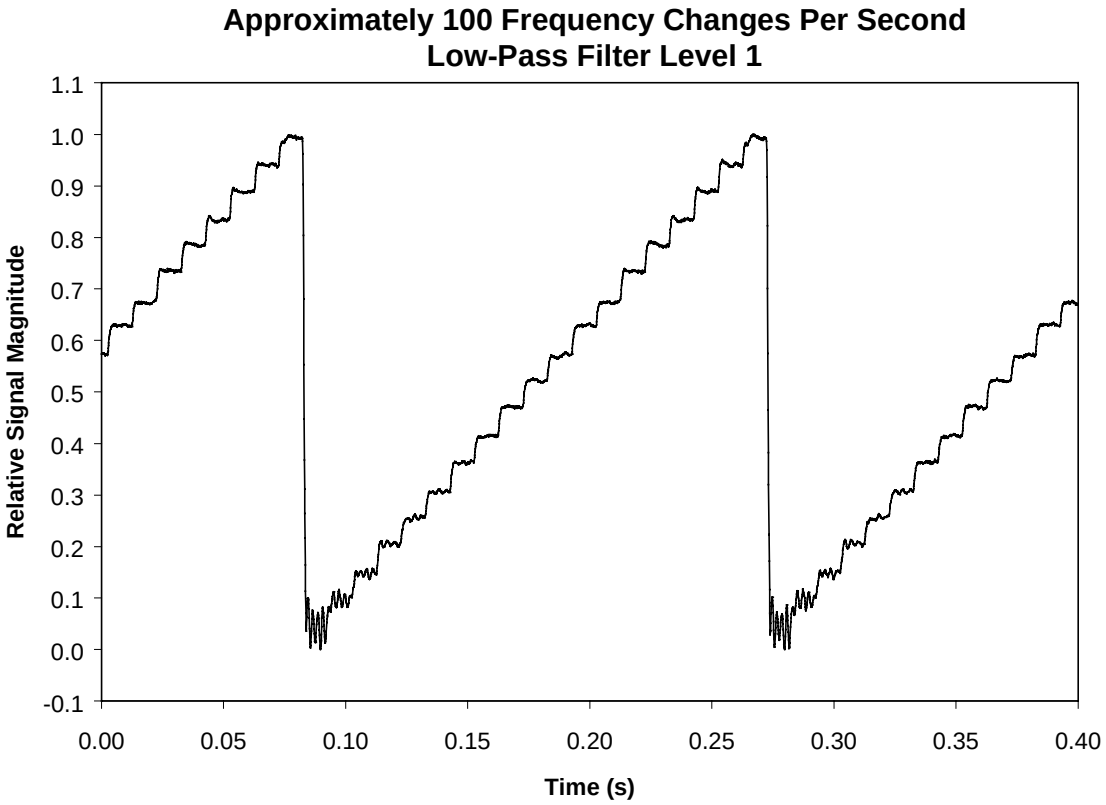

Figure 6.19 Improved appearance of staircase (when compared to Figure 6.18) as a result of decreasing the transmission speed.

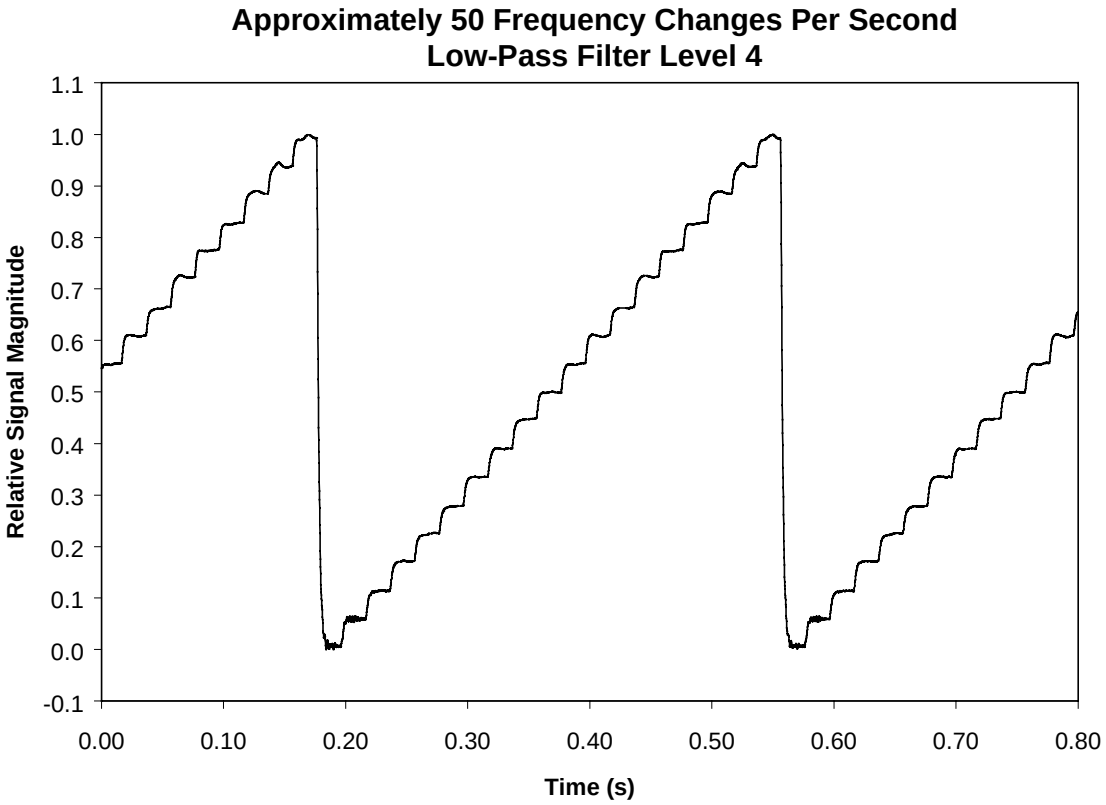

Figure 6.20 Continued improvement in the appearance of the staircase as a result of decreasing the transmission speed again and using a low-pass filter.

7. Descriptions of Demonstrations

7.1 Initial System (demonstrated 10/23/98)

An initial communication system was developed based on a two-tone frequency modulation of an ultrasonic carrier signal. The system utilized LabVIEW™ VIs for encoding a short, typed message and transmitting it ultrasonically through air at a distance of approximately 30 ft. At the receiver location, the ultrasound was received, and the typed message was decoded and displayed on a computer screen. The transmission was initiated via an ultrasonic trigger signal generated at the receiver location. The system was only capable of sending one short block of information and was incapable of the handshaking operations necessary to send longer messages and computer files. Speed of the system was approximately 15 characters per second (including computational time).

The VI platform provided a versatile means of controlling several parameters that were important to transmission speed and accuracy. Figures 7.1 and 7.2 show representative screen displays for the transmitter and receiver VIs used in the initial system, while Figures 7.3 and 7.4 illustrate the diagrams (programs) used by the VIs.

The system was demonstrated to the program monitor on October 23, 1998, in Oak Ridge.

7.2 Final System (demonstrated 7/16/99)

A major objective of this program was met with the development of a communication system for demonstration purposes. The system is based on a DFS method where individual alphanumeric characters are broken down into a sequence of two bits, with each bit having 16 possible levels and each bit level corresponding to a discrete ultrasonic frequency. Using this method, ASCII characters are transmitted one-bit-at-a-time and reconstructed by the receiver. LabVIEW™ VIs were developed and used in conjunction with specially designed electronics for transmission and reception/reconstruction of typed messages and computer files. This system provided improvements over the initial system in speed (over three times as fast) and provided a new ability to transmit long messages and computer files. This new ability was made possible by an ultrasonic triggering scheme between the receiver and the transmitter.

Figure 7.5 illustrates the basic functional elements of the system. A laptop computer running the transmitter program outputs a sequence of dc voltages (bit levels) to the VCO, which converts the dc voltages to ac voltages having discrete frequencies within the operating range of the ultrasonic transducer. Ultrasound is transmitted through the media (air, pipe, etc.) to the receiver location, where it is detected by an ultrasonic transducer and processed by the data receiver. The processed signals are then relayed to a laptop computer running the receiver program. Large data files are transmitted in blocks with an ultrasonic trigger signal being used to coordinate the block transmissions. The trigger signal is transmitted at the receiver location back to the transmitter location and received via ultrasound transducers operating at a frequency outside of the range used for data communication. The system presently uses a 40-kHz trigger signal and transmits data within an approximate range of 31 ± 1 kHz. Two different transducer models are used for communicating data and trigger signals, respectively. The inherent differences in the frequency responses of the two models enhance the separation between the trigger and data signals.

Figure 7.6 provides additional details about the data receiver electronics. In addition to signal preconditioning, two types of signal conversion are provided: frequency (phase) demodulation via a PLL and F-to-V conversion via an F-to-V integrated circuit. Sufficient controls are provided on the receiver box so that the processed signals are passed to the laptop computer with an optimum signal-to-noise ratio. Figure 7.7 similarly illustrates the internal functions of the trigger signal receiver box. In this case, amplifiers, filters, and an RMS-to-dc converter are used to enhance the trigger signal prior to sending it to the laptop computer for coordinating the data transmission. In both Figures 7.6 and 7.7, the indication of a "variable" parameter means that a control (e.g., potentiometer or multiposition switch) is provided for making adjustments of that parameter.

Electronic circuit diagrams for the data receiver are shown in Figures 7.8 through 7.12 (referenced to Figure 7.6), while the diagram for the trigger receiver is shown in Figure 7.13 (referenced to Figure 7.7). Circuits were constructed on general-purpose printed circuit cards but could be recreated on specially designed cards if desired.

As with the initial system, the VI platform provided a versatile means of controlling several parameters that were important to transmission speed and accuracy. Figures 7.14 (a through f) and 7.15 (a through n) show representative screen displays for the transmitter and receiver VIs used in the final system.

System performance tests were carried out by transmitting computer files across a 10-ft distance through air. The speed of the system was set at 75 bits per second, which equates to 37.5 characters per second. At this speed, data transmission was extremely reliable. Even compressed graphic files, where a single error in one bit can result in an unreadable file, were reliably transmitted. For example, Figure 7.16 shows a compressed file (gif format) that was transmitted by the system. This file depicts a floor plan of a building and contains 52303 pixels (193 x 271). The file was sent in 92 s, yielding an effective speed of 569 pixels per second. While the gif file is 2701 bytes in size, an uncompressed version (bmp format) of the same image is 54194 bytes in size. If the bmp version were sent via the same method and with the same speed, it would have required approximately 20 times the transmission time.

The system is capable of transmitting a variety of computer files. In addition to graphic files, text files and sound files can also be sent. For example, Figure 7.17 depicts a six-page text file, containing 3201 words constructed from 17256 characters (over 20000 characters, including the spaces). After compressing the file with a commercially available utility program, the compressed file (about 7 kB) was transmitted successfully in 3 min, 56 s at 75 bits per second.

Photos of the transmitter and receiver hardware are shown in Figures 7.18 and 7.19, respectively. As shown in these photos, the transmitter and receiver systems feature compact, modular elements that together perform the intended system functions. The system electronics require a power supply providing +12 V dc, -12 V dc, and common. Thus far, power has been supplied via linear (regulated) power supplies that plug into 120 V ac wall outlets; however, a battery supply could be utilized to provide complete portability.

On July 16, 1999, a program review meeting was held in Oak Ridge. The program accomplishments were discussed, and the ultrasonic communication final system was demonstrated.

Initial demonstrations utilized typed messages that were sent ultrasonically through air from the transmitter station (Figure 7.18) to the receiver station (Figure 7.19). For a second demonstration, the program monitor chose a computer file from many on the transmitter station

computer and transmitted it to the receiving station computer via the same ultrasonic link without assistance from the developers. A second visitor was able to open the file and demonstrate that it had been transferred flawlessly, again with no help from the developers.

7.3 Long-Range Ultrasonic Transfer (demonstrated 7/16/99)

For an additional demonstration for the program monitor, ultrasound (at 23 kHz and 30 kHz) was injected into a building instrument air pipe and detected at a remote location by a transducer that was simply taped to the pipe. The attenuation of the ultrasound signals was 5 orders of magnitude over the 110 ft (33 m) length of the pipe, which was in rough agreement with the laboratory absorption measurements on a straight galvanized pipe filled with air. This was a useful demonstration because it utilized a “real” pipe mounted in a building, rather than a “test” pipe in a laboratory.

Based on the laboratory absorption measurements (discussed in Section 4), it is estimated that the same signal sent through the 33-m instrument air pipe would have traveled an approximate distance of 15 m in the same pipe filled with water instead of air. Section 4 describes the benefits associated with directly coupling the ultrasound transducers to the water, rather than simply attaching them to the outside of the pipe. Laboratory tests have shown that direct coupling methods can provide up to three orders of magnitude improvement in signal strength when applied to water-filled galvanized pipe and six orders of improvement for water-filled PVC pipe. By increasing the transmitter power by three orders of magnitude, together with the impedance matching improvements of the direct-coupled transducers, an estimated six orders of magnitude of improvement is expected.

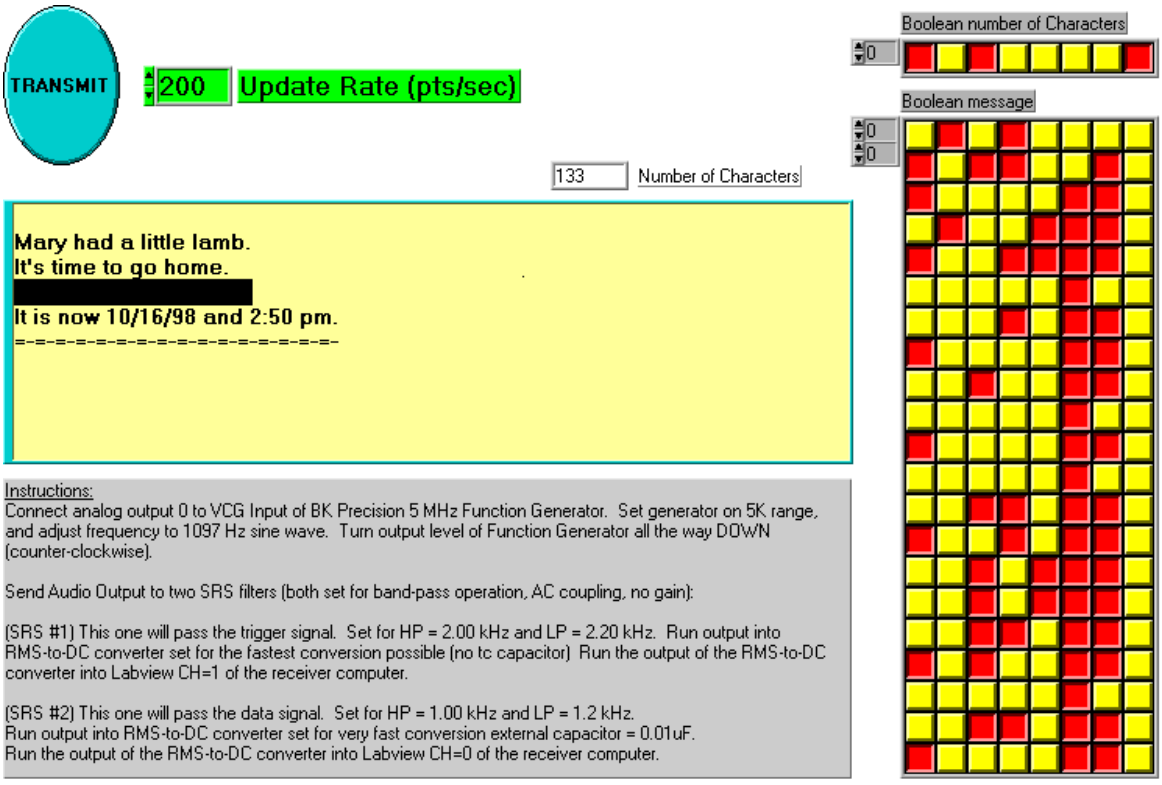

Figure 7.1 Screen display for the transmitter VI used in the initial system.

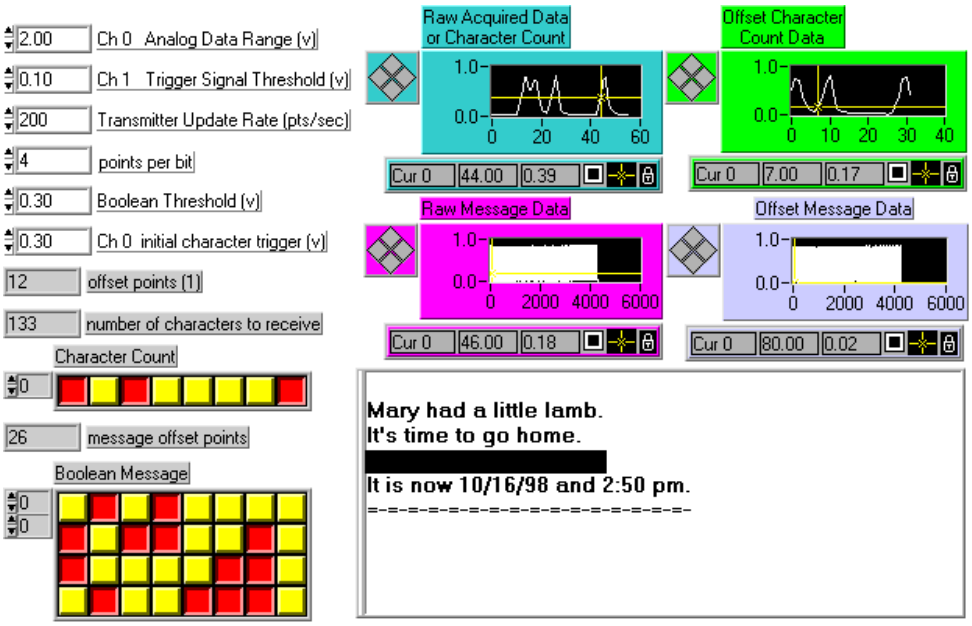

Figure 7.2 Screen display for the receiver VI used in the initial system.

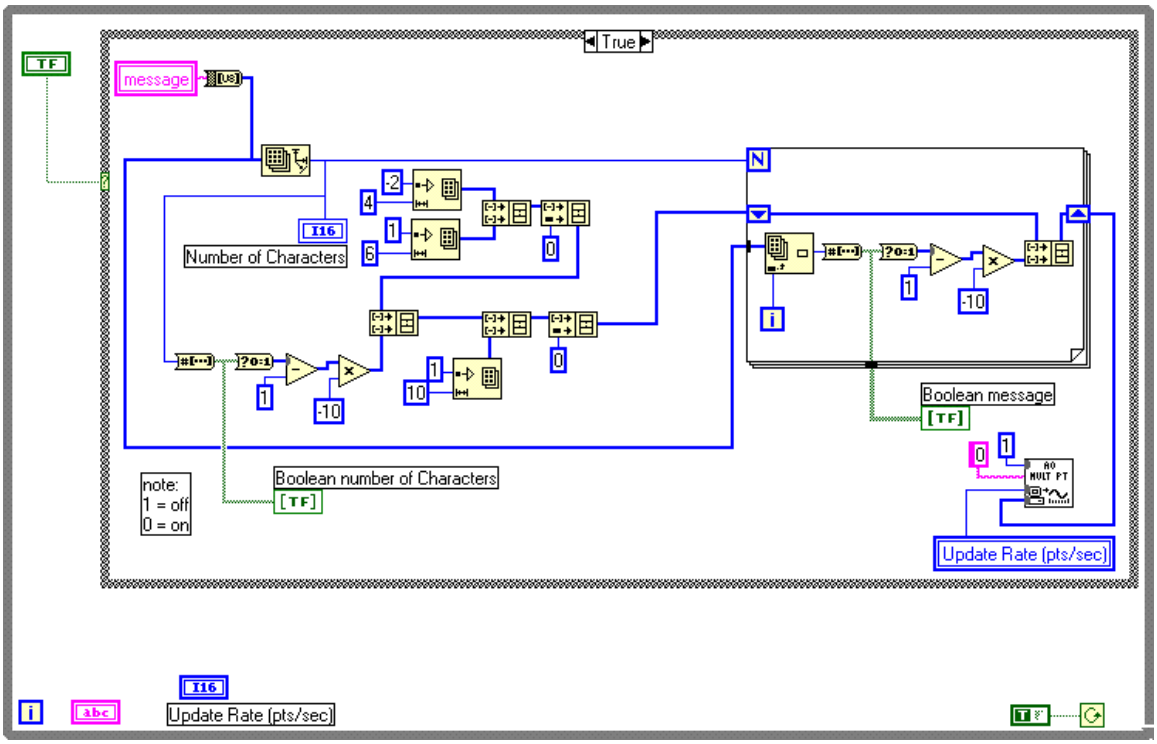

Figure 7.3 Diagram (program) for the transmitter VI used in the initial system.

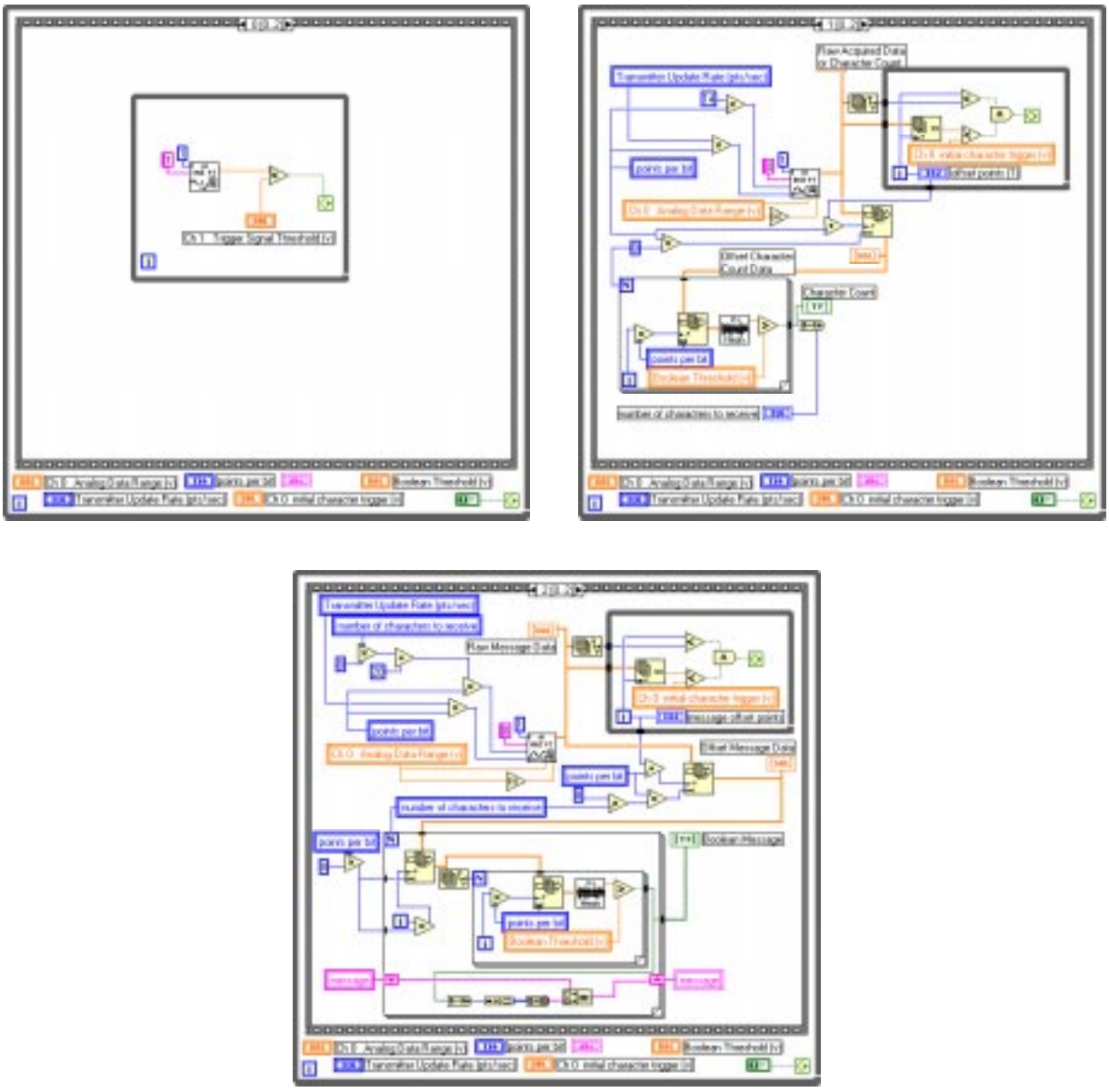

Figure 7.4 Diagram (program) for the receiver VI used in the initial system.

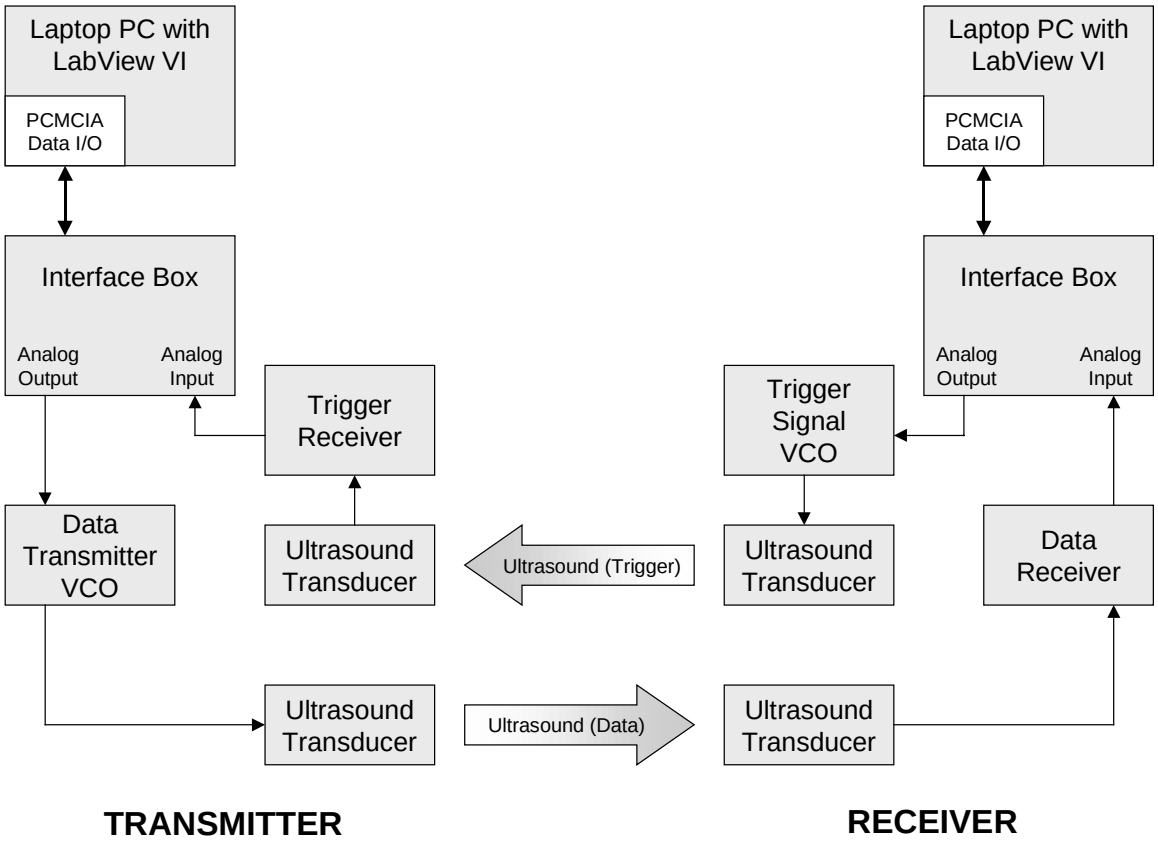

Figure 7.5 Simplified block diagram for the ultrasonic communication system developed for demonstration purposes.

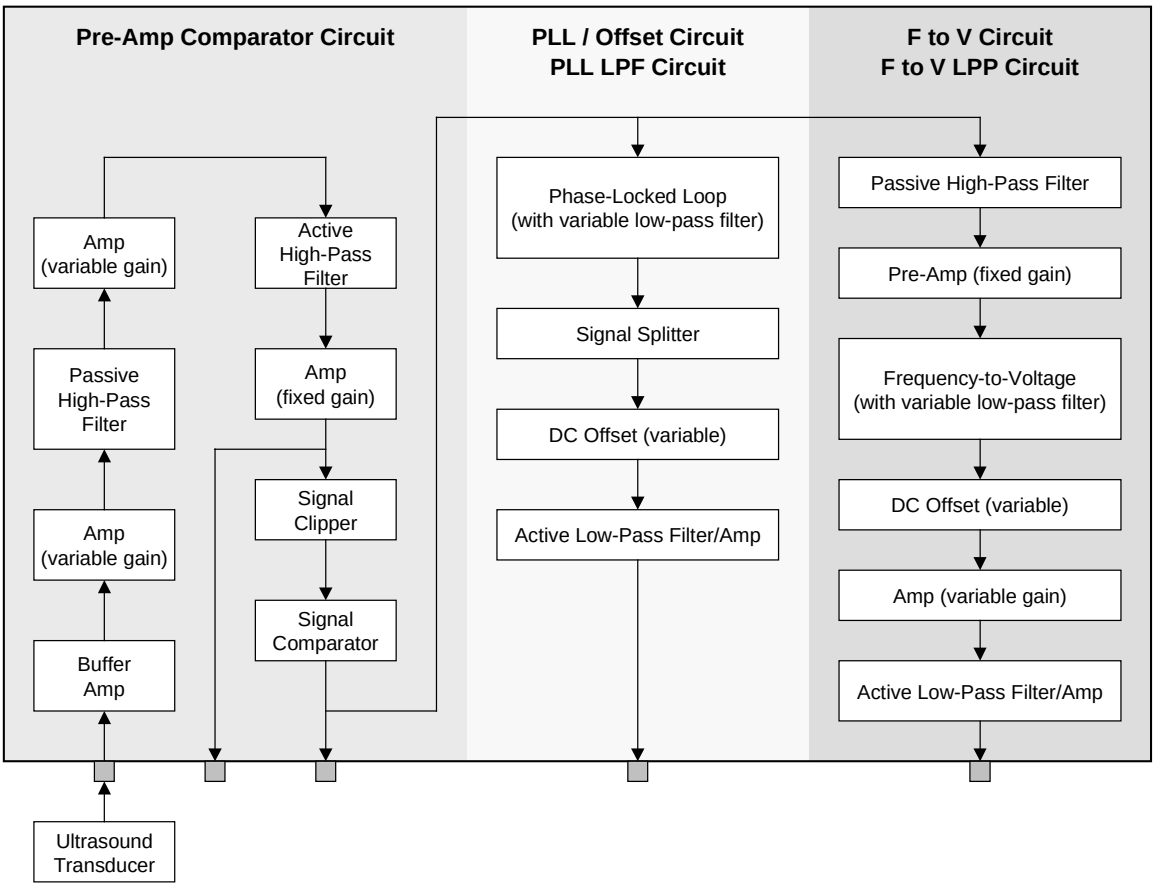

Figure 7.6 Functional diagram of the data receiver box used in the ultrasonic communication system.

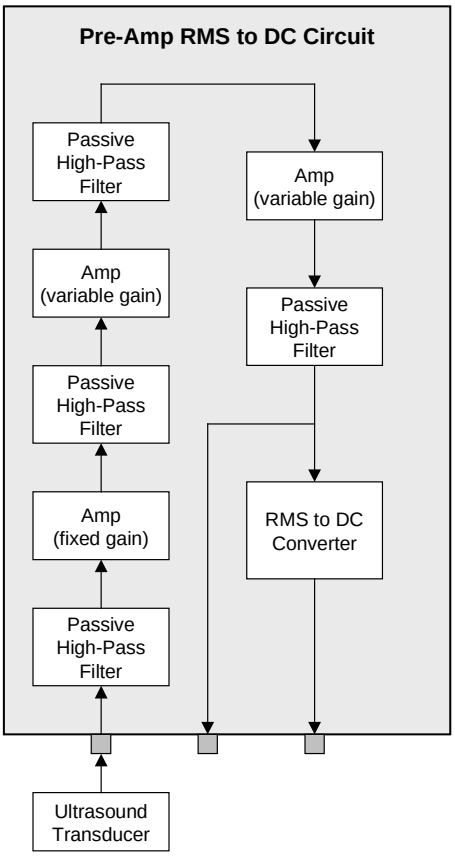

Figure 7.7 Functional diagram of the trigger signal receiver box used in the ultrasonic communication system.

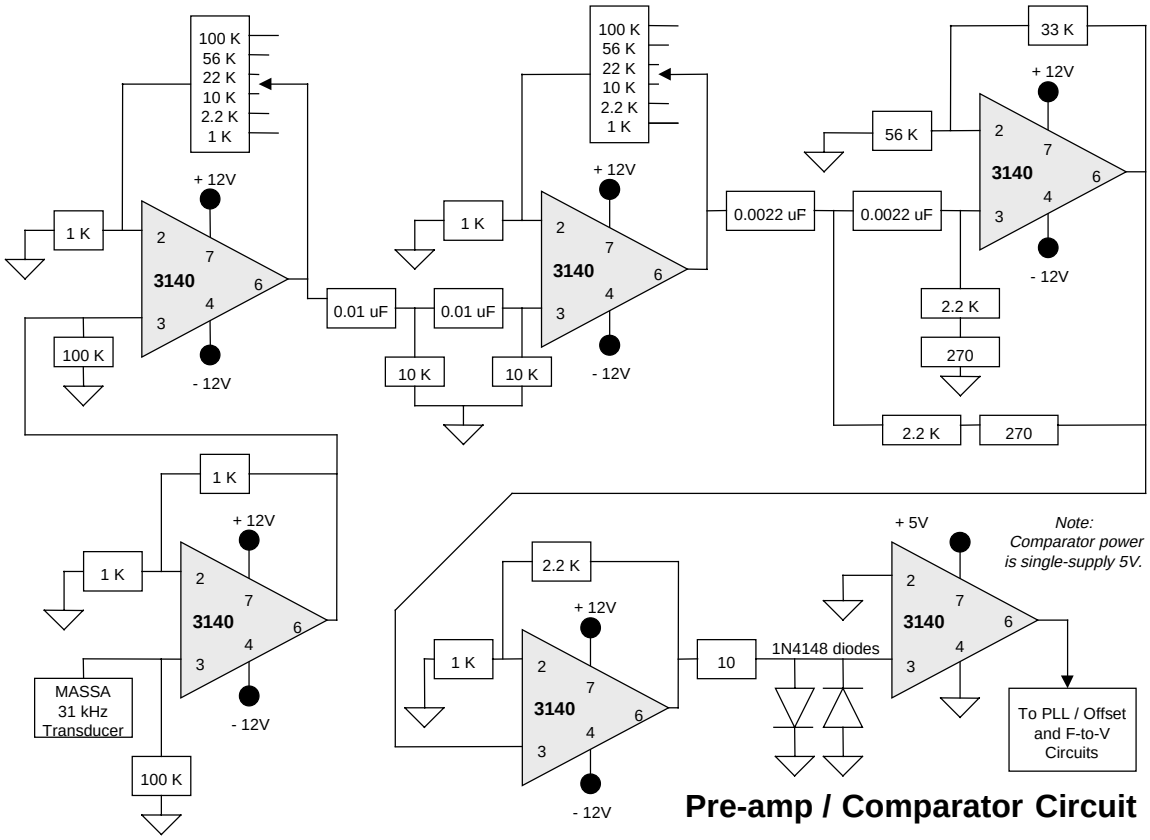

Figure 7.8 Circuit diagram for the pre-amp / comparator circuit used in the data receiver box.

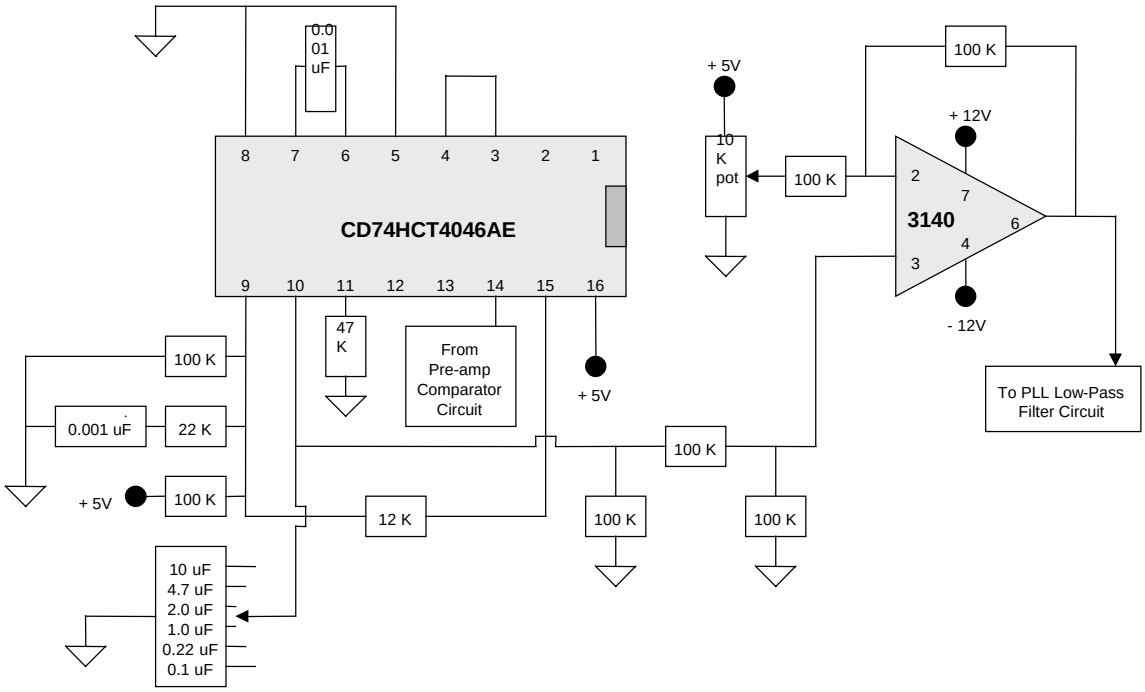

PLL / Offset Circuit

Figure 7.9 Circuit diagram for the PLL/offset circuit used in the data receiver box.

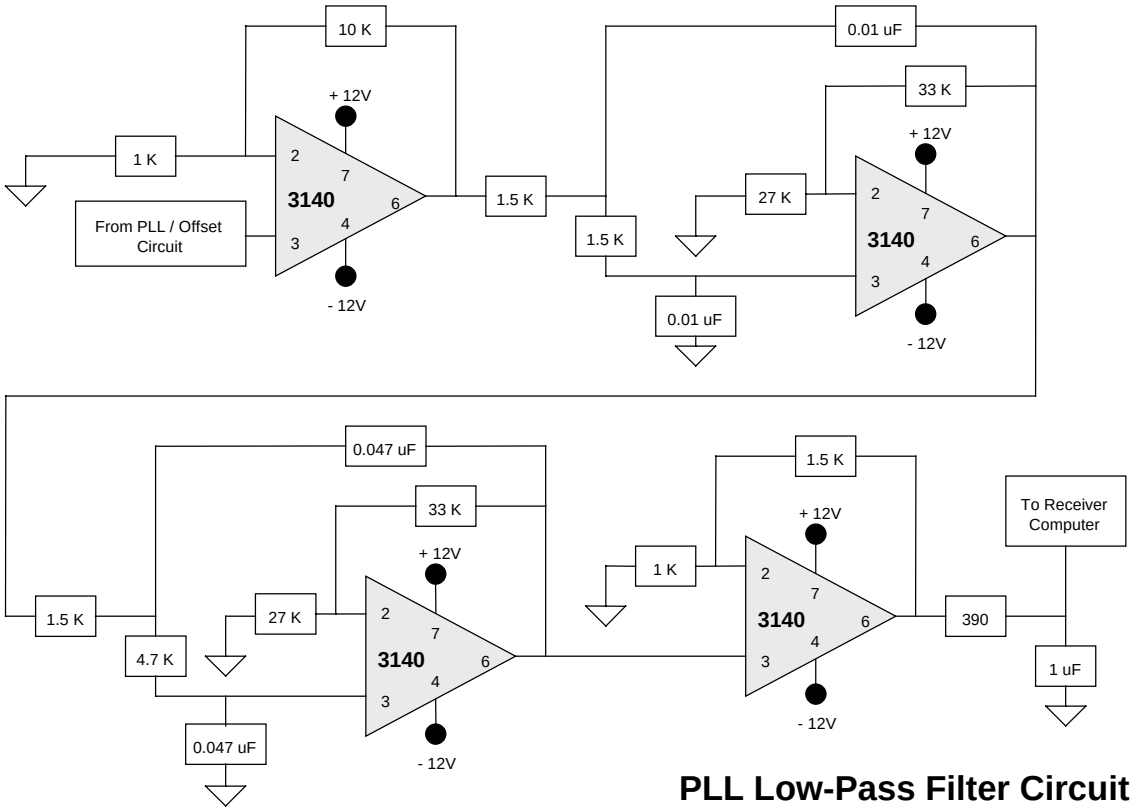

Figure 7.10 Circuit diagram for the PLL low-pass filter circuit used in the data receiver box.

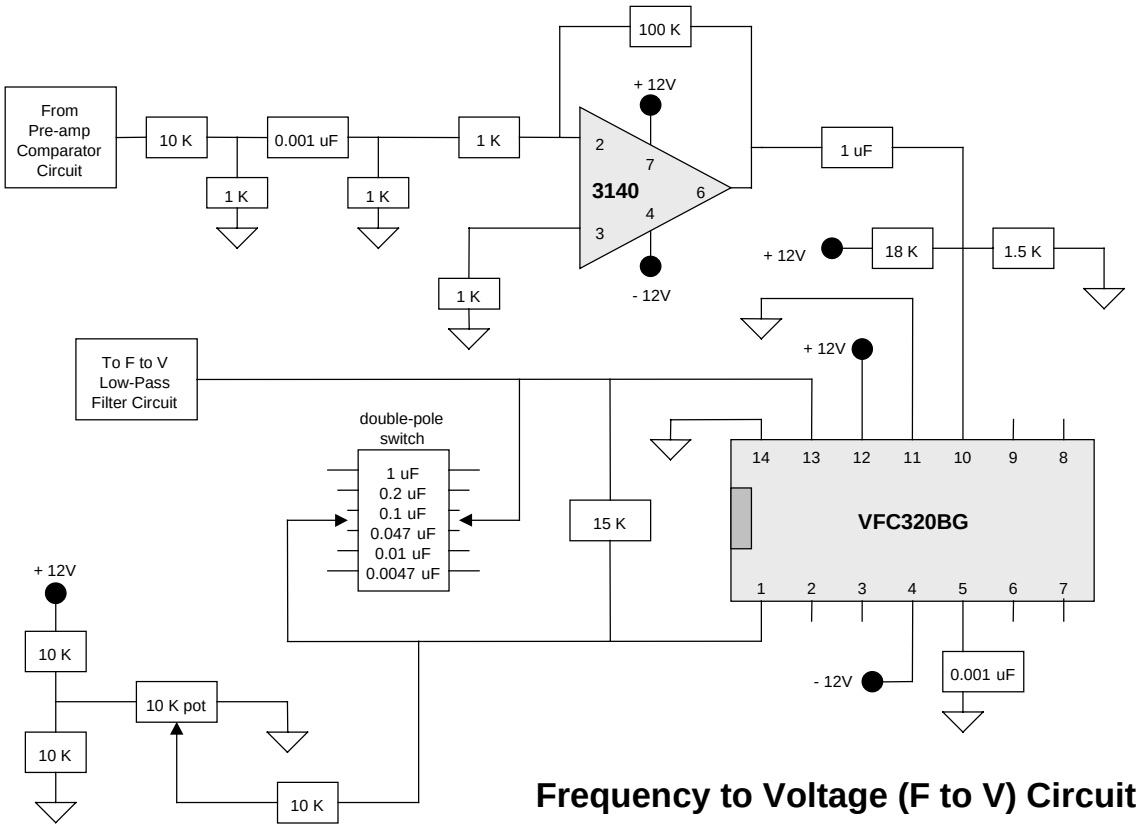

Figure 7.11 Circuit diagram for the F-to-V circuit used in the data receiver box.

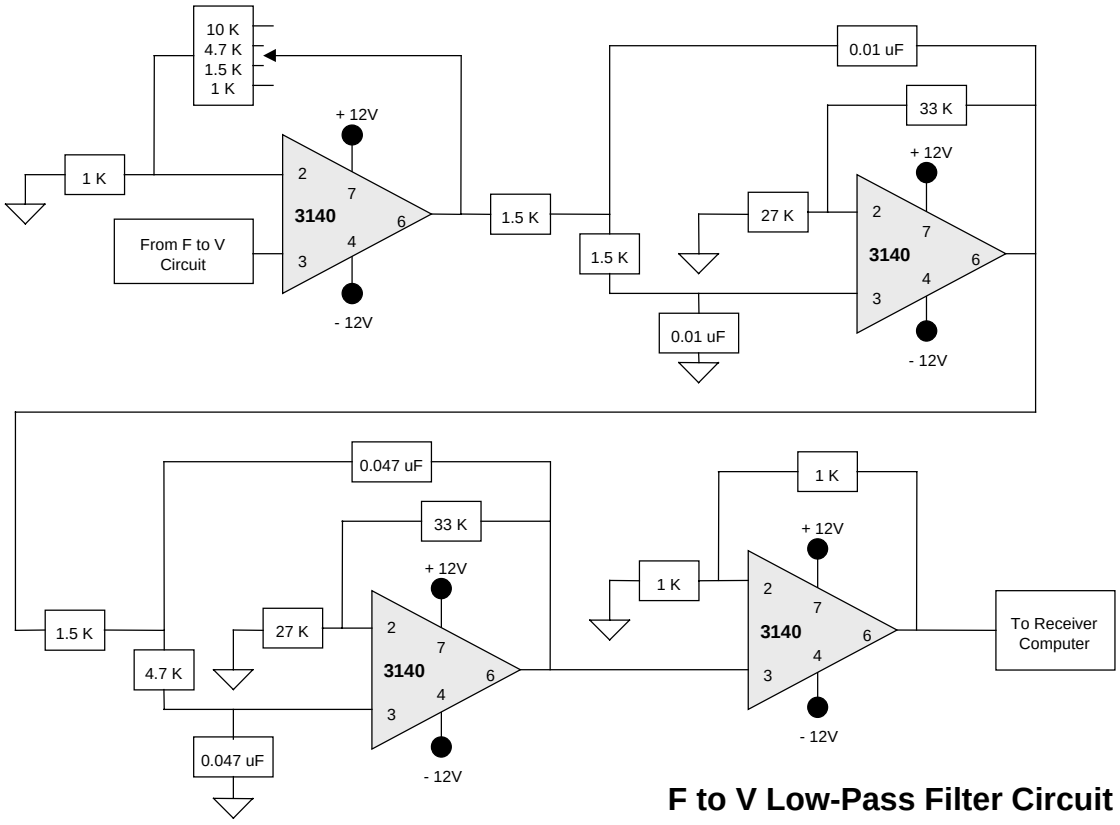

Figure 7.12 Circuit diagram for the F-to-V low-pass filter circuit used in the data receiver box.

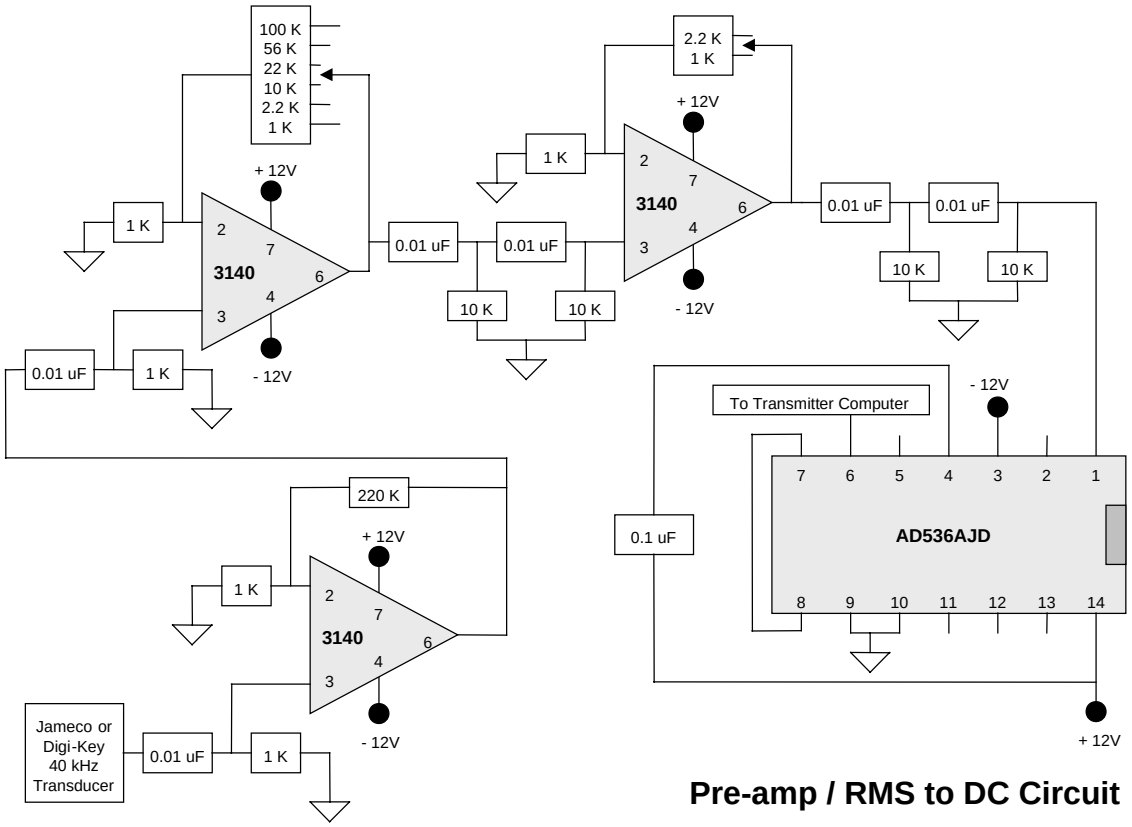

Figure 7.13 Circuit diagram for the preamplifier/RMS-to-dc circuit used in the trigger signal receiver box.

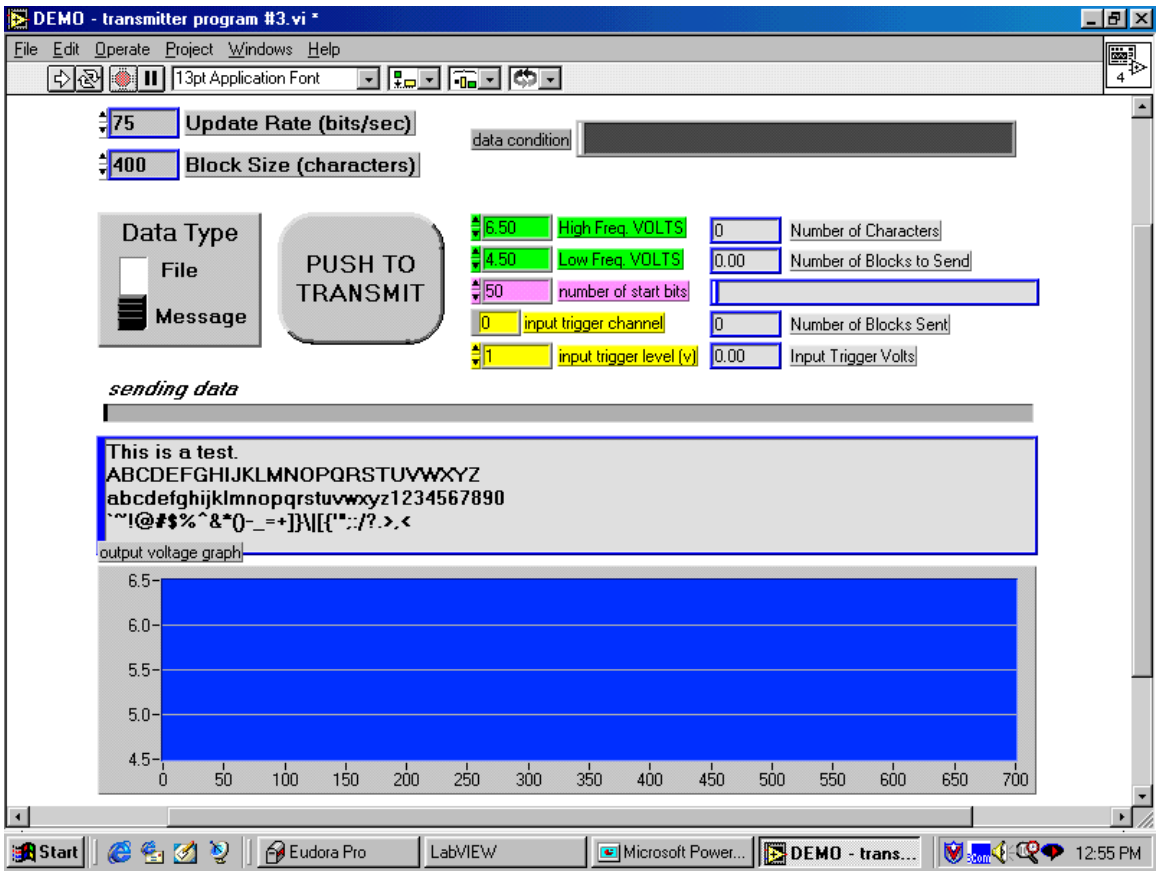

Figure 7.14a Front panel display of the ultrasonic transmitter VI.

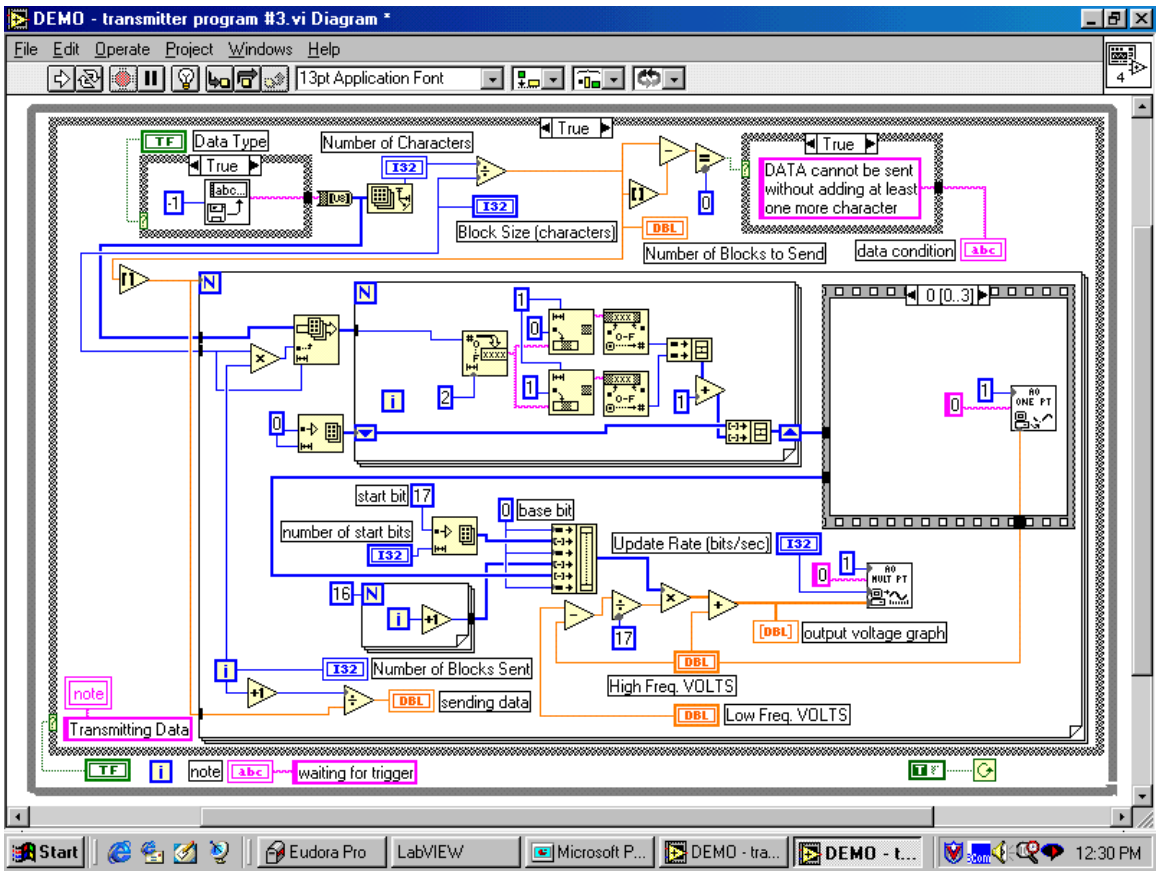

Figure 7.14b Diagram (page 1 of 5) of the ultrasonic transmitter VI.

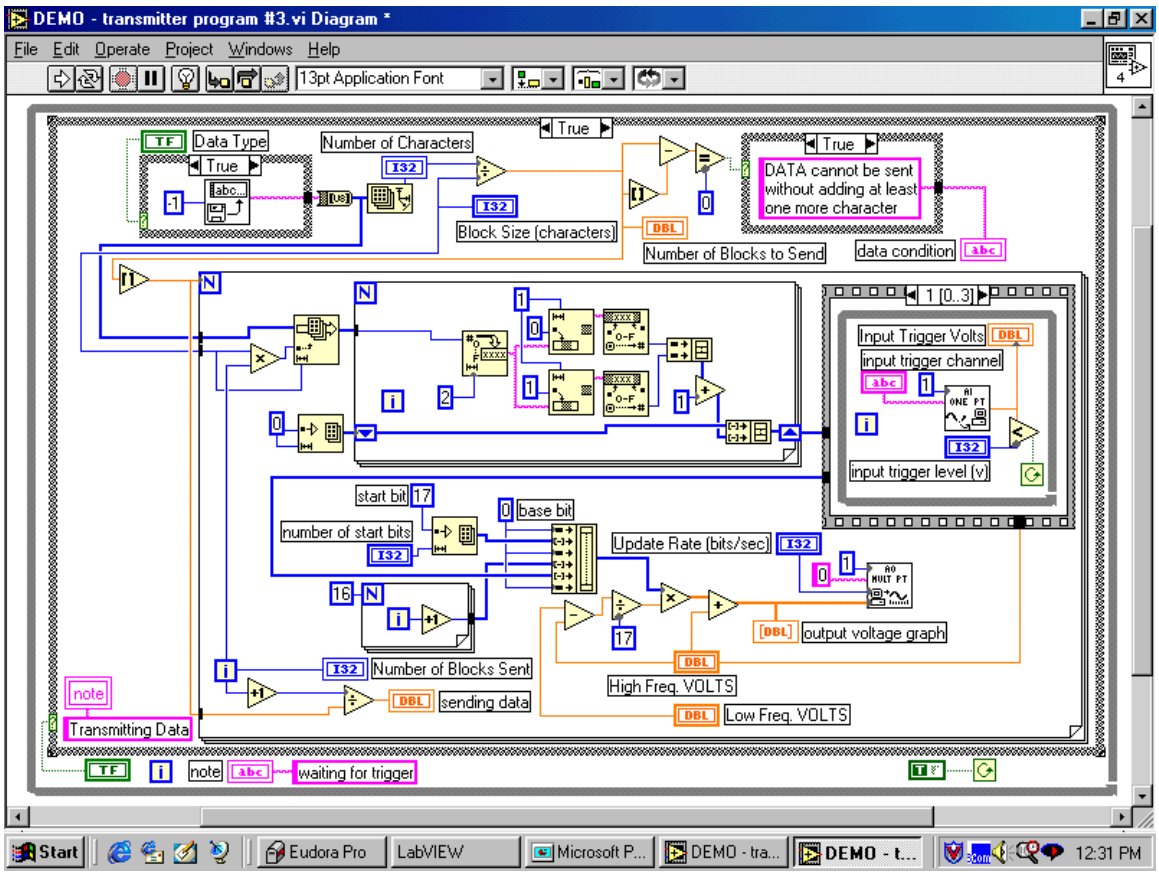

Figure 7.14c Diagram (page 2 of 5) of the ultrasonic transmitter VI.

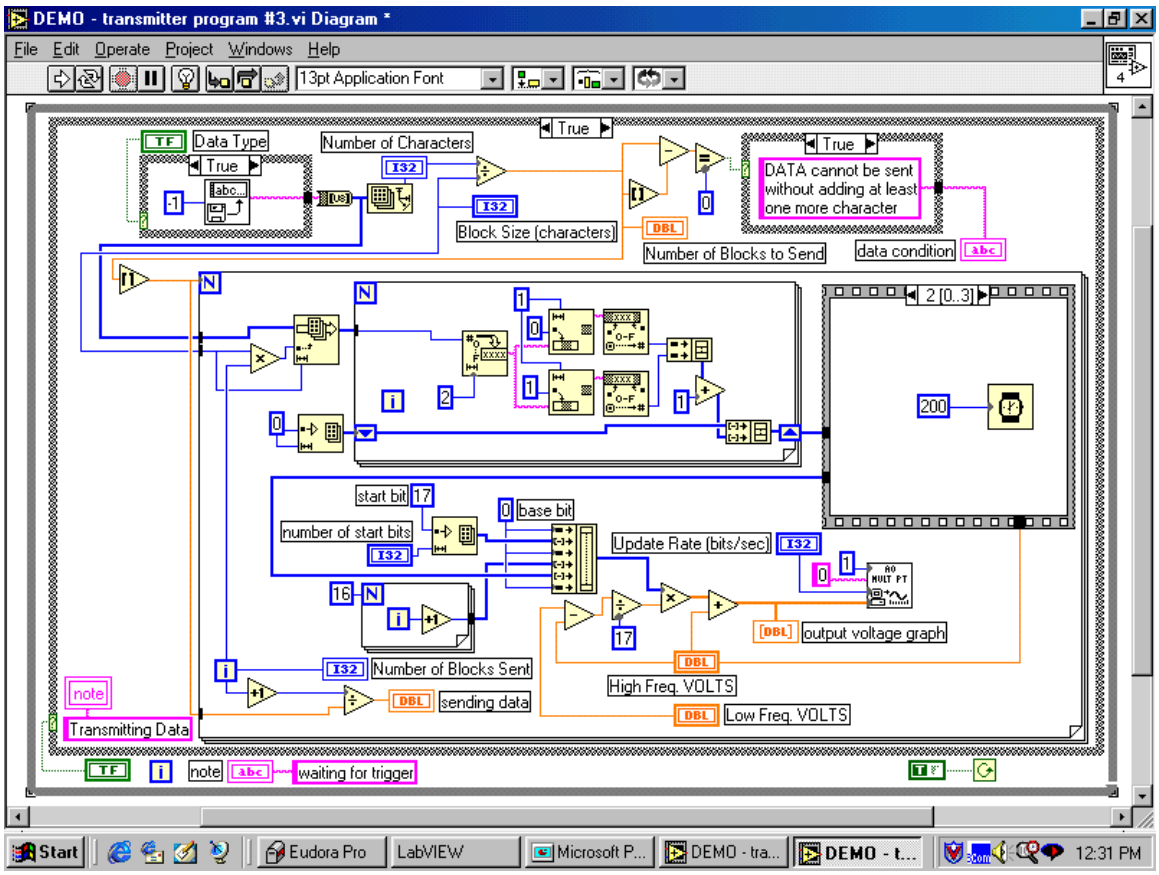

Figure 7.14d Diagram (page 3 of 5) of the ultrasonic transmitter VI.

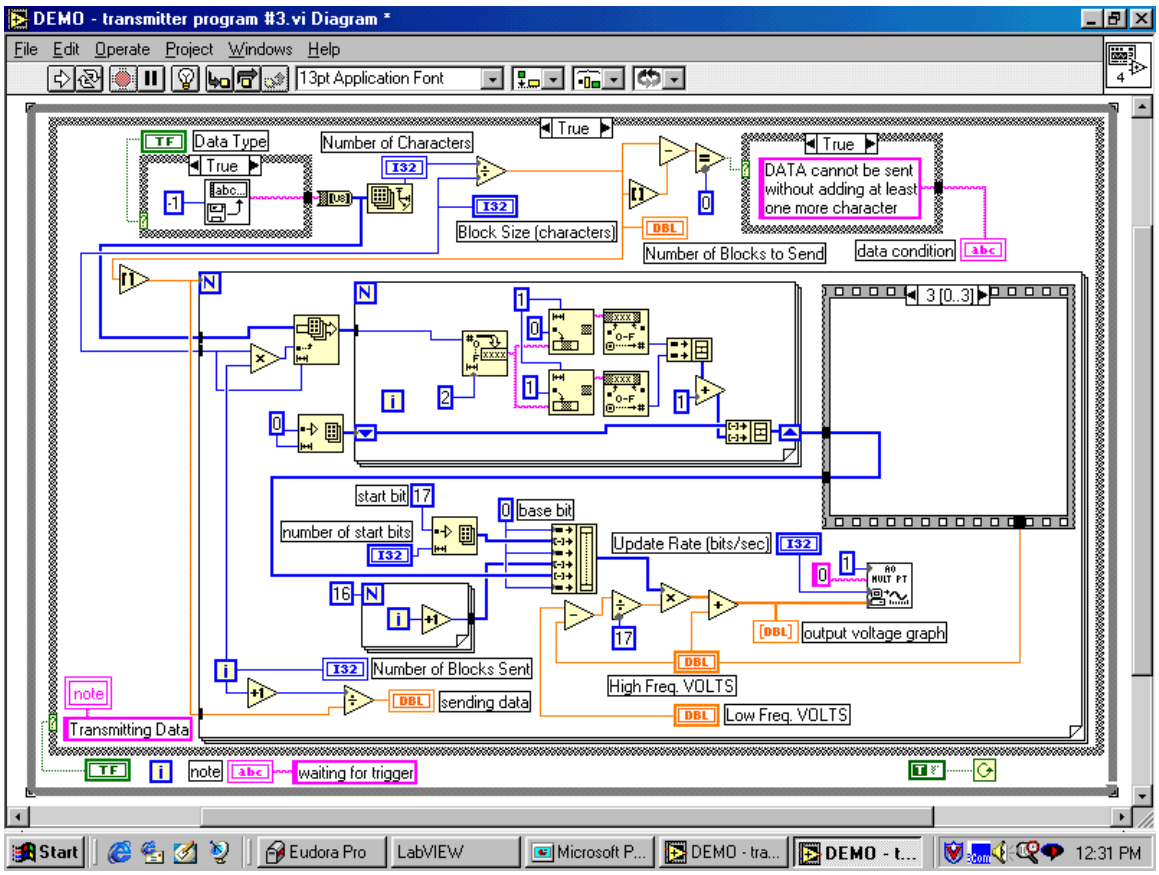

Figure 7.14e Diagram (page 4 of 5) of the ultrasonic transmitter VI.

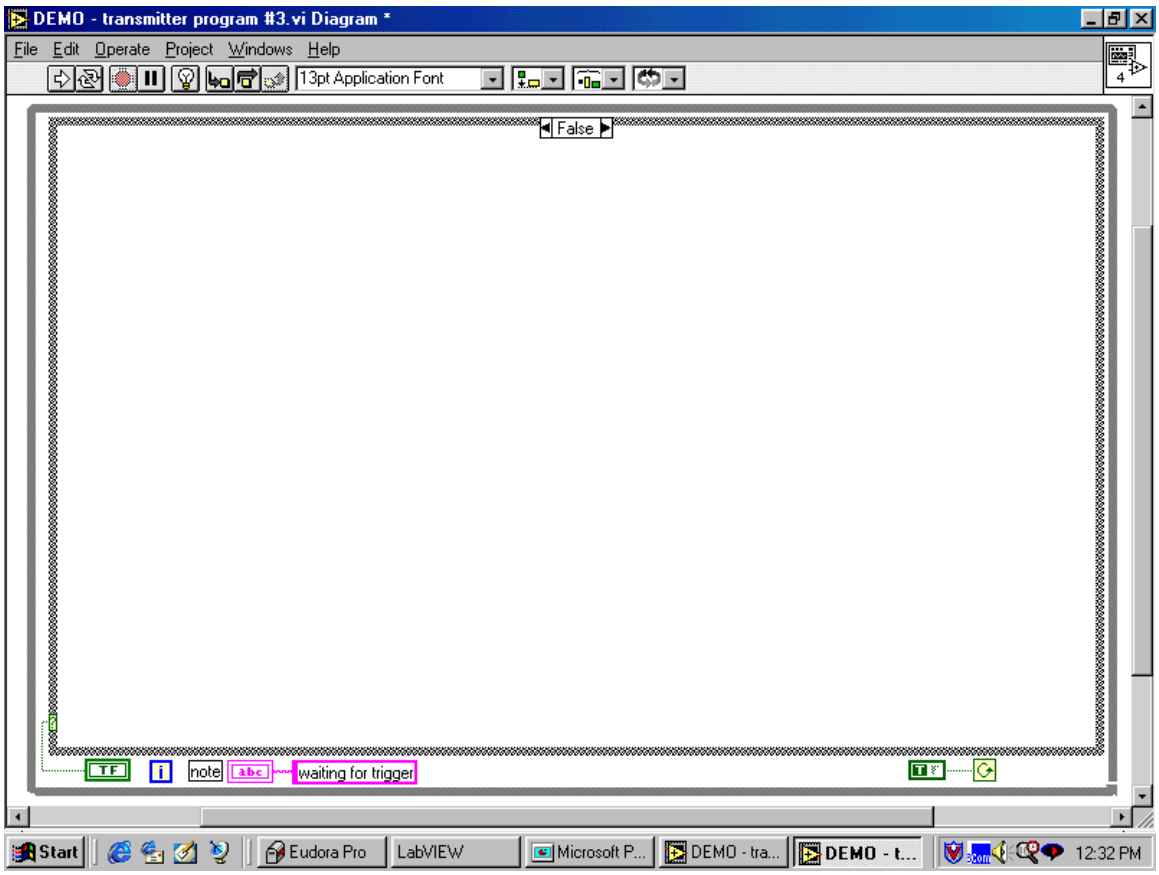

Figure 7.14f Diagram (page 5 of 5) of the ultrasonic transmitter VI.

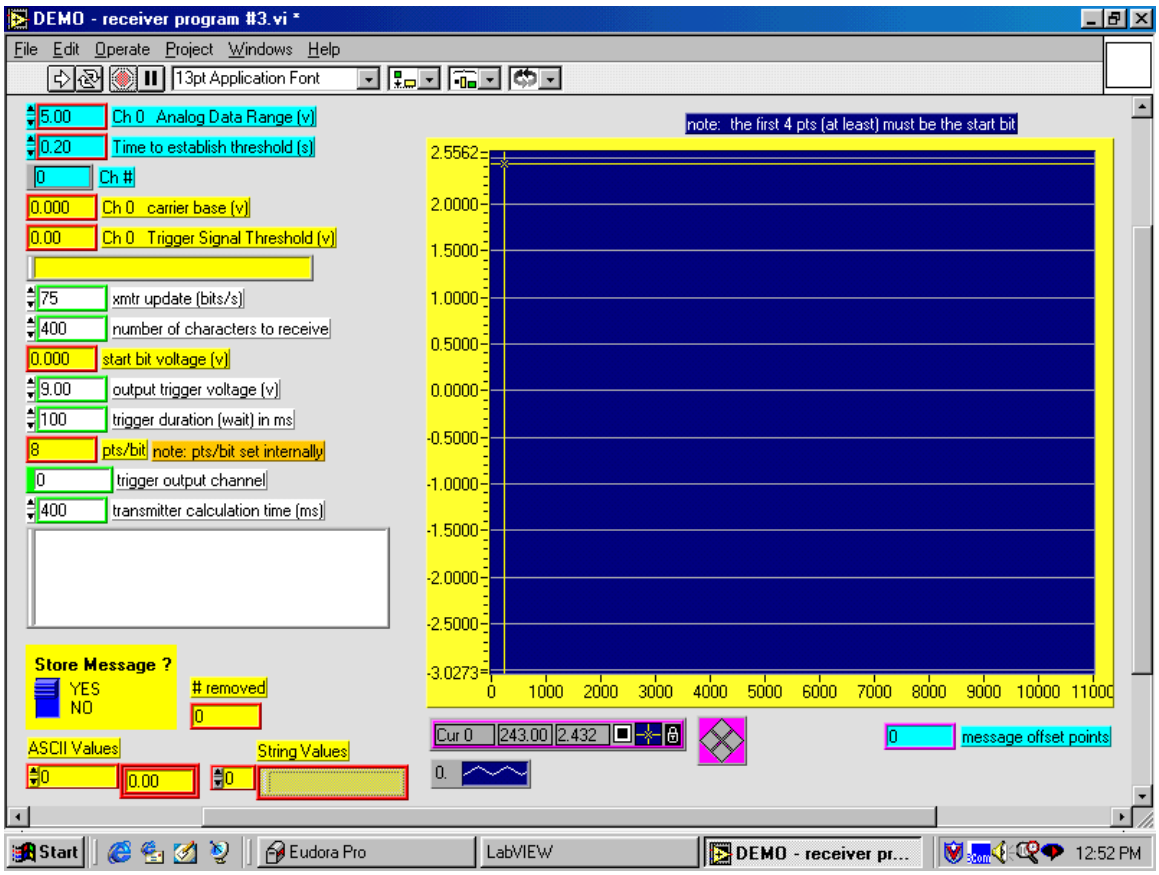

Figure 7.15a Front panel display of the ultrasonic receiver VI.

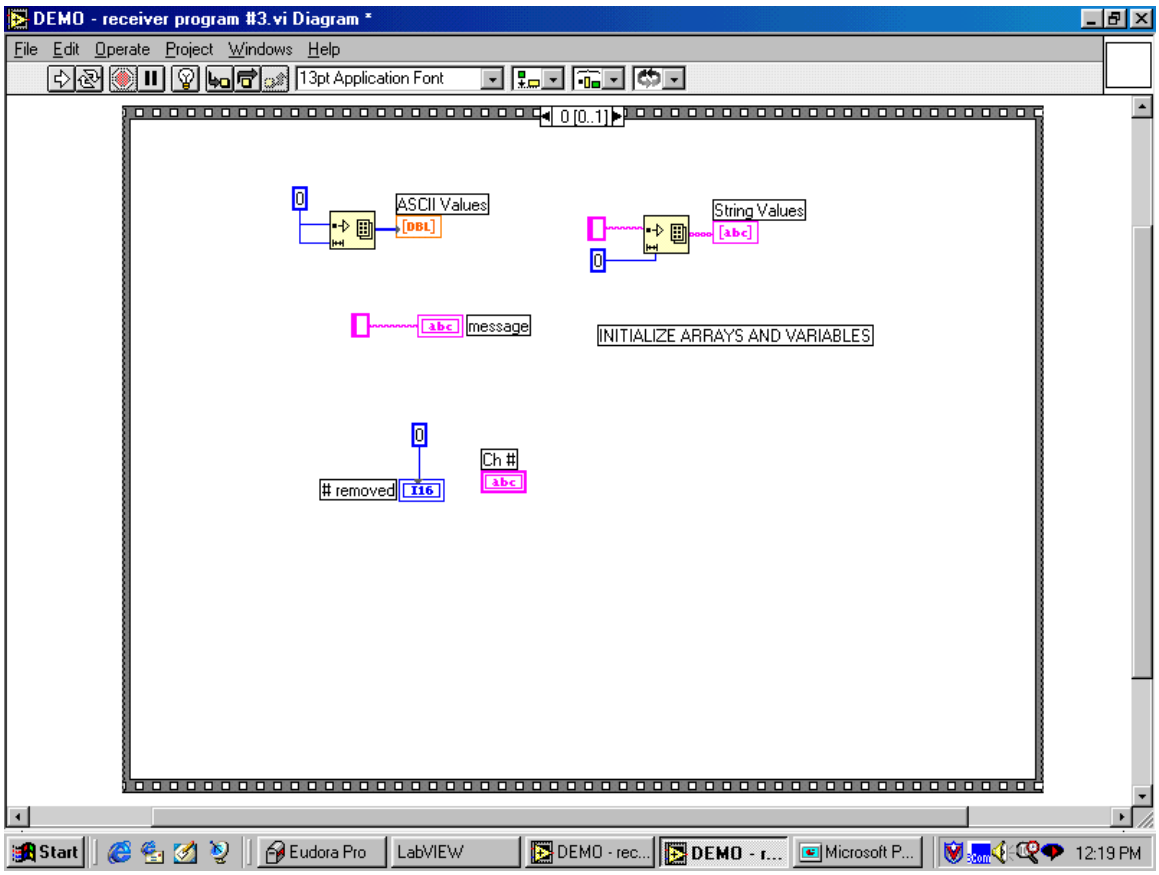

Figure 7.15b Diagram (page 1 of 13) of the ultrasonic receiver VI.

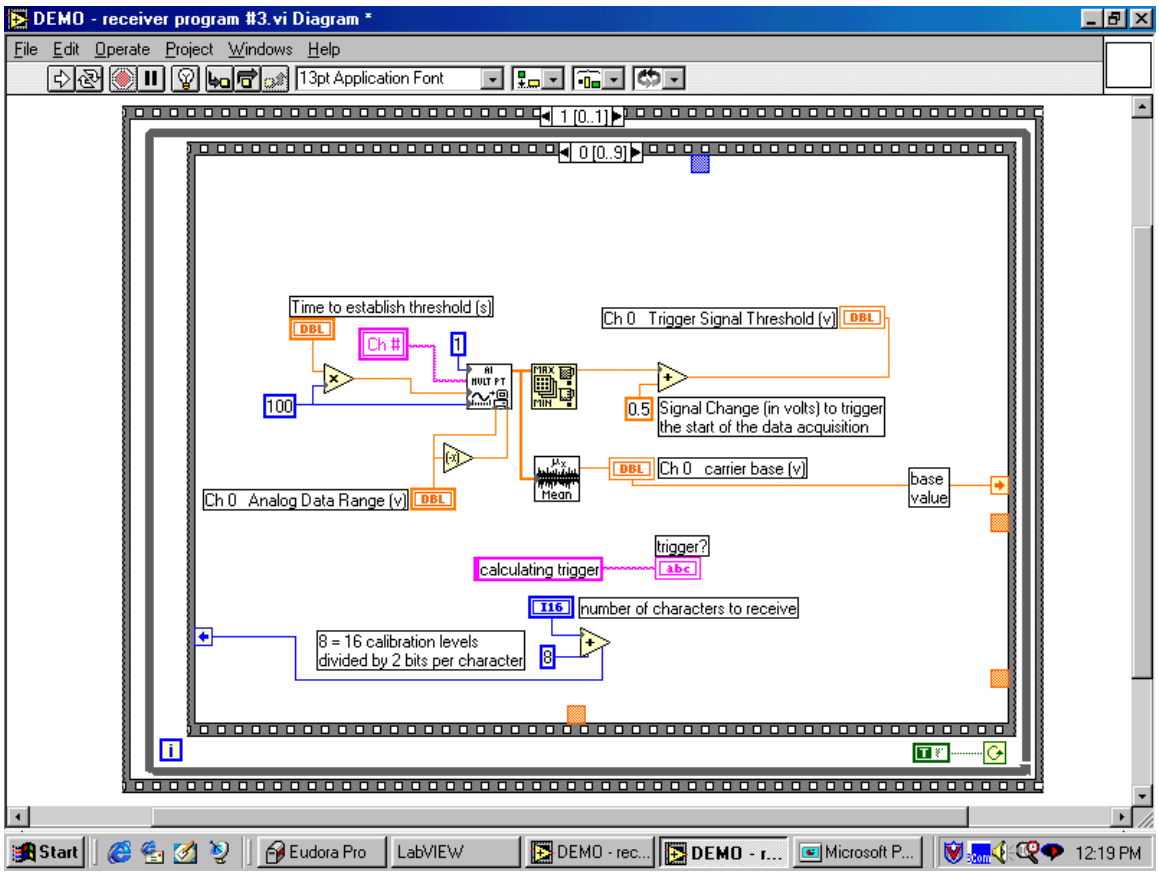

Figure 7.15c Diagram (page 2 of 13) of the ultrasonic receiver VI.

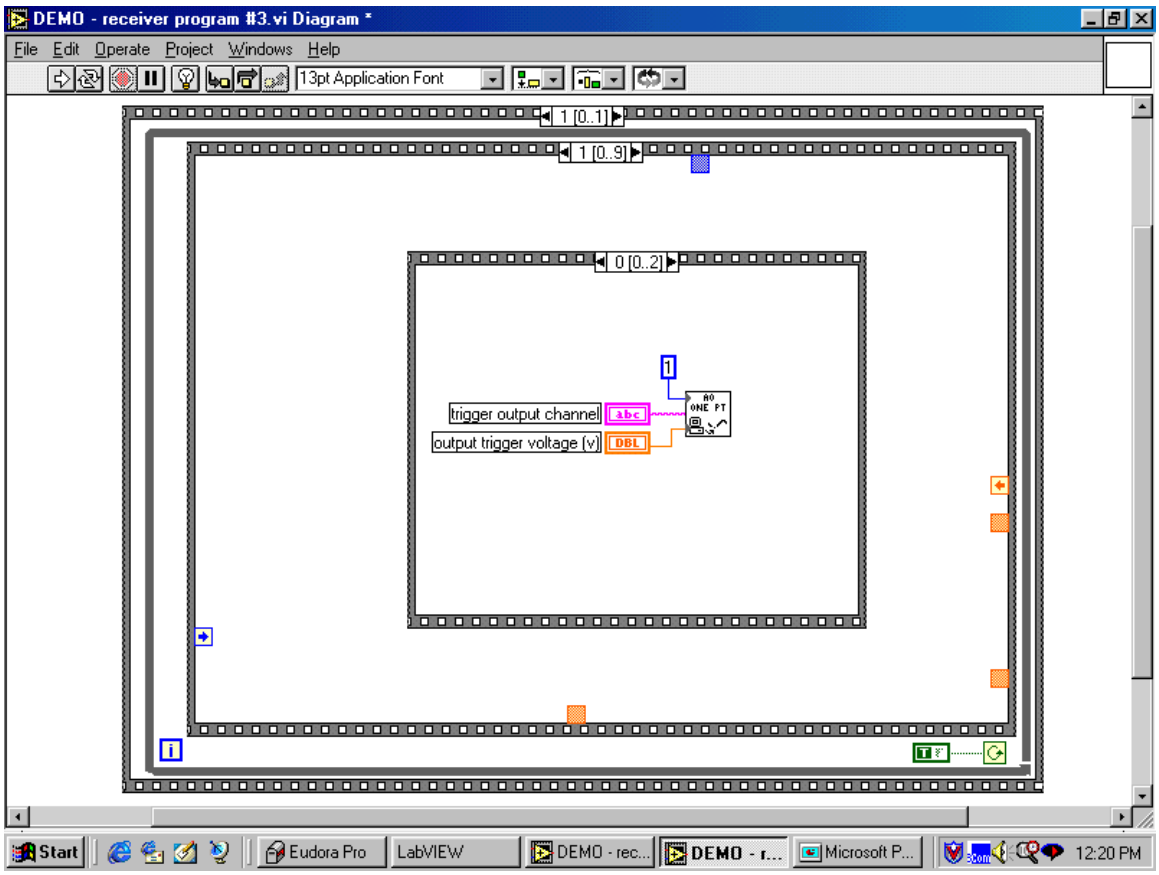

Figure 7.15d Diagram (page 3 of 13) of the ultrasonic receiver VI.

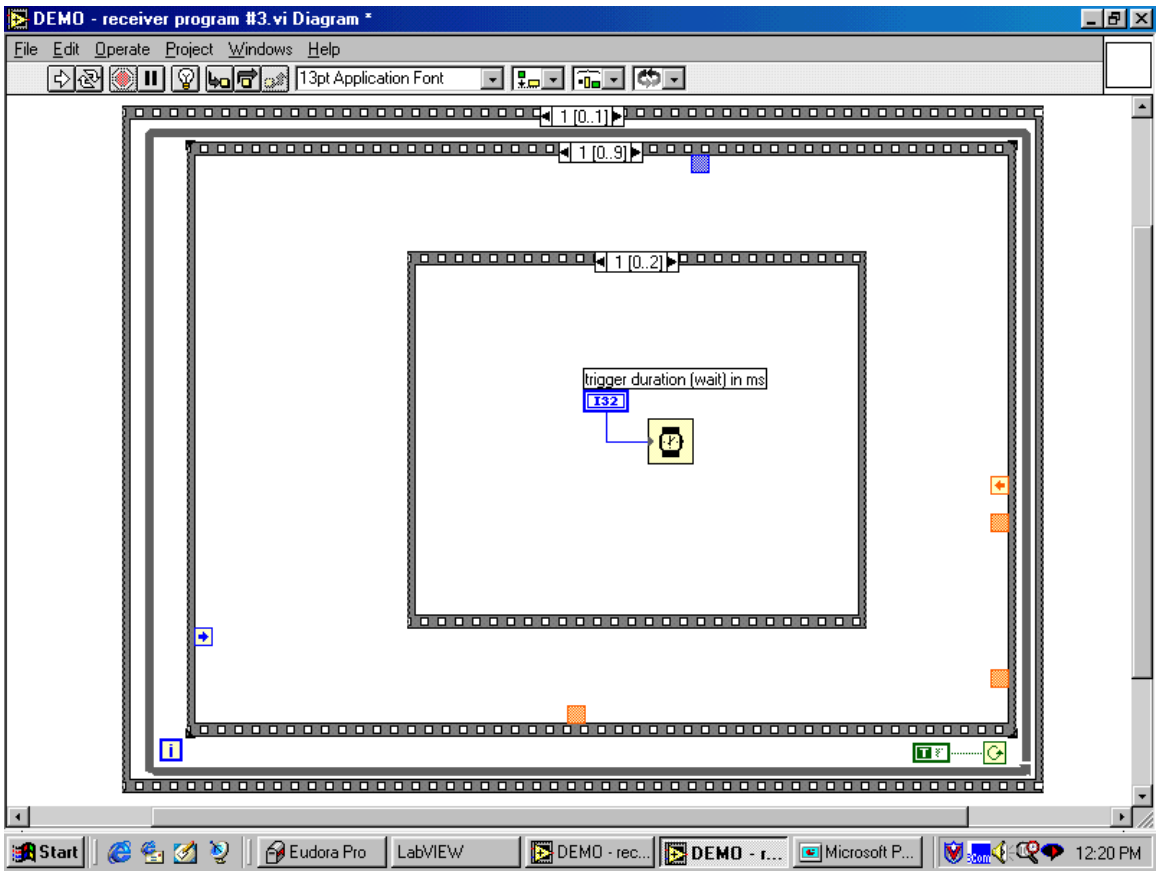

Figure 7.15e Diagram (page 4 of 13) of the ultrasonic receiver VI.

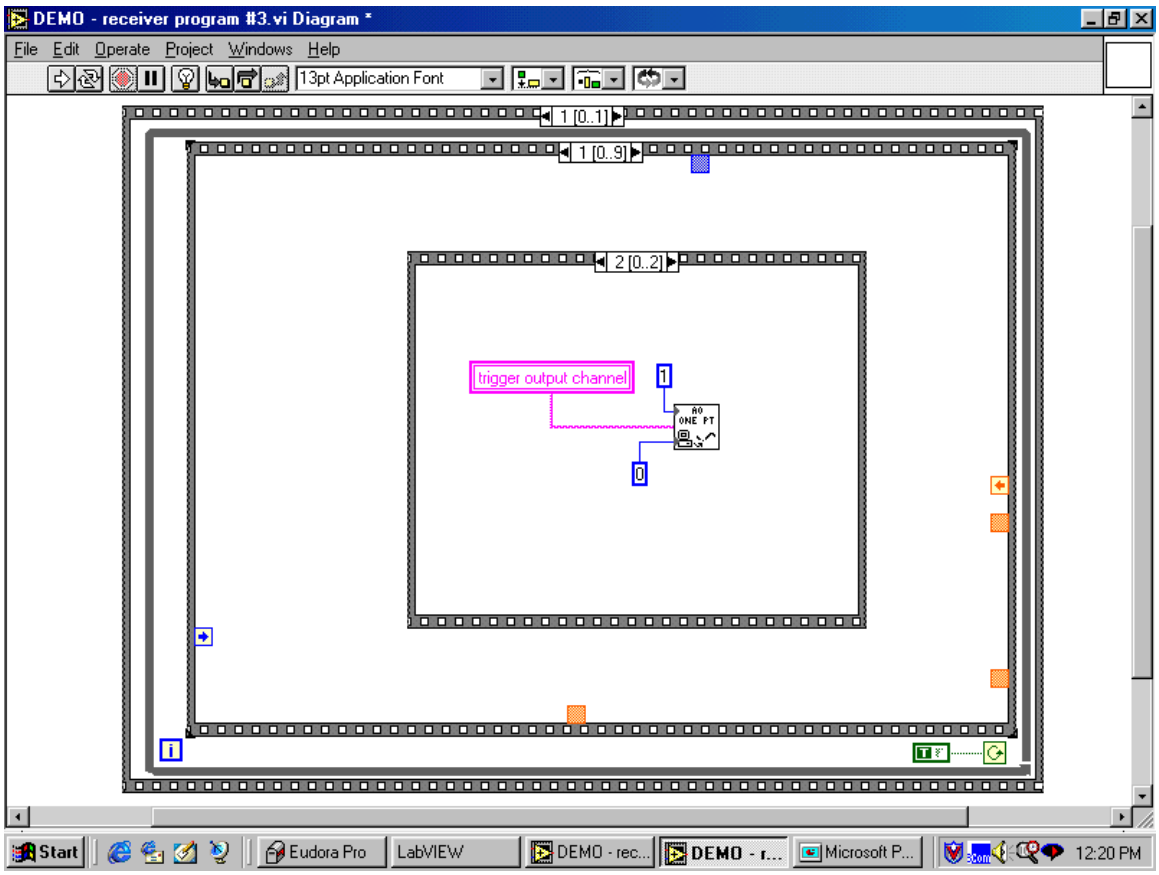

Figure 7.15f Diagram (page 5 of 13) of the ultrasonic receiver VI.

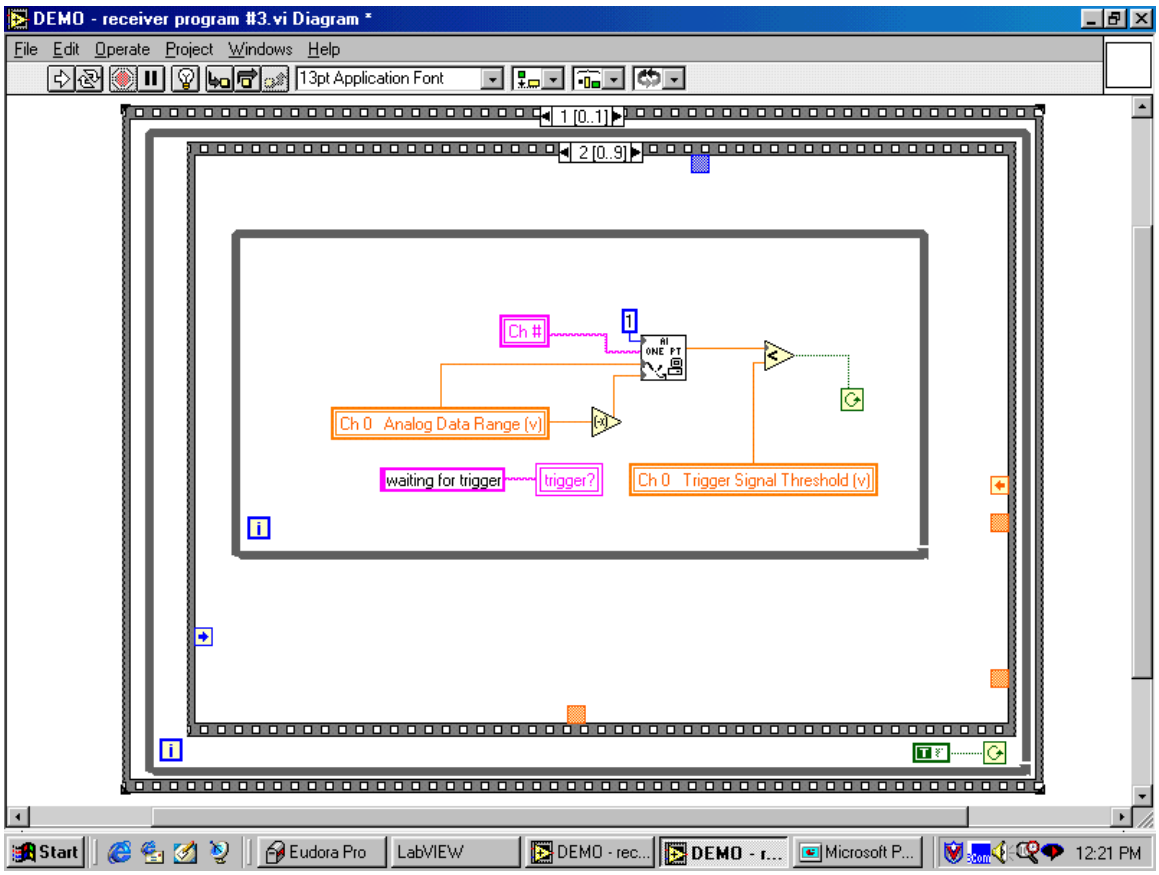

Figure 7.15g Diagram (page 6 of 13) of the ultrasonic receiver VI.

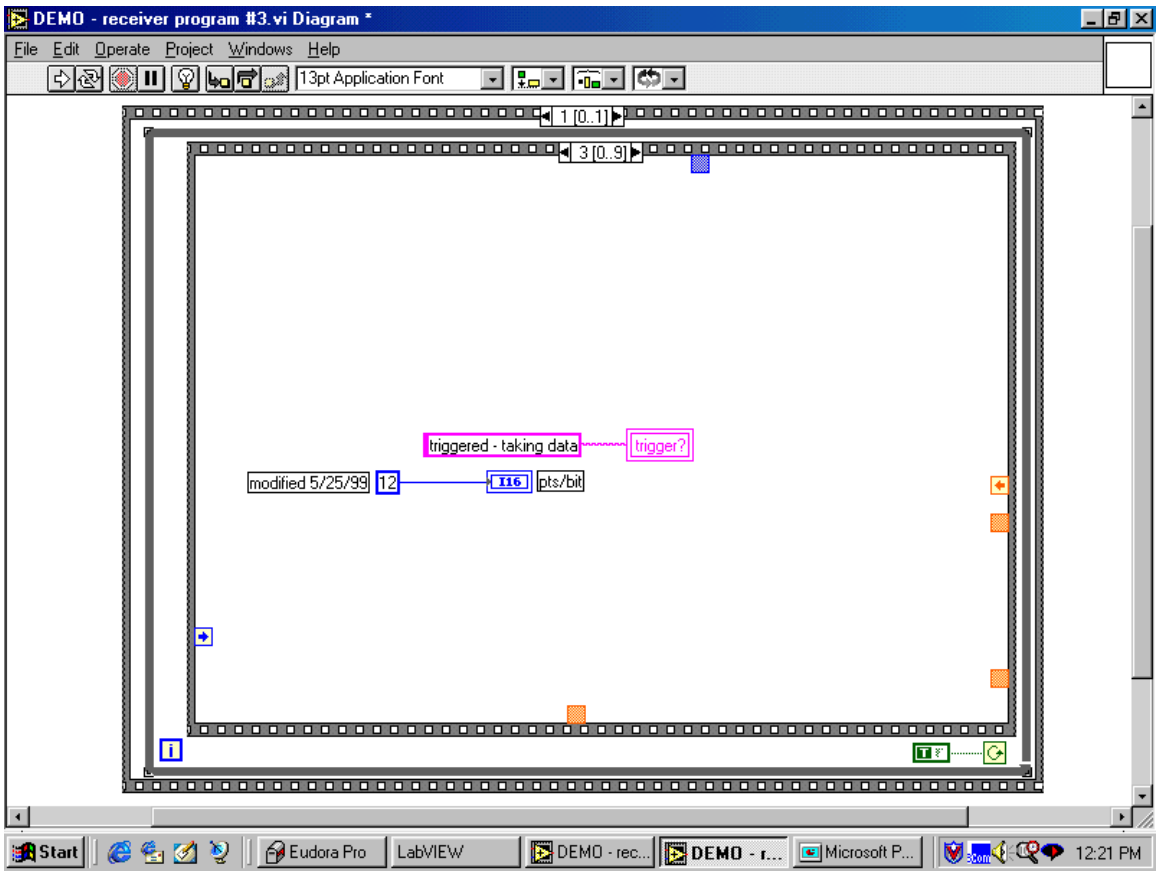

Figure 7.15h Diagram (page 7 of 13) of the ultrasonic receiver VI.

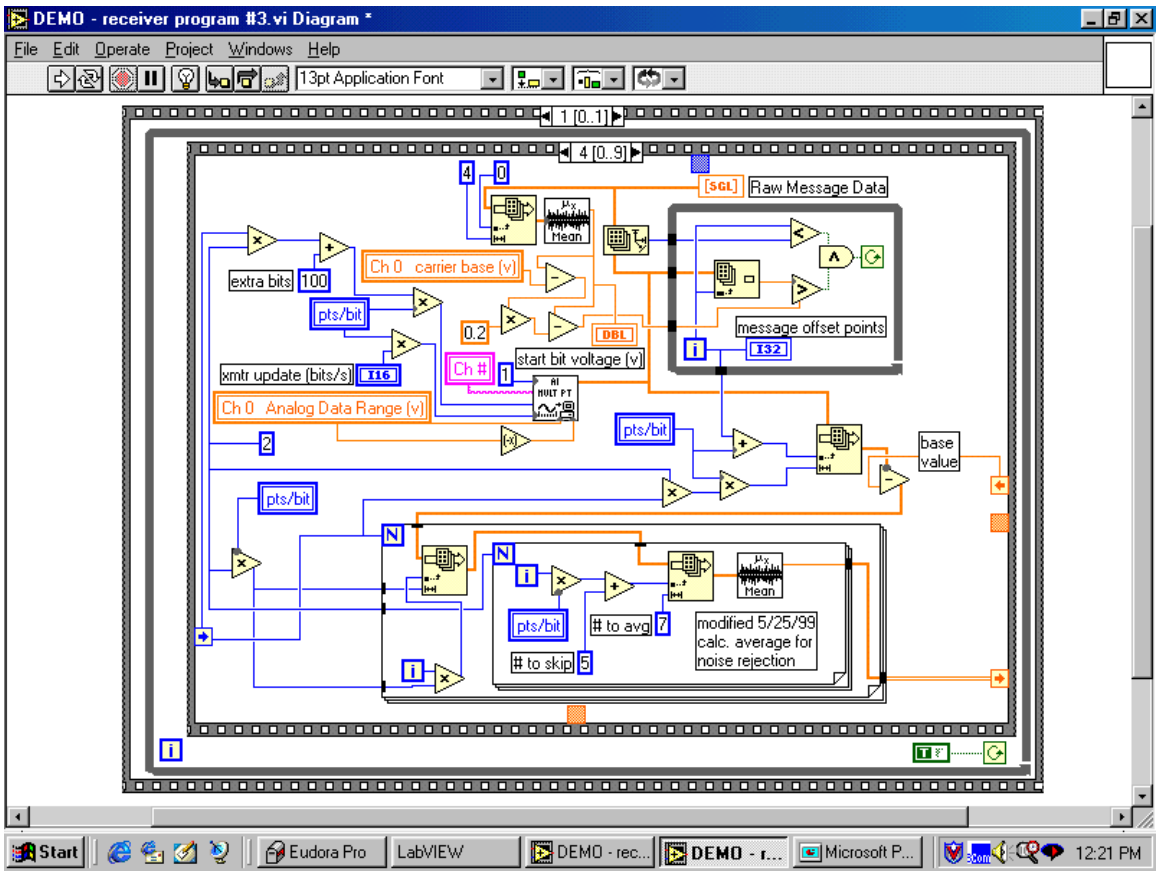

Figure 7.15i Diagram (page 8 of 13) of the ultrasonic receiver VI.

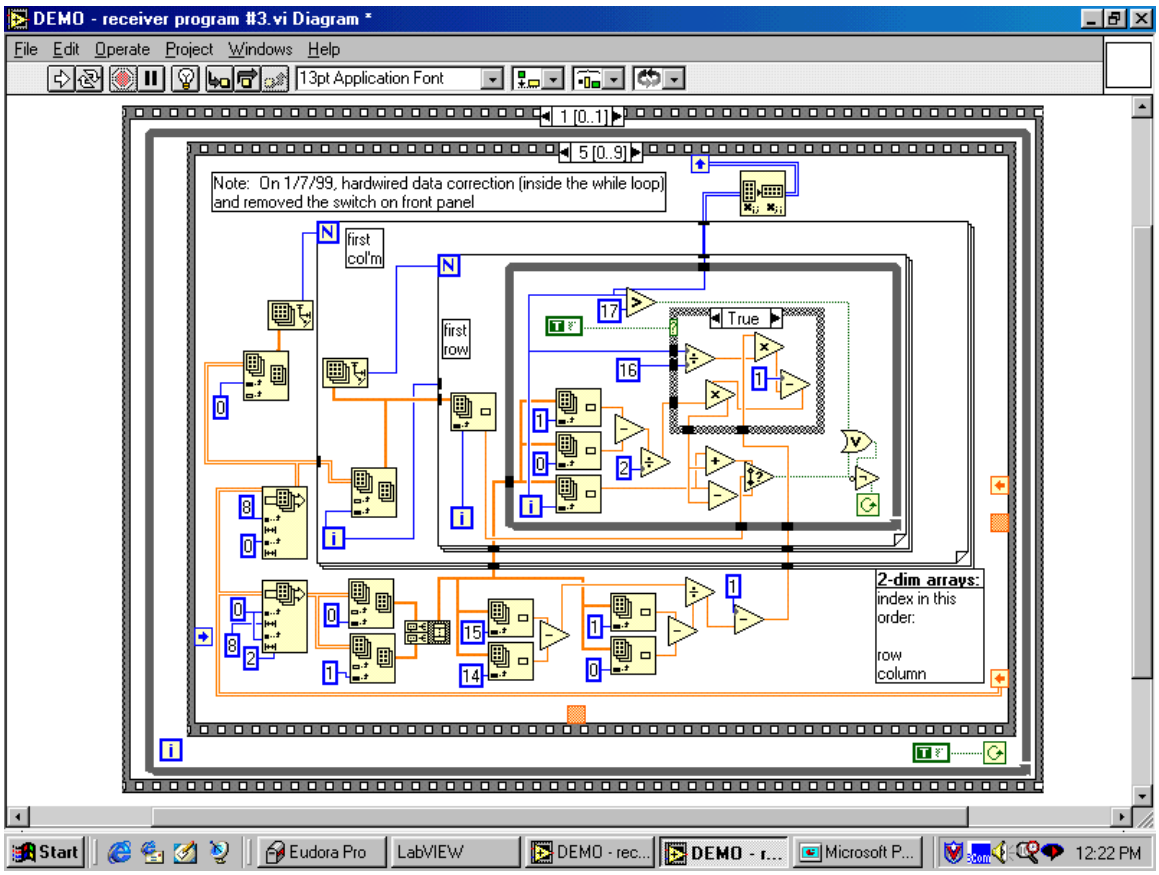

Figure 7.15j Diagram (page 9 of 13) of the ultrasonic receiver VI.

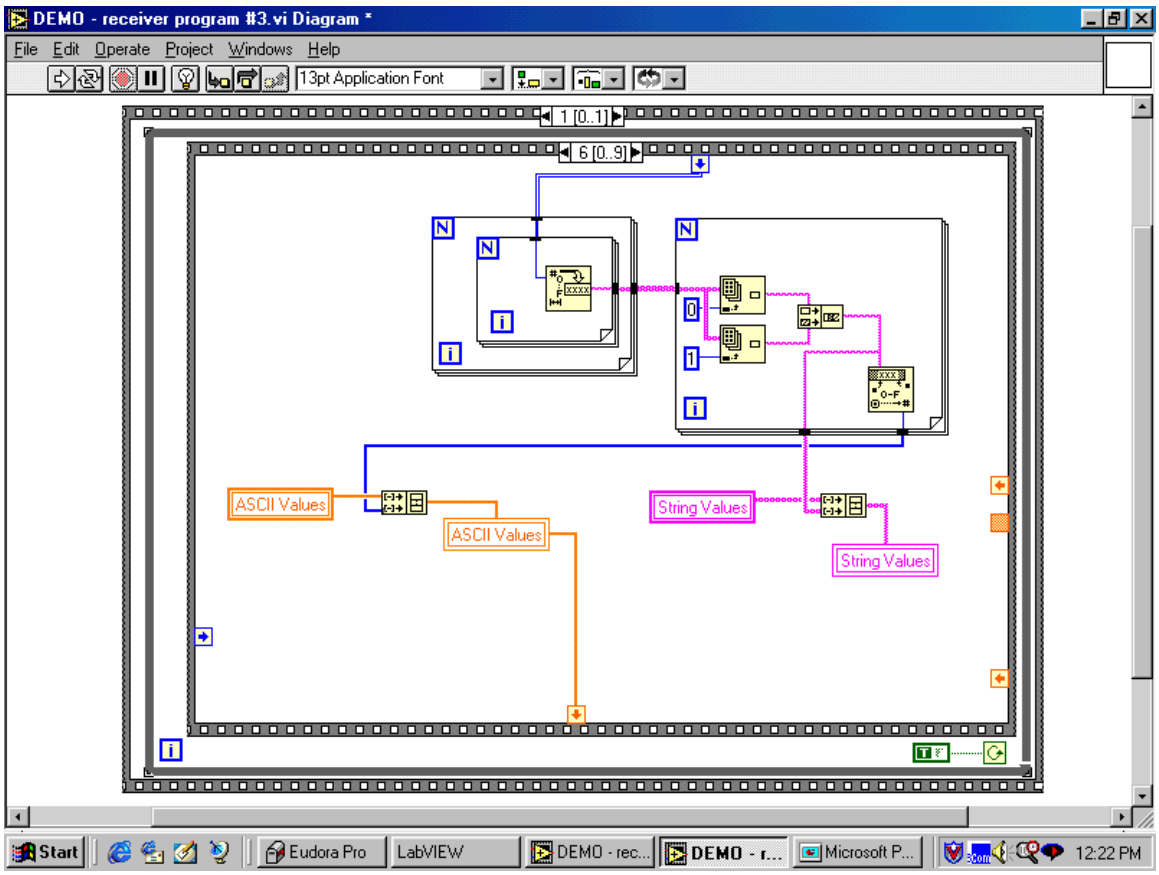

Figure 7.15k Diagram (page 10 of 13) of the ultrasonic receiver VI.

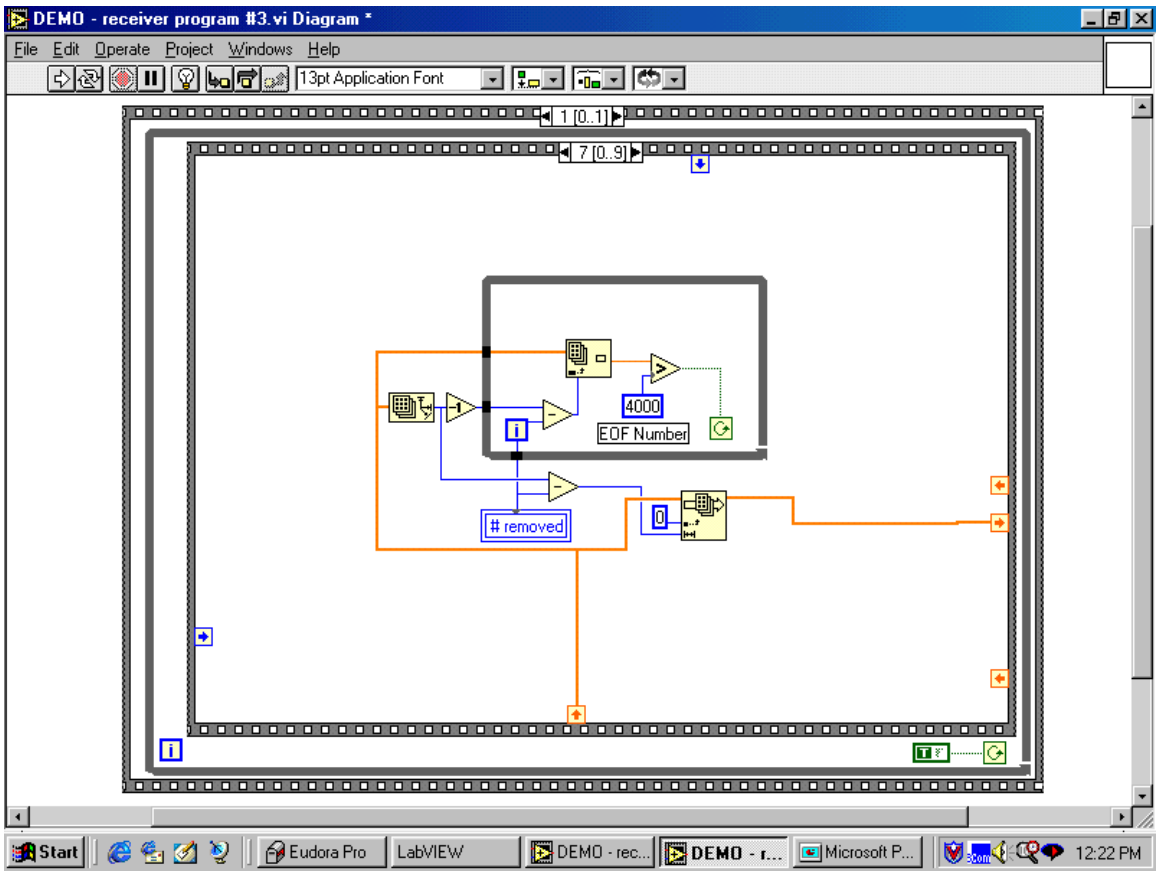

Figure 7.15l Diagram (page 11 of 13) of the ultrasonic receiver VI.

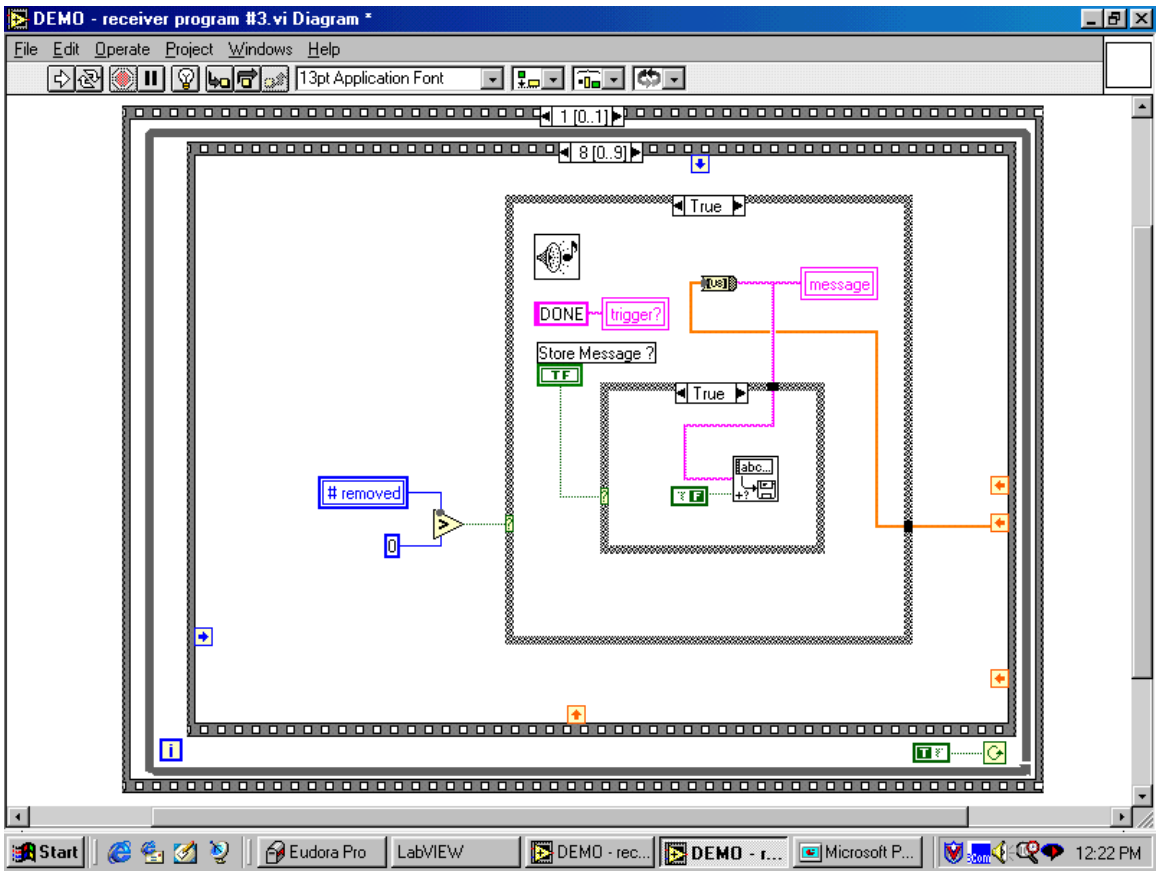

Figure 7.15m Diagram (page 12 of 13) of the ultrasonic receiver VI.

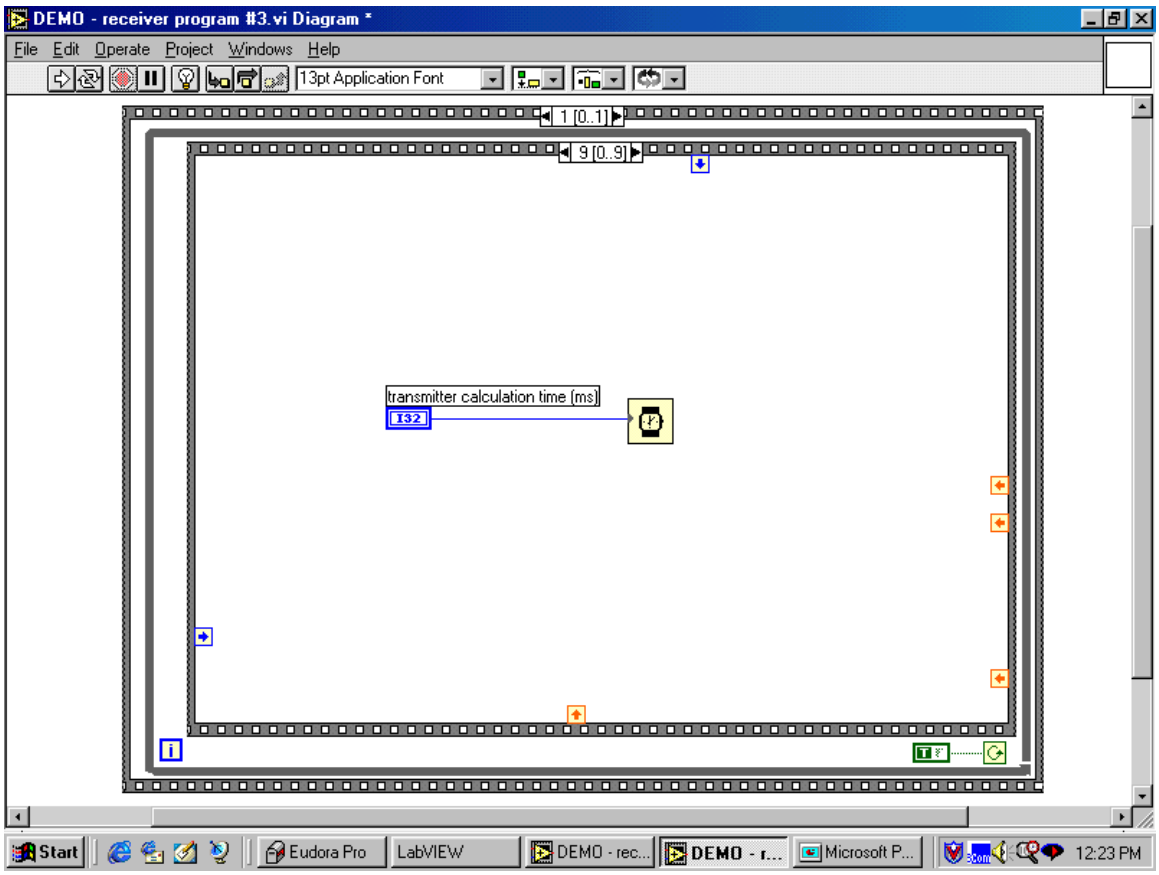

Figure 7.15n Diagram (page 13 of 13) of the ultrasonic receiver VI.

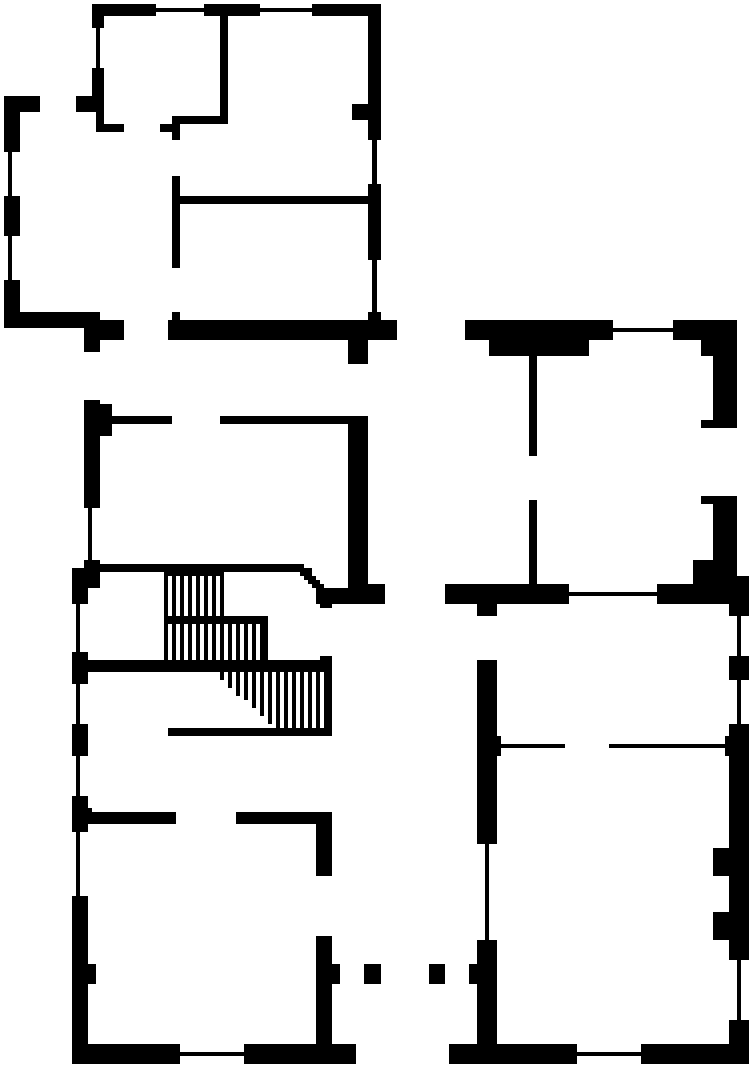

Figure 7.16 Graphic image used to test the ultrasonic communication system. The image (gif format) was reliably transmitted in 92 s, yielding an effective speed of 569 pixels per second.

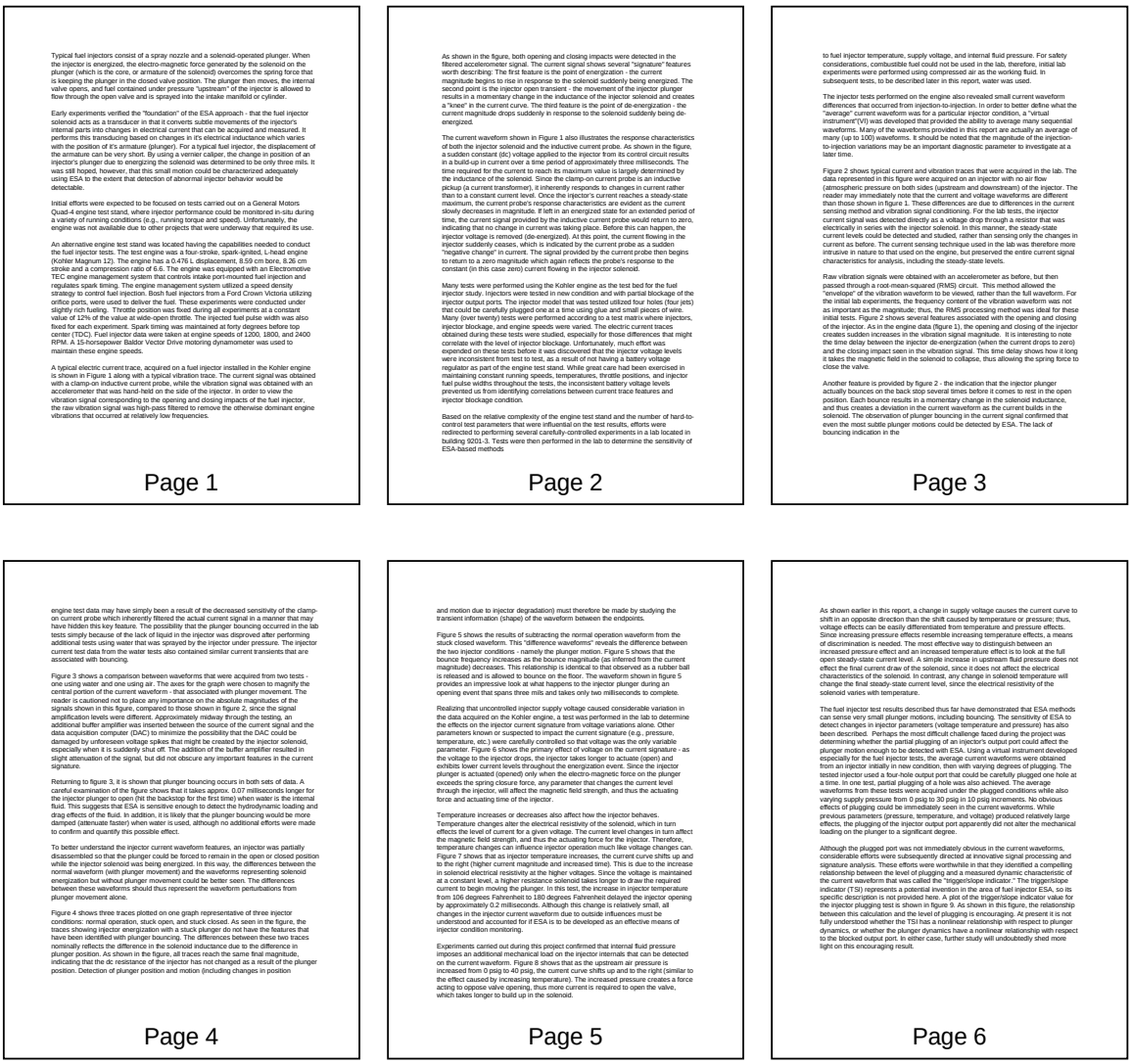
Typical fuel injectors consist of a spray nozzle and a solenoid-operated plunger. When the injector is energized, the electro-magnetic force generated by the solenoid on the plunger (which is the core, or armature of the solenoid) overcomes the spring force that is keeping the plunger in the closed valve position. The plunger then moves, the internal valve opens, and fuel contained under pressure "upstream" of the injector is allowed to flow through the open valve and is sprayed into the intake manifold or cylinder.
Early experiments verified the "foundation" of the ESA approach - that the fuel injector solenoid acts as a transducer in that it converts subtle movements of the injector's internal parts into changes in electrical current that can be acquired and measured. It performs this transducing based on changes in it's electrical inductance which varies with the position of it's armature (plunger). For a typical fuel injector, the displacement of the armature can be very short. By using a vernier caliper, the change in position of an injector's plunger due to energizing the solenoid was determined to be only three mils. It was still hoped, however, that this small motion could be characterized adequately using ESA to the extent that detection of abnormal injector behavior would be detectable.
Initial efforts were expected to be focused on tests carried out on a General Motors Quad-4 engine test stand, where injector performance could be monitored in-situ during a variety of running conditions (e.g., running torque and speed). Unfortunately, the engine was not available due to other projects that were underway that required its use.
An alternative engine test stand was located having the capabilities needed to conduct the fuel injector tests. The test engine was a four-stroke, spark-ignited, L-head engine (Kohler Magnum 12). The engine has a 0.476 L displacement, 8.59 cm bore, 8.26 cm stroke and a compression ratio of 6.6. The engine was equipped with an Electromotive TEC engine management system that controls intake port-mounted fuel injection and regulates spark timing. The engine management system utilized a speed density strategy to control fuel injection. Bosh fuel injectors from a Ford Crown Victoria utilizing orifice ports, were used to deliver the fuel. These experiments were conducted under slightly rich fueling. Throttle position was fixed during all experiments at a constant value of 12% of the value at wide-open throttle. The injected fuel pulse width was also fixed for each experiment. Spark timing was maintained at forty degrees before top center (TDC). Fuel injector data were taken at engine speeds of 1200, 1800, and 2400 RPM. A 15-horsepower Baldor Vector Drive motoring dynamometer was used to maintain these engine speeds.
A typical electric current trace, acquired on a fuel injector installed in the Kohler engine is shown in Figure 1 along with a typical vibration trace. The current signal was obtained with a clamp-on inductive current probe, while the vibration signal was obtained with an accelerometer that was hand-held on the side of the injector. In order to view the vibration signal corresponding to the opening and closing impacts of the fuel injector, the raw vibration signal was high-pass filtered to remove the otherwise dominant engine vibrations that occurred at relatively low frequencies.
Page 1
As shown in the figure, both opening and closing impacts were detected in the filtered accelerometer signal. The current signal shows several "signature" features worth describing: The first feature is the point of energization - the current magnitude begins to rise in response to the solenoid suddenly being energized. The second point is the injector open transient - the movement of the injector plunger results in a momentary change in the inductance of the injector solenoid and creates a "knee" in the current curve. The third feature is the point of de-energization - the current magnitude drops suddenly in response to the solenoid suddenly being de-energized.
The current waveform shown in Figure 1 also illustrates the response characteristics of both the injector solenoid and the inductive current probe. As shown in the figure, a sudden constant (dc) voltage applied to the injector from its control circuit results in a build-up in current over a time period of approximately three milliseconds. The time required for the current to reach its maximum value is largely determined by the inductance of the solenoid. Since the clamp-on current probe is an inductive pickup (a current transformer), it inherently responds to changes in current rather than to a constant current level. Once the injector's current reaches a steady-state maximum, the current probe's response characteristics are evident as the current slowly decreases in magnitude. If left in an energized state for an extended period of time, the current signal provided by the inductive current probe would return to zero, indicating that no change in current was taking place. Before this can happen, the injector voltage is removed (de-energized). At this point, the current flowing in the injector suddenly ceases, which is indicated by the current probe as a sudden "negative change" in current. The signal provided by the current probe then begins to return to a zero magnitude which again reflects the probe's response to the constant (in this case zero) current flowing in the injector solenoid.
Many tests were performed using the Kohler engine as the test bed for the fuel injector study. Injectors were tested in new condition and with partial blockage of the injector output ports. The injector model that was tested utilized four holes (four jets) that could be carefully plugged one at a time using glue and small pieces of wire. Many (over twenty) tests were performed according to a test matrix where injectors, injector blockage, and engine speeds were varied. The electric current traces obtained during these tests were studied, especially for those differences that might correlate with the level of injector blockage. Unfortunately, much effort was expended on these tests before it was discovered that the injector voltage levels were inconsistent from test to test, as a result of not having a battery voltage regulator as part of the engine test stand. While great care had been exercised in maintaining constant running speeds, temperatures, throttle positions, and injector fuel pulse widths throughout the tests, the inconsistent battery voltage levels prevented us from identifying correlations between current trace features and injector blockage condition.
Based on the relative complexity of the engine test stand and the number of hard-to-control test parameters that were influential on the test results, efforts were redirected to performing several carefully-controlled experiments in a lab located in building 9201-3. Tests were then performed in the lab to determine the sensitivity of ESA-based methods
Page 2
to fuel injector temperature, supply voltage, and internal fluid pressure. For safety considerations, combustible fuel could not be used in the lab, therefore, initial lab experiments were performed using compressed air as the working fluid. In subsequent tests, to be described later in this report, water was used.
The injector tests performed on the engine also revealed small current waveform differences that occurred from injection-to-injection. In order to better define what the "average" current waveform was for a particular injector condition, a "virtual instrument"(VI) was developed that provided the ability to average many sequential waveforms. Many of the waveforms provided in this report are actually an average of many (up to 100) waveforms. It should be noted that the magnitude of the injection-to-injection variations may be an important diagnostic parameter to investigate at a later time.
Figure 2 shows typical current and vibration traces that were acquired in the lab. The data represented in this figure were acquired on an injector with no air flow (atmospheric pressure on both sides (upstream and downstream) of the injector. The reader may immediately note that the current and voltage waveforms are different than those shown in figure 1. These differences are due to differences in the current sensing method and vibration signal conditioning. For the lab tests, the injector current signal was detected directly as a voltage drop through a resistor that was electrically in series with the injector solenoid. In this manner, the steady-state current levels could be detected and studied, rather than sensing only the changes in current as before. The current sensing technique used in the lab was therefore more intrusive in nature to that used on the engine, but preserved the entire current signal characteristics for analysis, including the steady-state levels.
Raw vibration signals were obtained with an accelerometer as before, but then passed through a root-mean-squared (RMS) circuit. This method allowed the "envelope" of the vibration waveform to be viewed, rather than the full waveform. For the initial lab experiments, the frequency content of the vibration waveform was not as important as the magnitude; thus, the RMS processing method was ideal for these initial tests. Figure 2 shows several features associated with the opening and closing of the injector. As in the engine data (figure 1), the opening and closing of the injector creates sudden increases in the vibration signal magnitude. It is interesting to note the time delay between the injector de-energization (when the current drops to zero) and the closing impact seen in the vibration signal. This time delay shows how it long it takes the magnetic field in the solenoid to collapse, thus allowing the spring force to close the valve.
Another feature is provided by figure 2 - the indication that the injector plunger actually bounces on the back stop several times before it comes to rest in the open position. Each bounce results in a momentary change in the solenoid inductance, and thus creates a deviation in the current waveform as the current builds in the solenoid. The observation of plunger bouncing in the current signal confirmed that even the most subtle plunger motions could be detected by ESA. The lack of bouncing indication in the
Page 3
engine test data may have simply been a result of the decreased sensitivity of the clamp-on current probe which inherently filtered the actual current signal in a manner that may have hidden this key feature. The possibility that the plunger bouncing occurred in the lab tests simply because of the lack of liquid in the injector was disproved after performing additional tests using water that was sprayed by the injector under pressure. The injector current test data from the water tests also contained similar current transients that are associated with bouncing.
Figure 3 shows a comparison between waveforms that were acquired from two tests - one using water and one using air. The axes for the graph were chosen to magnify the central portion of the current waveform - that associated with plunger movement. The reader is cautioned not to place any importance on the absolute magnitudes of the signals shown in this figure, compared to those shown in figure 2, since the signal amplification levels were different. Approximately midway through the testing, an additional buffer amplifier was inserted between the source of the current signal and the data acquisition computer (DAC) to minimize the possibility that the DAC could be damaged by unforeseen voltage spikes that might be created by the injector solenoid, especially when it is suddenly shut off. The addition of the buffer amplifier resulted in slight attenuation of the signal, but did not obscure any important features in the current signature.
Returning to figure 3, it is shown that plunger bouncing occurs in both sets of data. A careful examination of the figure shows that it takes approx. 0.07 milliseconds longer for the injector plunger to open (hit the backstop for the first time) when water is the internal fluid. This suggests that ESA is sensitive enough to detect the hydrodynamic loading and drag effects of the fluid. In addition, it is likely that the plunger bouncing would be more damped (attenuate faster) when water is used, although no additional efforts were made to confirm and quantify this possible effect.
To better understand the injector current waveform features, an injector was partially disassembled so that the plunger could be forced to remain in the open or closed position while the injector solenoid was being energized. In this way, the differences between the normal waveform (with plunger movement) and the waveforms representing solenoid energization but without plunger movement could be better seen. The differences between these waveforms should thus represent the waveform perturbations from plunger movement alone.
Figure 4 shows three traces plotted on one graph representative of three injector conditions: normal operation, stuck open, and stuck closed. As seen in the figure, the traces showing injector energization with a stuck plunger do not have the features that have been identified with plunger bouncing. The differences between these two traces nominally reflects the difference in the solenoid inductance due to the difference in plunger position. As shown in the figure, all traces reach the same final magnitude, indicating that the dc resistance of the injector has not changed as a result of the plunger position. Detection of plunger position and motion (including changes in position
Page 4
and motion due to injector degradation) must therefore be made by studying the transient information (shape) of the waveform between the endpoints.
Figure 5 shows the results of subtracting the normal operation waveform from the stuck closed waveform. This "difference waveforms" reveals the difference between the two injector conditions - namely the plunger motion. Figure 5 shows that the bounce frequency increases as the bounce magnitude (as inferred from the current magnitude) decreases. This relationship is identical to that observed as a rubber ball is released and is allowed to bounce on the floor. The waveform shown in figure 5 provides an impressive look at what happens to the injector plunger during an opening event that spans three mils and takes only two milliseconds to complete.
Realizing that uncontrolled injector supply voltage caused considerable variation in the data acquired on the Kohler engine, a test was performed in the lab to determine the effects on the injector current signature from voltage variations alone. Other parameters known or suspected to impact the current signature (e.g., pressure, temperature, etc.) were carefully controlled so that voltage was the only variable parameter. Figure 6 shows the primary effect of voltage on the current signature - as the voltage to the injector drops, the injector takes longer to actuate (open) and exhibits lower current levels throughout the energization event. Since the injector plunger is actuated (opened) only when the electro-magnetic force on the plunger exceeds the spring closure force, any parameter that changes the current level through the injector, will affect the magnetic field strength, and thus the actuating force and actuating time of the injector.
Temperature increases or decreases also affect how the injector behaves. Temperature changes alter the electrical resistivity of the solenoid, which in turn effects the level of current for a given voltage. The current level changes in turn affect the magnetic field strength, and thus the actuating force for the injector. Therefore, temperature changes can influence injector operation much like voltage changes can. Figure 7 shows that as injector temperatures increase, the current curve shifts up and to the right (higher current magnitude and increased time). This is due to the increase in solenoid electrical resistivity at the higher voltages. Since the voltage is maintained at a constant level, a higher resistance solenoid takes longer to draw the required current to begin moving the plunger. In this test, the increase in injector temperature from 106 degrees Fahrenheit to 180 degrees Fahrenheit delayed the injector opening by approximately 0.2 milliseconds. Although this change is relatively small, all changes in the injector current waveform due to outside influences must be understood and accounted for if ESA is to be developed as an effective means of injector condition monitoring.
Experiments carried out during this project confirmed that internal fluid pressure imposes an additional mechanical load on the injector internals that can be detected on the current waveform. Figure 8 shows that as the upstream air pressure is increased from 0 psig to 40 psig, the current curve shifts up and to the right (similar to the effect caused by increasing temperature). The increased pressure creates a force acting to oppose valve opening, thus more current is required to open the valve, which takes longer to build up in the solenoid.
Page 5
As shown earlier in this report, a change in supply voltage causes the current curve to shift in an opposite direction than the shift caused by temperature or pressure; thus, voltage effects can be easily differentiated from temperature and pressure effects. Since increasing pressure effects resemble increasing temperature effects, a means of discrimination is needed. The most effective way to distinguish between an increased pressure effect and an increased temperature effect is to look at the full open steady-state current level. A simple increase in upstream fluid pressure does not effect the final current draw of the solenoid, since it does not affect the electrical characteristics of the solenoid. In contrast, any change in solenoid temperature will change the final steady-state current level, since the electrical resistivity of the solenoid varies with temperature.
The fuel injector test results described thus far have demonstrated that ESA methods can sense very small plunger motions, including bouncing. The sensitivity of ESA to detect changes in injector parameters (voltage temperature and pressure) has also been described. Perhaps the most difficult challenge faced during the project was determining whether the partial plugging of an injector's output port could affect the plunger motion enough to be detected with ESA. Using a virtual instrument developed especially for the fuel injector tests, the average current waveforms were obtained from an injector initially in new condition, then with varying degrees of plugging. The tested injector used a four-hole output port that could be carefully plugged one hole at a time. In one test, partial plugging of a hole was also achieved. The average waveforms from these tests were acquired under the plugged conditions while also varying supply pressure from 0 psig to 30 psig in 10 psig increments. No obvious effects of plugging could be immediately seen in the current waveforms. While previous parameters (pressure, temperature, and voltage) produced relatively large effects, the plugging of the injector output port apparently did not alter the mechanical loading on the plunger to a significant degree.
Although the plugged port was not immediately obvious in the current waveforms, considerable efforts were subsequently directed at innovative signal processing and signature analysis. These efforts were worthwhile in that they identified a compelling relationship between the level of plugging and a measured dynamic characteristic of the current waveform that was called the "trigger/slope indicator." The trigger/slope indicator (TSI) represents a potential invention in the area of fuel injector ESA, so its specific description is not provided here. A plot of the trigger/slope indicator value for the injector plugging test is shown in figure 9. As shown in this figure, the relationship between this calculation and the level of plugging is encouraging. At present it is not fully understood whether the TSI has a nonlinear relationship with respect to plunger dynamics, or whether the plunger dynamics have a nonlinear relationship with respect to the blocked output port. In either case, further study will undoubtedly shed more light on this encouraging result.
Page 6

Figure 7.17 Six-page text file used to test the ultrasonic communication system. After compression, the file (zip format) was reliably transmitted in 3 min, 56 s, yielding an effective speed of over 85 characters per second.

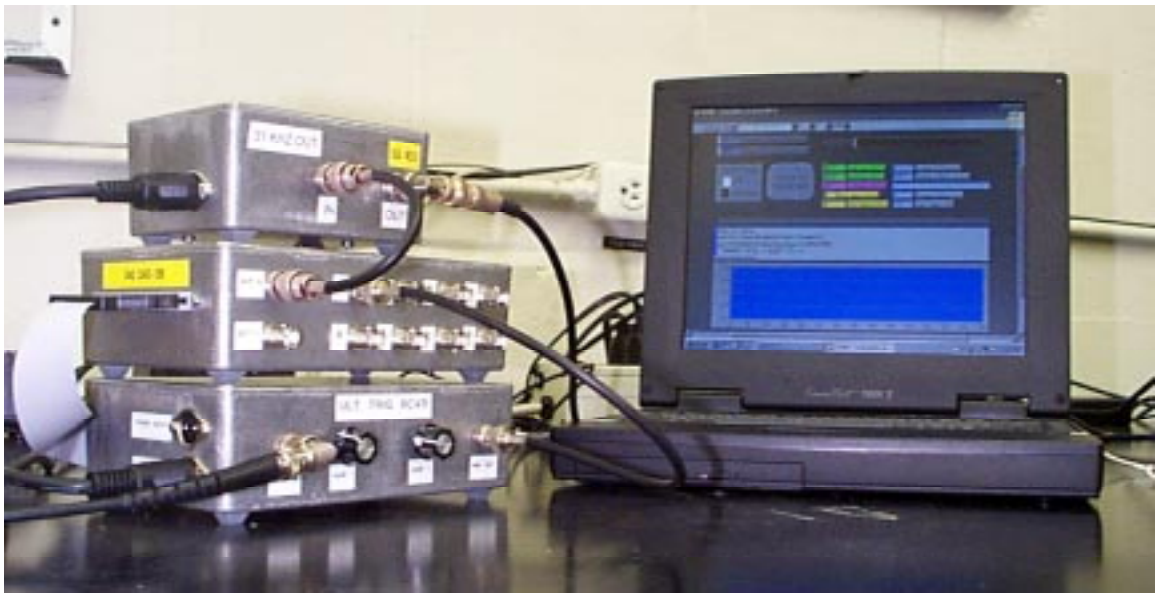

Figure 7.18 Ultrasonic communication transmitter system. The system includes a portable computer-based data I/O system, hardware VCO, trigger signal conditioning electronics, and ultrasonic transducers (not shown). This system was demonstrated for the program monitor on July 16, 1999, in Oak Ridge.

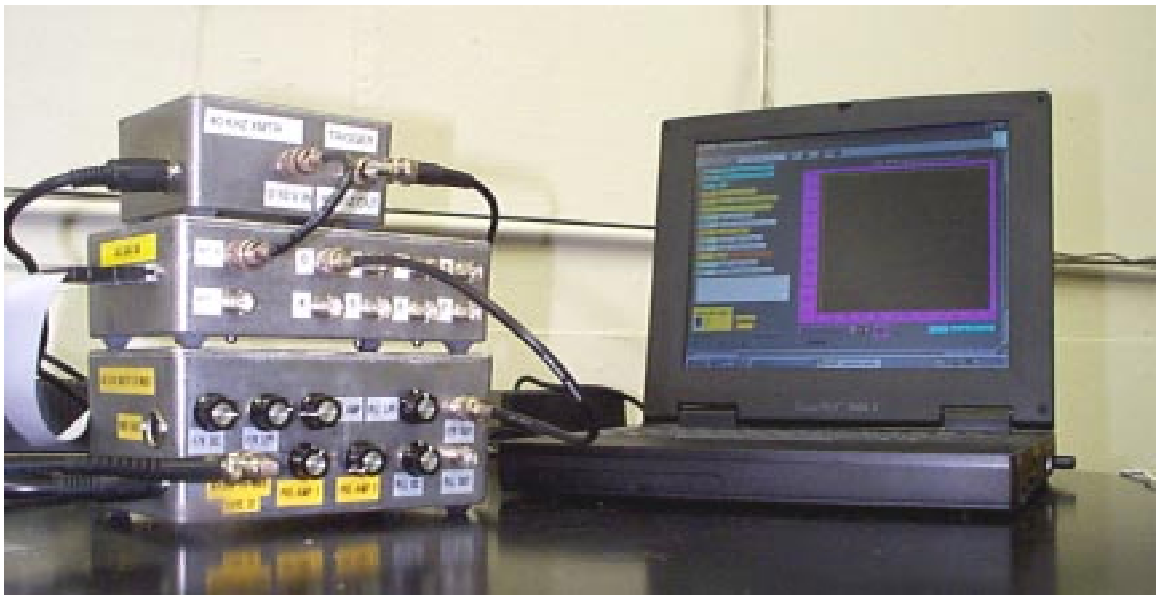

Figure 7.19 Ultrasonic communication receiver system. The system includes a portable computer-based data I/O system, hardware VCO, communication signal conditioning electronics, and ultrasonic transducers (not shown). This system was demonstrated for the program monitor on July 16, 1999, in Oak Ridge.

8. Conclusions and Recommendations

This Phase 1 project has been successful in identifying, exploring, and demonstrating methods for ultrasonic-based communication with an emphasis on the application of digital signal processing techniques. During the project, at the direction of the agency project monitor, particular attention was directed at sending and receiving ultrasonic data through air and through pipes that would be commonly found in buildings. Efforts were also focused on development of a method for transmitting computer files ultrasonically.

New methods were identified and evaluated for ultrasonic communication. These methods are based on a technique called DFS. With DFS, individual alphanumeric characters are broken down into a sequence of bits, and each bit is used to generate a discrete ultrasonic frequency. Characters are then transmitted one-bit-at-a-time, and reconstructed by the receiver. This technique was put into practice through the development of LabVIEW™ VIs. These VIs were integrated with specially developed electronic circuits to provide a system for demonstrating the transmission and reception/reconstruction of typed messages and computer files.

Tests were performed to determine the envelope for ultrasound transmission through pipes (with and without water) versus through air. The practical aspects of connections, efficient electronics, impedance matching, and the effect of damping mechanisms were all investigated. These tests resulted in a considerable number of reference charts that illustrate the absorption of ultrasound through different pipe materials, both with and without water, as a function of distance. Ultrasound was found to be least attenuated by copper pipe and most attenuated by PVC pipe. Water in the pipe provides additional damping and attenuation of ultrasonic signals. Dramatic improvements are observed, however, in ultrasound signal strength if the transducers are directly coupled to the water, rather than simply attaching them to the outside of the pipe.

A major accomplishment of this project was the development and integration of hardware and software into a fully functional ultrasonic communication system for demonstration purposes. The development of this system was a major deliverable of this project and has been successfully demonstrated to the program monitor.

Major system considerations are discussed in this report, including signal conditioning electronics, speed and distance of transmission, triggering and noise filtering, and error checking. The methods employed by this system are believed to be capable of transmitting information over long distances (greater than 200 ft) under ideal conditions, and under extreme conditions if several improvements are made.

Several improvements are suggested as follow-on work. Brief descriptions of these activities follow:

1. Continue to identify and develop methods for minimizing the detrimental effects of extraneous noise and multipath effects observed when transmitting ultrasonic signals through various media. Methods to be explored would include single-frequency pulse width modulation and phase modulation, modulated carrier, and modulated standing wave. These methods may substantially improve the signal-to-noise ratio of the communication link by exploiting the unique nature of ultrasound. In addition, noise rejection circuitry and error checking techniques would be explored and optimized in order to provide 100% accurate information exchange between two sites, even if the media (air, liquid, or solid) contains a high level of ambient noise.

2. Develop transducers that are optimized for connection to different media of interest. New transducer designs, assemblies, and impedance-matching schemes should provide substantial advantages over commercially available transducers that are used in off-design ways (e. g., using an air transducer for coupling ultrasound to pipes or coupling transducers directly to water).

3. Further improve efficiency and minimize size of the communication system by

   - optimizing electronics to meet a specific performance specification,
   - optimizing software (VI) to run faster, with less computational time, and
   - designing and prototyping new application-specific integrated circuits.

4. Explore the transmission of ultrasound through pipe elbows, mounting brackets, and couplings. The attenuation of ultrasound through these elements should be determined in order to best apply the techniques described in this report on real pipe systems.

5. Explore the effect of running water on the transmission of ultrasound through pipes. Investigate the effects of pipe vibrations that are induced by various external sources.

These improvements can evolve the demonstration system into a package that fits a specific sponsor requirement. A field-ready system can be laptop-computer-based, or computer-less, depending on the intended application.

All major objectives outlined in the Phase 1 project statement of work have been addressed and met. This project has produced a substantial body of knowledge that builds on the initial ORNL 1993 work and is believed to be integral to the further development of a field-ready ultrasonic communication system.

Acknowledgments

The authors are grateful for the contributions provided by several people throughout this project. Jeanie Shover provided continuous support by providing communication continuity among the staff and by buying parts and equipment over the past year with amazing speed and accuracy. The authors would also like to thank Curt Ayers and Ned Clapp, Jr., for their generous contribution of ideas throughout the project and for their review of this report. Curt Ayers also designed and built several circuits early in the project which were useful in determining subsequent direction of project developments. George Ott and Cliff White made helpful suggestions regarding integrated circuits and test equipment. Rickey White generously made his laboratory space and equipment available to the authors as well.

References

Manufacturer Information

- Hitachi Semiconductor Selection Guide
- Questlink.com: Internet based semiconductor database
- Piezo Materials Characteristics, APC International, LTD.
- Application Notes for APC Materials
- Catalog #3, Piezo Systems, Inc.
- Motorola Specification Sheet for 45-kHz transducer
- MASSA Model TR-89/B Series Specification sheet
- Jameco 40 kHz Ultrasound Sensor Specification Sheet

Papers

- P. A. Meyer, "Improved sound field Penetration Using Piezo Composite Transducers," NDTnet, Vol. 2, No-08, Aug. 1997.
- D. Reiss, 'E-M Surface Waves, HTTP://web.mit.edu/afs/athena.mit.edu
- J. Eyre and J. Bier, "DSPs court the consumer," IEEE Spectrum, pp. 47-51, Mar, 1999.
- V. A. Krasil'nikov, "Sound and ultrasound waves," NSF, Wash. DC, Israel Program for Scientific Translations, Jerusalem, 1963.

Patents

- US4348904 Acoustic impedance matching device
- US4356422 Ultrasound transducer for enhancing signal reception in ultrasound equipment
- US4427912 Ultrasound transducer for enhancing signal reception in ultrasound equipment

- US4872347 Multiple frequencies from single crystal
- US4907207 Ultrasound transducer having astigmatic transmission/reception characteristic
- US5054470 Ultrasonic treatment transducer with pressurized acoustic coupling
- US5291090 Curvilinear interleaved longitudinal-mode ultrasound transducers
- US5410208 Ultrasound transducers with reduced side-lobes and method for manufacture thereof
- US5418759 Ultrasound transducer arrangement having an acoustic matching layer
- US5446332 Ultrasonic transducer
- US5505205 Interface element for medical ultrasound transducer
- US5575289 Flow meters
- US5663502 Thickness measurement